理學博士 學位論文

ODAM mediates junctional epithelium attachment to tooth and tumorigenesis

치아치은 접합과 암 발생 과정에서 ODAM의 기능적 특성

2015년 8월

서울대학교 대학원

치의과학과 세포 및 발생생물학 전공

이 혜 경

ODAM mediates junctional epithelium attachment to tooth and tumorigenesis

지도교수 박 주 철

이 논문을 이학박사학위논문으로 제출함

2015년 4월

서울대학교 대학원

치의과학과 세포 및 발생생물학 전공

이 혜 경

이혜경의 박사학위논문을 인준함

2015년 6월

위 원 장 정 진 하 (인)

부위원장 박 주 철 (인)

위 원 이 승 복 (인)

위 원 이 장 희 (인)

위 원 조 성 원 (인)

ODAM mediates junctional epithelium attachment to tooth and tumorigenesis

By

Hye-Kyung Lee

Advisor:

Prof. Joo-Cheol Park, D.D.S., Ph.D.

A thesis submitted fulfillment of the requirement for the degree of Doctor of philosophy in Seoul National University

June, 2015

Chin Ha Chung

Joo-Cheol Park

Lee Seungtae

Sung-Won Cho

Lee Jong Hee

ABSTRACT

ODAM mediates junctional epithelium attachment to tooth and tumorigenesis

Hye-Kyung Lee

Department of Cell and Developmental Biology

School of Dentistry

The Graduate School

Seoul National University

(Directed by Prof. Joo-Cheol Park, Ph.D.)

The odontogenic ameloblast-associated protein (ODAM) is known to play important roles in ameloblast differentiation, enamel mineralization, periodontal regeneration, and tumorigenesis. However, the underlying mechanism of ODAM function in various tissues remains largely unknown.

The expression pattern and subcellular localization of ODAM was highly variable and dependent on cell types and their differentiation states, and that functional correlations exist in tooth and various cancer cells. During amelogenesis, Odam was localized in the

nucleus, cytoplasm, and extracellular matrix (ECM) of ameloblasts. Runt-related transcription factor 2 (Runx2) regulated the expression of Odam and nuclear Odam served an important regulatory function in the mineralization of enamel through the regulation of matrix metalloproteinase-20 (MMP-20).

ODAM was expressed in normal junctional epithelium (JE) of healthy tooth but was absent in pathologic pocket epithelium of diseased periodontium. In periodontitis and peri-implantitis, ODAM was extruded from JE following onset with JE attachment loss and detected in gingival crevicular fluid. Odam-mediated RhoA signaling resulted in actin filament rearrangement by interacting with Rho guanine nucleotide exchange factor 5 (Arhgef5). These results suggest that ODAM expression in JE reflects healthy periodontium, and that JE adhesion to the tooth surface is regulated via fibronectin/laminin-integrin-Odam-Arhgef5-RhoA signaling.

Furthermore, ODAM has roles in inducing cancer cell adhesion, in part through binding, a positive regulator of Rho GTPases. ODAM-mediated RhoA signaling resulted in actin filament rearrangement by activating phosphatase and tensin homolog (PTEN) and inhibiting the phosphorylation of AKT. ODAM overexpression decreased motility, increased adhesion, and inhibited the metastasis of breast cancer cell line MCF7 cells.

These results suggest that ODAM regulates MMP-20 in the nucleus, ODAM mediated cell adhesion by activating RhoA signaling in the cytoplasm, and the cytoplasmic ODAM was released in ECM after inflammation.

Keywords: ODAM · ARHGEF5 · RhoA · Junctional epithlium · Cancer · cell adhesion

Student Number: 2011-31199

CONTENTS

LIST OF TABLES AND FIGURES

CHAPTER I. GENERAL INTRODUCTION

Enamel is a great bioceramic designed to bear mechanical forces for decades while being subjected to continuous changes in pH, temperature, and microbial challenges, all that without the ability to regenerate. ability [1]. The enamel mineral builds up at the organic matrix during the maturation stage. Although some important progresses have been made toward identifying essential mechanisms and molecules in these processes [2-4], the developmental continuum of ameloblasts at the maturation stage has been reported on a only histological level [5, 6]. With teeth eruption, the reduced enamel epithelium fuses with the oral epithelium and then is transformed into junctional epithelium (JE). The JE eventually offers the adhesion around teeth. Therefore, it is of crucial significance to obstruct invasion of oral microbes. However, the molecular composition for attachment of the JE and the mineralized tooth remains undefined [7]. In this paper, I focused on the odontogenic ameloblast-associated protein (ODAM) and briefly summarized its role in enamel and the JE.

1. Discovery

ODAM is initially identified as the protein in potentially specific odontoblasts by suppression subtractive hybridization and is named OD-314 [8]. Also, ODAM is identified as the important protein related with the amyloid deposits of calcifying epithelial odontogenic tumors and is called APin (for Amyloid in Pindborg tumors) [9].

In addition, It is discovered by the signal trap screening approach using rat incisor enamel is named EO-009 [10]. It has been renamed ODAM because of its considerable expression in enamel-associated epithelial cells [11, 12].

2. Genomic localization, organization, and protein characteristics

The genomic location of *ODAM* contains in chromosome 5 that clusters for genes involved in enamel, saliva, bone, and milk (small integrin-binding ligand N-linked glycoproteins, SIBLING family) [13]. *ODAM* gene sequence is conserved in mammalian genomes [12]. *ODAM* is composed of 12 exons and has the predicted protein mass of 28.3kD. However, its presence is revealed by western blot analysis, albeit at a higher than predicted molecular mass due to post-translation. ODAM proteins contain an N-terminal signal peptide and are secreted [12, 14]. ODAM have the rich glutamine and proline and the positions of glutamine and proline are predicted to be phosphorylated at a large number of serine and threonine residues and O-glycosylated at various positions. ODAM expression is striking in secretory-stage ameloblasts, maturation-stage ameloblasts, and JE, but present in other tissues including mammary gland, nasal gland, and salivary gland [12], indicating diverse biological roles.

3. Roles in enamel formation

ODAM is expressed in from secretory- to maturation-stage ameloblasts during enamel formation [14]. The first report shows that ODAM involves the enamel formation and highly expresses during amelogenesis [11]. ODAM proteins are localized in the

ameloblast-enamel interface with closer to the cell surface [15]. The data related with ODAM knockout mice has not been reported. Further studies on the regulatory molecular mechanism of enamel mineralization by ODAM have indicated that intracellular ODAM proteins are phosphorylated by the bone morphogenetic protein receptor type IB (BMPR-IB)-mediated action by BMP-2 and then regulates the signaling pathways related with ameloblast differentiation [16]. Interestingly, after injury, recombinant ODAM proteins show the induction of odontoblast differentiation and dentin mineralization using *in vitro* cell culture system and *in vivo* dental pulp capping experiments [17].

4. Roles in the junctional epithelium

ODAM is localized in the pericellular of JE [11]. ODAM is not expressed in the JE after gingivectomy or orthodontic tooth movement and gets back its normal expression condition after the regeneration of gingival tissue [18, 19]. Remarkably, the expression of ODAM is induced in epithelial rests of Malassez (ERM) after gingivectomy or orthodontic tooth movement and ODAM is reexpressed during regeneration [19, 20], indicating that ODAM may function effectively in periodontal regeneration. However, functional studies have not been published. Recently, the *in vitro* model system for junctional, sulcular and gingival epithelium formation has identified ODAM expression to describe the JE's feature [21].

5. Roles in tumors

In addition to the potential roles in enamel formation and the JE regeneration, some

papers have studied the ODAM expression and function in cancers as it is initially found in Pindborg tumors [9, 22]. ODAM has also been discovered in tumors of epithelial origin such as breast, gastric, and lung. It has been suggested as a prognostic marker for breast tumor [23, 24]. In addition, the expression of ODAM has confirmed in certain odontogenic tumors [25, 26]. ODAM expression has also been reported in odontoblasts, osteoblasts and diverse cancer cells [27]. The first report, which shows the functional role of ODAM in tumors, has shown that it hinder tumorigenic characteristics in MDA-MB231 and the mice transplantating ODAM-expressing tumor cells cause significantly reduced tumor growth and their metastasis inability to metastasize [23]. Further molecular study shows that ODAM function by inducing the tumor suppressor phosphatase and tensin homolog (PTEN) and inhibiting the apoptosis-blocking PI3 kinase/AKT pathway [28].

6. Rationale and outline of the thesis experiments

A key purpose of this thesis is to investigate the mechanisms of ODAM function in enamel formation, JE attachment, and tumor metastasis. To achieve this goal, I performed the study of 1) the localization and expression of ODAM, 2) roles of ODAM during amelogenesis 3) the mechanism of JE attachment to the tooth surface for the formation of an epithelial barrier against periodontal pathogens in healthy and inflamed periodontal tissues, and 4) the roles of ODAM in the migration and invasion of cancer cells *in vitro* and *in vivo*.

CHAPTER II.

Expression pattern, subcellular localization, and functional implications of ODAM in ameloblasts, odontoblasts, osteoblasts, and various cancer cells

* This Chapter has been largely reproduced from an article published by Lee HK. and Park JC. (2012). Gene Expr Patterns., 12(3-4):102-108.

I. ABSTRACT

During tooth development and tumorigenesis, the odontogenic ameloblast-associated protein (ODAM) is involved in cellular differentiation and matrix protein production. However, the precise function of ODAM remains largely unknown. To suggest new functional roles of ODAM, it was investigated the cellular expression and subcellular localization of ODAM in tooth and cancer cells. Odam was expressed in ameloblasts, odontoblasts, and osteoblasts *in vivo* and *in vitro*. Furthermore, Odam was localized in both the nucleus and cytoplasm of Mmp-20 expressing ameloblasts and odontoblasts, but only in the cytoplasm of non-Mmp-20 expressing osteoblasts. The extracellular secretion of Odam was not observed in odontoblasts and osteoblasts, but was seen in ameloblasts. In addition, ODAM was discovered in the nucleus, cytoplasm, and extracellular matrix of various cancer cells. These results suggest that the expression pattern and subcellular localization of ODAM is highly variable and dependent on cell types and their differentiation states, and that functional correlations exist between ODAM and MMP-20. This study provides the first evidence for ODAM in multiple cellular compartments of differentiating odontogenic and cancer cell lines with important functional implications.

II. INTRODUCTION

The odontogenic ameloblast-associated protein (ODAM, FLJ20512) was originally cloned from the human KATO III cell line [29] and has been detected in calcifying epithelial odontogenic tumor-associated amyloids [9]. ODAM is expressed in ameloblasts, odontoblasts, lactating mammary glands, nasal and salivary glands, tongue, gingival tissue, the reducing enamel organ, junctional epithelia, and epithelial cell rests of Malassez [8, 12, 20]. ODAM has been implicated in diverse functions such as ameloblast differentiation, enamel maturation, junctional epithelia formation and regeneration, and tumor growth and metastasis [12, 14, 23]. However, the precise function of ODAM remains largely unknown.

In ameloblasts, nuclear Odam serves an important regulatory function in the mineralization of enamel through the regulation of matrix metalloproteinase-20 (Mmp-20) [14]. The cytoplasmic expression of Odam in junctional epithelia and epithelial cell rests of Malassez suggests that this protein may be involved in periodontal healing and regeneration at early time-points following the disruption of periodontal integrity [18, 20]. Nevertheless, the subcellular localization of Odam and its functional implications has not yet been clarified.

MMP-20 expression has been detected in ameloblasts, odontoblasts, and pathological tissues, including the ghost cells of calcifying odontogenic cysts, odontogenic tumors, and human breast carcinomas [30-33]. MMP-20, which plays an important role in the degradation of amelogenin, is synthesized and secreted by ameloblasts. Enamel formation is severely defective in Mmp-20-deficient mice because Mmp-20-mediated amelogenin

degradation is believed to be essential for the axial growth of enamel crystals [33, 34]. MMP-20 may also be involved in breast carcinogenesis, as MMP-20 is expressed at diverse stages even though it is much greater levels in late stages of cancer than in the early stages [32]. MMP-20 is able to fragment the primary structural proteins of the basement membrane and extracellular matrix as well as certain host defense proteins encircling the tumor, but not native fibrillar collagens. Therefore, MMP-20 may participate in the basement membrane and extracellular matrix modeling required for oral carcinoma cell invasion and metastasis formation [35]. I have recently shown that Mmp-20 transcription is induced by recruitment of Odam on the Mmp-20 promoter in ameloblasts [14]. However, besides ameloblasts, very little is known about cells coexpressing ODAM and MMP-20 and the functional correlations between ODAM and MMP-20 in various normal and cancer cells.

In the present study, I investigated the cellular expression and subcellular localization of ODAM in ameloblasts, odontoblasts, osteoblasts, and various cancer cells to determine correlations between ODAM and MMP-20 and define new functional roles of ODAM.

III. MATERIALS AND METHODS

1. Tissue preparation and immunohistochemistry

All mouse experiments were approved by the Seoul National University Institutional Animal Care and Use Committee. Mandibles and maxillae from 10-day-old mice were decalcified in a 10% EDTA (pH 7.4) solution at 4°C and processed for immunohistochemistry for immunohistochemistry. Deparaffinized sections were immersed in 0.6% H_2O_2 in methanol for 20 min to quench endogenous peroxidase activity. They were then pre-incubated with 1% bovine serum albumin in phosphate buffered saline (PBS) for 30 min and incubated overnight at 4°C with a rabbit polyclonal ODAM (1:50) antibody. Affinity-purified rabbit polyclonal anti-ODAM antibody using its target antigen was newly generated against amino acids residues 102-114 of ODAM. The following day, the sections were incubated for 3 h at room temperature with the secondary antibody and reacted with avidin-biotin-peroxidase complex (Vector) in PBS for 30 min. After color development with 0.05% 3, 3'-diaminobenzidine tetrahydrochloride (Vector), the samples were counterstained with hematoxylin.

2. Cell culture

Immortalized ameloblast-lineage cells (ALC) were kindly provided by Dr. T. Sugiyama (Akita University School of Medicine, Akita, Japan). ALCs were cultured in Minimum essential medium supplemented with 5% heat inactivated fetal bovine serum, 10 ng/ml of the recombinant human epithelial growth factor (Sigma-Aldrich), and antibiotic-antimycotic (Invitrogen) in a 5% CO_2 atmosphere at 37°C. Another ameloblast

cell line, LS8, was kindly provided by Dr. ML Snead (University of Southern California, LosAngeles, CA). MDPC-23 odontoblast-like cells (Dr. JE nör, University of Michigan, Ann Arbor, MI), MG-63 human osteoblast-like cells (ATCC), H1299 human metastatic lung cancer cells (ATCC), AGS human stomach cancer cells (ATCC), and HeLa human uterine cervix cancer cells (ATCC) were cultured in Dulbecco's modified eagle's medium supplemented with 10% fetal bovine serum. MCF-7 non-invasive human breast cancer cells (ATCC), SK-BR-3 non-invasive human breast cancer cells (ATCC), and MDA-MB-231 invasive human breast cancer cells (ATCC) were cultured in RPMI 1640. MCF-10A normal human breast cells (ATCC) were cultured in a 1:1 mixture of Dulbecco's modified Eagle's medium and F12 medium supplemented with 5% horse serum (Gibco), hydrocortisone (0.5 μg/ml; Sigma-Aldrich), insulin (10 μg/ml; Sigma–Aldrich), epidermal growth factor (20 ng/ml; Sigma-Aldrich), and penicillin-streptomycin (100 μg/ml each; Gibco).

3. Plasmid construction

Odam cDNA was constructed and verified as described previously [14]. The green fluorescent protein (GFP)-tagged *Odam* gene was placed into pEGFP-C3 (BD Biosciences).

4. Immunofluorescence

To locate endogenous Odam, ALC, MDPC-23, MG-63, or LS8 cells were seeded in chambered cover glasses at a density of 1×10^5 cells per well. The cells were transiently

transfected with the GFP-tagged *Odam* expression construct. The cells were then washed with PBS, fixed with 4% paraformaldehyde in PBS for 10 min at room temperature, and permeabilized for 4 min in PBS containing 0.5% Triton X-100. After washing, cells were incubated with anti-Odam antibody (1:200 dilution) in blocking buffer (2% BSA in PBS) for 2 h and then incubated with FITC-conjugated anti-rabbit IgG (1:200 dilution; Amersham Pharmacia). After the washing step, the cells were visualized under a fluorescence microscope (AX70; Olympus, Japan). Chromosomal DNA in the nucleus was stained using DAPI.

5. Preparation of cytoplasmic and nuclear protein extracts

The cells were collected by centrifugation at 3000 rpm for 5 min at 4°C. Cell lysis was performed in ice-cold hypotonic lysis buffer [10 mM HEPES (pH 7.9), 10 mM KCl, 0.1% Nonidet P-40 (NP-40)], supplemented with protease inhibitors (Roche) for 15 min. The nuclear and cytoplasmic fractions were separated by centrifugation at 3000 rpm for 5 min at 4°C. The resulting supernatant (the cytoplasmic fraction) was stored at 4°C until further analysis. The membrane pellet was resuspended in ice-cold hypertonic lysis buffer [10 mM HEPES (pH 7.9), 150 mM NaCl, 1% NP-40, 0.25% sodium deoxycholate, 10% glycerol], supplemented with protease inhibitors and incubated for 15 min at 4°C. The soluble fraction was isolated by centrifugation at 3000 rpm for 5 min at 4°C. The resulting supernatant (the nuclear fraction) was stored at 4^{o}C until further analysis.

6. Western blot analysis

Proteins were extracted from cell lysates after lysis in NP-40 lysis buffer (50 mM Tris-Cl, pH 7.4; 150 mM NaCl; 1% NP-40; 2 mM EDTA, pH 7.4; and protease inhibitor). The samples were separated on denaturing 10–12% Tris-HCl polyacrylamide gels and transferred to nitrocellulose membranes. The membranes were blocked for 1 h with 5% non-fat dry milk in PBS containing 0.1% Tween 20 (PBS-T), washed with PBS-T, and incubated overnight with primary antibodies diluted in PBS-T (1:1000) at 4°C. Commercially available primary antibodies used were goat polyclonal anti-MMP-20 (sc-26926; Santa Cruz), goat polyclonal lamin B antibody (sc-6216; Santa Cruz), and rabbit anti-GAPDH IgG (sc-25778; Santa Cruz). After washing, the membranes were incubated with goat anti-rabbit-IgG (sc-2004; Santa Cruz) and rabbit anti-goat-IgG (sc-2768; Santa Cruz) conjugated with horseradish peroxidase for 1h. The labeled protein bands were detected using an enhanced chemiluminescence system (Dogene, MA), and the bands were measured using densitometric analysis of the autoradiograph films.

IV. RESULTS

1. Expression of Odam in ameloblasts, odontoblasts, and osteoblasts of developing mice teeth

In our first series of experiments, I aimed to determine the expression pattern of Odam protein during ameloblast, odontoblast, and osteoblast differentiation in developing mice molars by immunohistochemistry. At postnatal day 0, Odam was observed in neither the enamel organ nor dental papilla at the early bell stage of tooth development (Fig. 1A), but it detected in osteoblasts of developing alveolar bone (Fig. 1B). At postnatal days 3, inner enamel epithelial cells differentiated into secretory ameloblasts at cusp tip and secreted enamel matrix. Differentiated odontoblasts also secreted unmineralized pre-dentin and formed mineralized dentin matrix. Odam protein was clearly observed in both the nucleus and cytoplasm of secretory-stage ameloblasts and the interface between ameloblasts and enamel layer (Fig. 1C and D). It was also detected in enamel, dentin matrix, pre-dentin, and underlying odontoblasts (Fig. 1C and D). At postnatal days 10, the ameloblasts showed strong immunoreactivity against Odam in the cytoplasm, the interface between ameloblasts and enamel layer, and enamel matrix (Fig. 1E and F). In addition, Odam was localized in odontoblast processes (Fig. 1F). At postnatal days 14, enamel matrix formation was almost completed and enamel surface was covered with maturation-stage ameloblasts. Odam immunostaining was observed in the cytoplasm of ameloblasts and the interface between ameloblasts and mineralized enamel layer (Fig. 1G and H). However, in predentin and odontoblast processes, the expression levels of Odam decreased compared to those of postnatal days 3 (Fig. 1G and H). These results showed

that the localization of Odam was stage-specific during ameloblast and odontoblast differentiation *in vivo*.

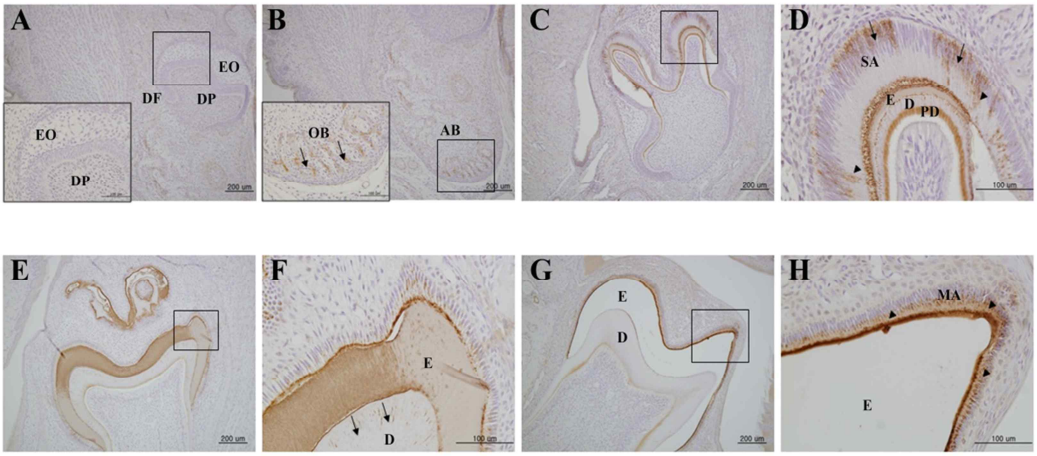

Figure 1. Localization of Odam protein in the developing mandibular molars of mice by immunohistochemistry.

(A) Odam was not observed in a developing tooth bud at early bell stage. (B) Odam expression in osteoblasts (arrows) at postnatal day 0. Closed boxes showed the enlargement of small boxes in A and B, respectively. (C, D) Panel D, the enlargement of box in C, showed Odam expression in the nucleus (arrows) and cytoplasm (arrowheads) of secretory-stage ameloblasts, the interface between ameloblasts and enamel layer, and predentin at postnatal days 3. (E, F) Panel F, the enlargement of box in E, Odam was clearly detected in the interface between ameloblasts and enamel layer, enamel matrix, and odontoblast processes (arrows) at postnatal days 10. (G, H) Panel H, the enlargement of box in G, showed Odam expression in the cytoplasm (arrowheads) of maturation-stage ameloblasts and the interface between ameloblasts and enamel layer at postnatal days 14. EO, enamel organ; DP, dental papilla; DF, dental follicle; OB, osteoblast; AB, alveolar bone; SA, secretory-stage ameloblast; E, enamel; D, dentin; PD, pre-dentin; MA,

maturation-stage ameloblast.

2. In vitro subcellular localization of Odam protein in ameloblastic ALC and LS8, odontoblastic MDPC-23, and osteoblastic MG-63 cells

The subcellular localization of the Odam protein was further investigated in cultured ALC, LS8, MDPC-23, and MG-63 cells using indirect immunofluorescence. Odam immunostaining revealed a strong mesh-like pattern in the nucleus and cytoplasm of ALC, LS8, and MDPC-23 cells. However, in MG-63 cells, Odam was expressed only in the cytoplasm (Fig. 2A). To exclude non-specific antibody binding and confirm the subcellular localization of Odam, a GFP-tagged rat *Odam* construct was transfected into ALC, MDPC-23, and MG-63 cells. Similar to the endogenous Odam, the exogenous GFP-tagged Odam protein was observed in the nucleus and cytoplasm with a similar mesh-like pattern in ALC and MDPC-23 cells (Fig. 2B). In contrast to free GFP distributed throughout the cytoplasm, GFP-Odam protein appeared as punctuate bodies in the cytoplasm of MG-63, but the precise nuclear localization could not be determined (Fig. 2B).

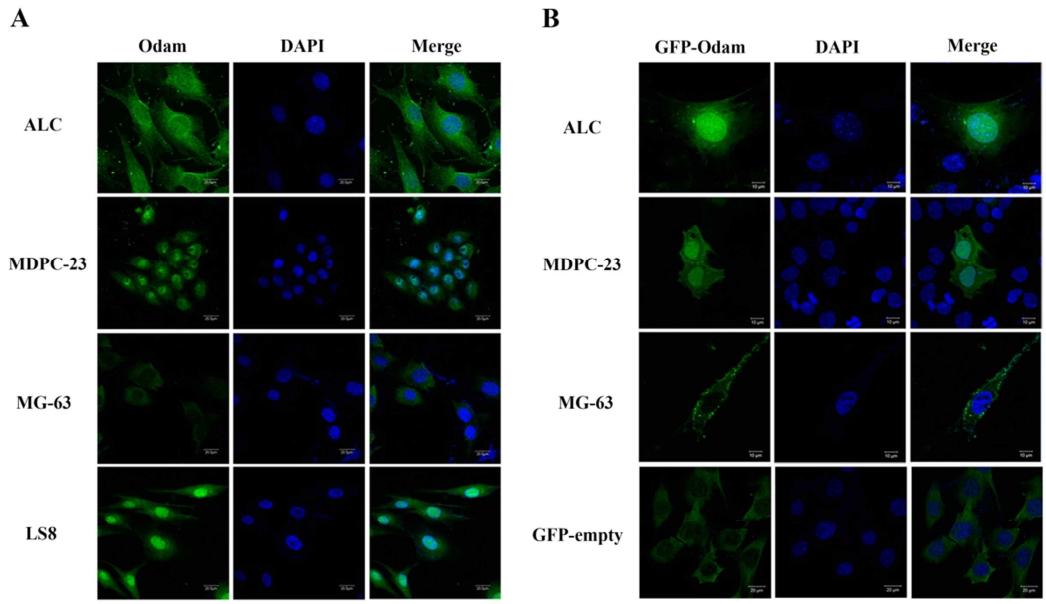

Figure 2. Subcellular localization of Odam protein in ameloblastic ALC and LS8, odontoblastic MDPC-23, and osteoblastic MG-63 cells *in vitro* by immunofluorescence.

(A) Endogenous Odam was detected with anti-Odam antibodies in ALC, MDPC-23, MG-63, and LS-8 cells. Endogenous Odam was located in the nucleus and cytoplasm of ALC, MDPC-23, and LS-8 cells. In MG-63 cells, Odam was primarily localized to the cytoplasm. (B) Exogenous Odam in ALC, MDPC-23, and MG-63 cells was detected by immunofluorescence after transfection of the GFP-tagged *Odam* construct into the cells. Exogenous Odam was also expressed in the nucleus and cytoplasm of ALC and MDPC-23 cells. Nuclei were stained with DAPI.

3. Correlative expression of Odam and Mmp-20 proteins in ameloblastic ALC and LS8, odontoblastic MDPC-23, and osteoblastic MG-63 cells in vitro

To confirm the expression of Odam in tooth-specific cell lines, I analyzed the expression of Odam and Mmp-20 in ALC, LS8, MDPC-23, and MG-63 cells by western blot. ALC, MDPC-23, and LS8 cells expressed both Odam and Mmp-20 protein, while MG-63 expressed Odam protein but not Mmp-20 protein (Fig. 3A). Next, I investigated the subcellular localization of Odam in these cells. Odam protein found in both the nucleus and cytoplasm of ALC, MDPC-23, and LS8 cells, but only in the cytoplasm of MG-63 cells (Fig. 3B). In our previous study, Odam was detected in ameloblasts culture media and I determined that the Odam signal peptide played an important role in Odam protein secretion [14]. Here, I investigated whether odontoblasts and osteoblasts also secrete Odam protein. Endogenous Odam protein was localized in intracellular compartments of ALC, MDPC-23, MG-63, and LS8 cells in the presence or absence of brefeldin A, an inhibitor of protein secretion. In contrast, secreted Odam was not detected in odontoblastic MDPC-23 and osteoblastic MG-63 cells, but was found in ameloblastic ALC and LS8 cells. In addition, Odam secretion was inhibited by brefeldin A in ALC and LS8 cells (Fig. 3C).

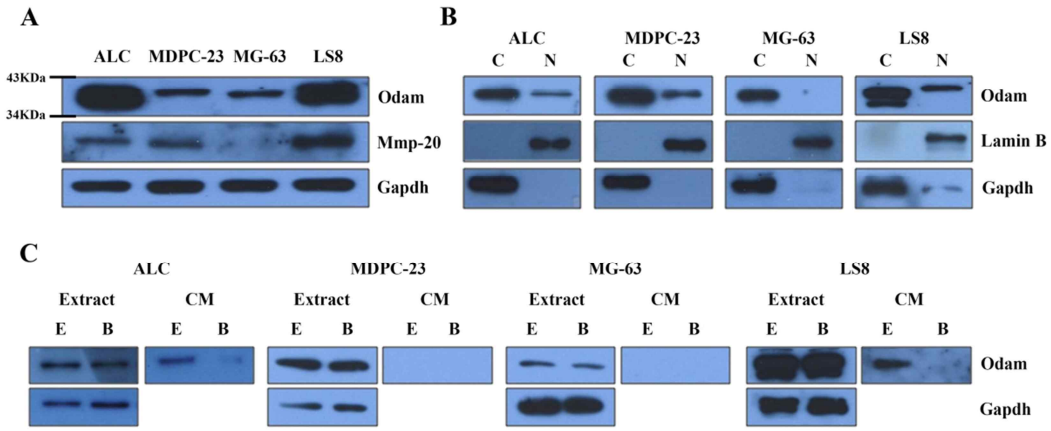

Figure 3. Intracellular and extracellular localization of Odam and Mmp-20 in ameloblastic ALC and LS8, odontoblastic MDPC-23, and osteoblastic MG-63 cells as measured by western blot.

(A) The cell lysates from ALC, MDPC-23, MG-63, and LS8 cells were analyzed by western blot using antibodies against Odam and Mmp-20. Endogenous Odam was expressed in these cell lines, but Mmp-20 proteins were detected in ALC, MDPC-23, and LS8 cells. (B) The cell lysates were separated to nuclear and cytoplasmic fractions and were analyzed for Odam proteins by western blot. Odam was expressed in the nucleus and cytoplasm of ALC, MDPC-23, and LS8 cells, but it was only found in the cytoplasm of MG-63 cells. The nuclear and cytoplasmic fractions blotted with antibodies to Gapdh as a cytoplasmic marker and lamin B1 as a nuclear marker. (C) The Odam protein in cell lysates and conditioned media (CM) were analyzed by western blot. A strong Odam signal was observed in the cell lysates and CM of ALC and LS8 cells. However, Odam was detected in cell lysates of MDPC-23 and MG-63 cells, but not in the CM from these cells. C, cytoplasm; N, nucleus; E, cell extract; B, brefeldin A.

4. Correlative expression of ODAM and MMP-20 proteins in various cancer cells in vitro

ODAM was strongly expressed in the nucleus and cytoplasm of benign structures including ducts, vessels, adenosis, and epithelial hyperplasia. In contrast, ODAM showed uniformly weak cytoplasmic staining in the malignant cells [23]. To infer the function of ODAM in various cancer cells, it was examined the expression levels and patterns of ODAM and MMP-20 by western blot. Although the expression of ODAM protein was relatively low in H1299 cells, it was strongly expressed in AGS, HeLa, MCF-7, and SK-BR-3 cancer cells and MCF-10A human breast epithelial cells. However, ODAM protein was not detected in MDA-MB231 invasive breast cancer cells (Fig. 4A). MMP-20 expression was observed in HeLa, MCF-10A, SK-BR-3, and MDA-MB231 cells (Fig. 4A).

To examine the subcellular localization of ODAM in various cancer cell lines, it was analyzed ODAM expression by western blot after subcellular fractionation. ODAM was found to be expressed in both the nucleus and cytoplasm of HeLa, and MCF-10A cells, but only in the cytoplasmic compartment of H1299, AGS, MCF-7, and SK-BR-3 cells (Fig. 4B). Although, nuclear localization of ODAM did not completely coincide with MMP-20 expression in these cell types, the similar expression patterns observed between ODAM and MMP-20 may suggest correlative functional roles for these proteins.

I also assessed the extracellular secretion of ODAM in H1299, AGS, HeLa, MCF-10A, MCF-7, SK-BR-3, and MDA-MB231 cells by western blot. Endogenous ODAM protein was expressed in the intracellular compartments of H1299, AGS, HeLa, MCF-10A,

MCF-7, and SK-BR-3 cells in the presence or absence of brefeldin A. The extracellular secretion of ODAM was also observed in these cells. However, in MDA-MB231 cells, ODAM was only detected in the conditioned media, but not in the cell lysates (Fig. 4C).

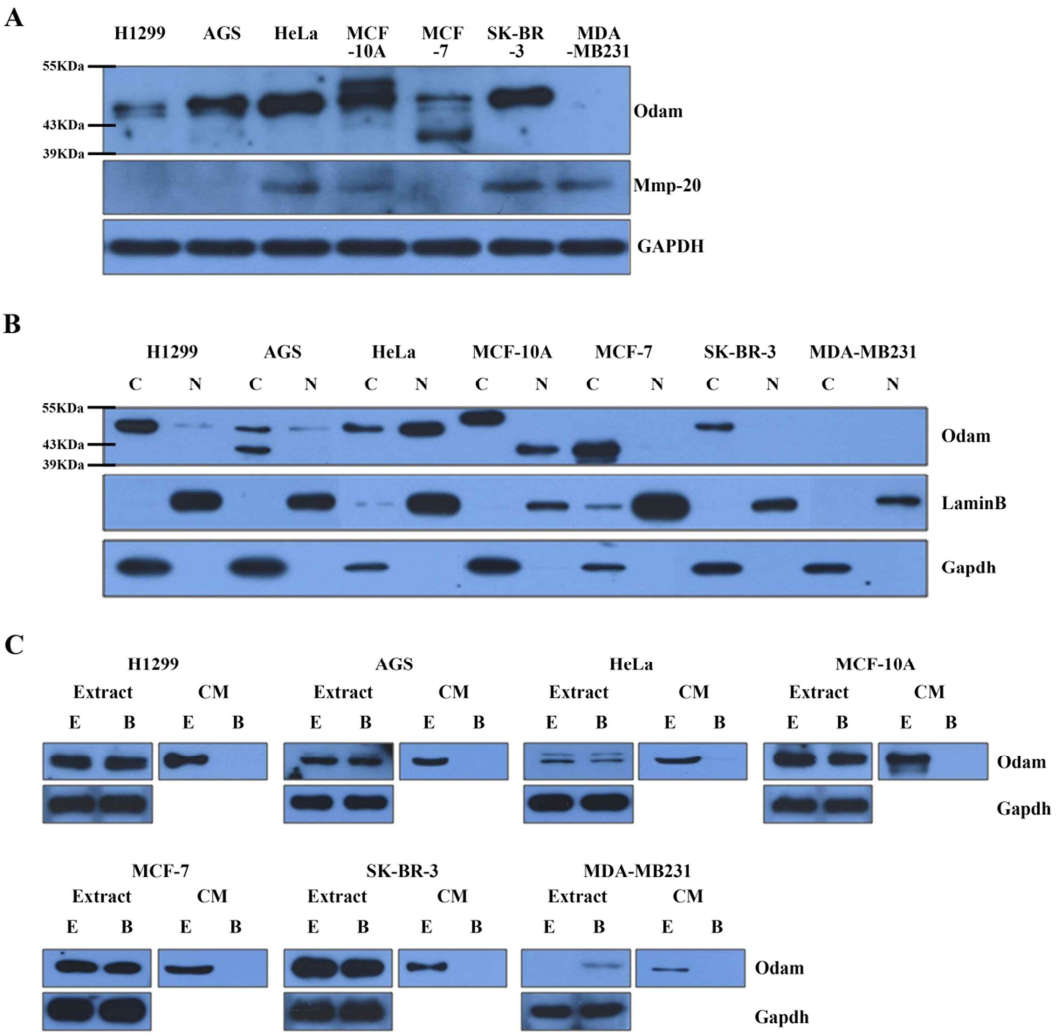

Figure 4. Intracellular and extracellular localization of ODAM and MMP-20 expression in cancer cells, as measured by western blot.

(A) The indicated cell lysates were analyzed by western blot using antibodies against ODAM and MMP-20. ODAM was expressed in all but the MDA-MB231 cells, but MMP-20 proteins were only detected in HeLa, MCF-10A, SK-BR-3, and MDA-MB231

cells. (B) The cell lysates were separated into nuclear and cytoplasmic fractions and were analyzed for ODAM protein by western blot. ODAM was strongly expressed in the nucleus and cytoplasm of HeLa, and MCF-10A cells, but it was found only in the cytoplasm of H1299, AGS, MCF-7, and SK-BR-3 cells. The nuclear and cytoplasmic fractions blotted with antibodies to GAPDH (cytoplasmic marker) and lamin B1 (nuclear marker). (C) The ODAM protein in cell lysates and CM were analyzed by western blot. A strong ODAM signal was observed in both the cell lysates and CM of H1299, AGS, HeLa, MCF-10A, MCF-7, and SK-BR-3 cells; however, ODAM was detected in the MDA-MB231 cell lysates, but not in the CM from these cells. C, cytosol; N, nucleus; E, cell extract; B, brefeldin A.

V. DISCUSSION

Generally, amelogenesis is subdivided into three main functional stages, including the presecretory, secretory, and maturation. Each stage is also subdivided into early, mid, and late phases. A previous controversy concerned whether Odam is expressed in secretory-stage ameloblasts. In our previous studies, it was determined that Odam is expressed in secretory-stage ameloblasts and is localized to the nucleus and cytoplasm both *in vivo* and *in vitro* [11, 14]. However, it has been reported that Odam is expressed exclusively in maturation-stage ameloblasts during amelogenesis [12]. Recently, in early to mid-maturation stage of amelogenesis, the expression of Odam was observed in the cytoplasm of ameloblasts and the interface between ameloblasts and mineralized enamel layer [36]. This discrepancy might result from difficulties in clearly delineating the subdivision of the stages during the continuous amelogenesis process. Part of the secretory stage by our classification might correspond to the early maturation stage classified by other researchers. In the present study, I showed Odam protein in the nuclei and cytoplasm of secretory-stage ameloblasts using a new antibody, unlikely previous antibody [11]. These findings suggest the nuclear localization of Odam in tooth and cancer cells and its functional implications during tooth and cancer development.

Dentin matrix protein 1 (Dmp1) is an acidic phosphoprotein that plays an important role in mineralized tissue formation through the initiation of nucleation and modulation of mineral phase morphology [37-39]. It is expressed in all developing dental structures including the dental lamina, enamel organ, dental papilla, ameloblasts odontoblasts, and dentinal tubules [40]. Similar to Odam, Dmp1 is present in the nucleus and cytoplasm of

certain cell types and can also be found in the extracellular matrix. For example, Dmp1 resides in the nucleus, cytoplasm, and extracellular matrix of osteoblasts depending on their differentiation state suggesting a bifunctional role for this protein, as a transcriptional regulator of specific genes that control osteoblast differentiation before it is exported into the extracellular matrix [41]. Dmp1 was found in the cytoplasm and plasma membrane in the mineralized extracellular matrix of tooth and bone [41]. Thus, it has been postulated to play an important role in mineralized tissue formation by initiating and modulating deposition during the mineral phase [37]. Therefore, the variable localization of Odam indicates that it has various cellular activities in tooth and cancer development that are similar to Dmp1.

Secreted Odam was localized to junctional epithelium-tooth interfaces. Based on these expression patterns, it was suggested that secreted Odam might mediate the adhesion of junctional epithelial cells to the tooth surface, indicating multiple potential regulatory functions [12]. Odam, like a number of other cell-adhesion molecules such as the cadherins [42] and claudin [43], has been shown to reside in the cytoplasm, nuclear/perinuclear regions, and at the cell surface [44]. Furthermore, Odam contains six PDZ-binding motifs, which are found in several tight junction (TJ) proteins, including claudin-4 and ZO, which have been implicated in malignant transformation, cell signaling, and breast tumor cell invasion [24]. Certain TJ proteins, such as ZO-1, are to be coexpressed in the nucleus and extracellular matrix, and some TJ proteins also serve prominent roles in signal transduction [45]. In the present study, ODAM was expressed in the cytoplasm and extracellular matrix of cancer cells and tissues. Furthermore, despite

the absence of intracellular ODAM expression, MDA-MB231 invasive breast cells secreted ODAM protein. These results suggest important roles for extracellular ODAM in neoplastic transformation and tumor cell invasion similar to TJ proteins. Together with the biochemical fractionation, our results also indicate that ODAM is a cytoplasmic, nuclear, and extracellular matrix protein in cancer cells, which is consistent with the predicted role of Odam in tooth development.

MMPs are a family of zinc-dependent endopeptidases that play important roles in tooth development, tumor invasion, and metastasis. Many reports on MMP2, MMP9, and MMP-20 have demonstrated that the production and activation of these proteins is dramatically increased in tooth development and breast cancer, and their expression may also be related to the tooth development and metastasis of cancer cells [32, 34]. MMP-20 plays an important role in the progression of tumor invasion [33] . Consistent with a previous report [14], the expression of MMP-20 correlated with nuclear ODAM expression in most of the investigated cells excluding SK-BR-3 cancer cells in this study. These finding suggest that nuclear ODAM and MMP-20 together may have important roles in transcriptional regulation not only during tooth development but also tumorigenesis and metastasis.

In the present study, intracellular and extracellular expression pattern of ODAM was investigated in tooth and cancer cells *in vivo* and *in vitro*. Odam was present in developing ameloblasts, odontoblasts, osteoblasts, and various cancer cells including human lung, stomach, uterine cervix, and breast cancer cells. Interestingly, in odontogenic ameloblasts and odontoblasts, the nuclear localization of Odam correlated

with Mmp-20 expression. The extracellular secretion and expression of ODAM protein was observed in most cancer cells and tissues which were investigated in this study. These findings suggest that ODAM may be implicated in tumorigenesis. It can be also used as novel clues for understanding the function of ODAM in other various cells. Based on the observation presented here, I propose that ODAM has diverse functions that vary with protein location in various cell lines: nuclear ODAM appears to be associated with MMP-20 regulation and tumorigenesis, and additional functions may take place in the cytoplasm and extracellular matrix.

CHAPTER III.

Odam cooperates with Runx2 and modulates enamel mineralization via regulation of Mmp-20

* This Chapter has been largely reproduced from an article published by Lee HK. and Park JC. (2010). J Cell Biochem., 111(3):755-767.

I. ABSTRACT

I have previously reported that the odontogenic ameloblast-associated protein (Odam) plays important roles in enamel mineralization through the regulation of matrix metalloproteinase-20 (Mmp-20). However, the precise function of Odam in Mmp-20 regulation remains largely unknown. The aim of the present study was to uncover the molecular mechanisms responsible for Mmp-20 regulation. The subcellular localization of Odam varies in a stage-specific fashion during ameloblast differentiation. During the secretory stage of amelogenesis, Odam was localized to both the nucleus and cytoplasm of ameloblasts. However, during the maturation stage of amelogenesis, Odam was observed in the cytoplasm and at the interface between ameloblasts and the enamel layer, but not in the nucleus. Secreted Odam was detected in the conditioned medium of ameloblast-lineage cell line (ALC) from days 14-21, which coincided with the maturation stage of amelogenesis. Interestingly, the expression of Runx2 and nuclear Odam correlated with Mmp-20 expression in ALC. I therefore examined whether Odam cooperates with Runx2 to regulate Mmp-20 and modulate enamel mineralization. Increased expression of Odam and Runx2 augmented Mmp-20 expression, and Runx2 expression enhanced expression of Odam, although overexpression of Odam did not influence Runx2 expression. Conversely, loss of Runx2 in ALC decreased ODAM expression, resulting in down-regulation of Mmp-20 expression. Increased Mmp-20 expression accelerated amelogenin processing during enamel mineralization. Our data suggest that Runx2 regulates the expression of Odam and that nuclear Odam serves an important regulatory function in the mineralization of enamel through the regulation of

Mmp-20 apart from a different, currently unidentified, function of extracellular Odam.

II. INTRODUCTION

Dental enamel formation is divided into secretory, transition, and maturation stages [46]. During the secretory stage, tall columnar ameloblasts secrete specialized proteins, including amelogenin [47], ameloblastin [48], and enamelin [47] into the enamel matrix. Two novel molecules, odontogenic ameloblast-associated protein (Odam) and amelotin (Amtn) have recently been described as members of the secretory calcium-binding phosphoprotein (SCPP) gene cluster [13, 49, 50].

The cDNA transcript of ODAM (FLJ20512) was originally cloned from the human KATO III cell line [29] and has been detected in calcifying epithelial odontogenic tumor (CEOT)-associated amyloids designated as Apin [9]. ODAM has also been reported to be a gastric and breast cancer-specific gene based on the analysis of gene expression data [51]. Rat Odam protein was identified from the secretome profile of rat enamel organ cells using the signal trap method [10]. Odam contains a cleavable signal peptide and an abundance of glutamine and proline residues and is expressed in ameloblasts during the secretory and maturation stage of enamel development [10, 11]. The association of high Odam expression with enamel maturation suggests a possible role for this protein in the final phases of enamel formation [12]. In addition to ameloblasts, Odam is also expressed in odontoblasts, lactating mammary glands, nasal and salivary glands, tongue, and gingival tissue [8, 12]. Taken together, these data suggest a broad physiological role for Odam; however, the precise function of Odam remains largely unknown.

Matrix metalloproteinase-20 (Mmp-20, also known as enamelysin) and Kallikrein-4 (Klk4) have also been shown to function in enamel formation. Mmp-20, which plays an

important role in the degradation of amelogenin, is synthesized and secreted by ameloblasts. The amelogenin degradation induced by Mmp-20 is believed to be essential for the axial growth of enamel crystals. During the maturation stage, low columnar ameloblasts synthesize and secrete less enamel matrix protein, but instead synthesize and secrete Klk-4, which degrades enamel proteins to promote enamel crystal thickening. During this stage, ameloblasts develop either a ruffle-end or a smooth-end, which plays an important role in the mineralization and maturation of enamel by removing water and enamel matrix degradation products, as well as transporting calcium [34, 52]. Although there have been advances in our understanding of enamel formation, further studies are required to understand the precise mechanism underlying enamel mineralization.

In ameloblasts and other types of cells, the expression of Mmp-20 correlates with Odam expression. Mmp-20 is primarily expressed in ameloblasts, although transient expression has been detected in odontoblasts [52]. Mmp-20 expression has also been detected in pathological tissues, including the ghost cells of calcifying odontogenic cysts [30], odontogenic tumors [31], and human breast carcinomas [32].

Runx2, which is stimulated by BMP-2 or TGF-β, controls downstream factors that act on the development of the enamel organ epithelium [53]. The importance of Runx2 in amelogenesis is evidenced by the lack of enamel in the incisor tooth germs of Runx2-deficient mice. Runx2 is also present in late secretory- and maturation-stage ameloblasts [54]. The promoter of the gene encoding ameloblastin, an extracellular matrix protein that may play a role in enamel crystal formation in the developing dentition, contains two Runx2-binding sites [55]. The Odam promoter also contains Runx2-binding sites [56],

suggesting that Runx2 may be involved in the early stages of enamel organ formation as well as tooth morphogenesis, and might also play a direct role in the formation of tooth enamel.

Recently, I reported that Odam is primarily involved in mineralization of enamel that is mediated by up-regulating expression of Mmp-20 [11]. The aim of the present study was to determine whether Runx2 and Odam co-operate to regulate the expression of Mmp-20, thereby modulating enamel mineralization.

III. MATERIALS AND METHODS

1. Tissue preparation and Immunohistochemistry

All experiments involving animal were performed according to the Dental Research Institute guidelines of the Seoul National University. Mandibles and maxillae of 16-day-old mice were decalcified in 10% EDTA (pH 7.4) at 48C and processed for immunohistochemistry. ODAM expression was detected using an ABC kit (Vector Lab) with rabbit anti-rat ODAM antibody (0.2mg/ml) as the primary antibody and a biotin-labeled goat anti-rabbit IgG (1:200) as the secondary antibody. ODAM-specific antibodies were obtained by affinity purification of the ODAM antisera that had been produced by immunizing rabbits with a synthetic peptide (STSPKPDTGNF or QGGQAGQPDFSQQ; Peptron, Seoul, Korea), corresponding to the sequence of 241 through to 251 or 102 through to 114 of the 278-residue rat ODAM as previously described [Park et al., 2007].

2. Cell culture

Ameloblast lineage cells (ALCs) were cultured on collagen-coated dishes in MEM supplemented with 5% FBS, 10 ng/ml recombinant human epithelial growth factor (EGF; Sigma-Aldrich), and an antibiotic-antimycotic agent (Invitrogen) in a 5% CO_2 at 37°C. MDPC-23 odontoblast-like cells (Dr. JE nör, University of Michigan, Ann Arbor, MI) and C_2C_{12} mouse myoblast cells (ATCC) were cultured in DMEM with 10% fetal bovine serum.

3. Reverse transcription-PCR (RT-PCR) analysis

Total RNA was extracted from MDPC-23 cells as well as pulp tissue using TRIzol® reagent according to the manufacturer's instructions (Invitrogen). Total RNA (2 μg) was reverse transcribed for 1 h at 50°C with 0.5 mg Oligo dT and 1 μl (50 IU) Superscript III enzyme (Invitrogen) in a 20 μl reaction. One microliter of the RT product was PCR amplified using the primer pairs. RT products were amplified by PCR using the primer pairs (Table. 1). The following PCR conditions were used: 94°C for 30 sec; 55°C for 30 sec; and 72°C for 1 min for 30 cycles. The PCR products were electrophoresed in a 1% agarose gel, stained with ethidium bromide, and visualized under ultraviolet light.

Table 1. The list for RT-PCR primer

Gene name		Primer
Runx2	forward	5'-TCT GGC CTT CCT CTC TCA GT-3'
	reverse	5'-TAT GGA GTG CTG CTG GTC TG-3'
Odam	forward	5'-ATG TCC TAT GTG GTT CCT GT-3'
	reverse	5'-TTA TGG TTC TCT TAG GCT ATC-3'
Mmp-20	forward	5'-AGC TGT GAG CAA CTG ATG ACT GGA-3'
	reverse	5'-ACA GCT AGA GCC AAG AAC ACA CCT-3'
Amelogenin	forward	5'-CCA GAG CAT GAT AAG GCA GC-3'
	reverse	5'-GAA CTG GCA TCA TTG GTT GC-3'
Enamelin	forward	5'-GAC CTA TGC CAT GAT GCC TG-3'
	reverse	5'-CGC TGA TAA CGG CTG AGT GT-3'
Ameloblastin	forward	5'-AAA AGG AGA AGG TCC AGA AG-3'
	reverse	5'-GCG GAA GGA TAG TAA GTG T-3'
Klk4	forward	5'-ACA AAC CCT TTA TAG GAG CC-3'
	reverse	5'-AAT TAA AAT TTG GGC CTA CC-3'
Gapdh	forward	5'-ACC ACA GTC CAT GCC ATC AC-3'
	reverse	5'-TCC ACC ACC CTG TTG CTG T-3'

4. Plasmids, Cloning, and Recombinant Odam (rOdam)

All cDNAs were constructed using standard methods and verified by sequencing. Constructs encoding Flag (2×)- or HA-tagged full-length *Odam* were inserted into pcDNA3 (Invitrogen, Carlsbad, CA, USA). Based on the 19-nucleotide *Odam siRNA* sequence (5'-AAGTGCCTCAAGATCAAAC-3') selected using the siRNA Target Finder and design Tool (Ambion, Austin, TX, USA), plasmid expressing *Odam siRNA* was prepared using the pSilencer 1.0-U6 siRNA expression vector (Ambion) according to the manufacturer's instructions. mMmp-20 was inserted into pGL3-basic vector (Invitrogen).

The coding region of Odam was amplified by PCR using the following primers: 5'-caggctgctagcatgtcctatgtggttcc-3' and 5'-gtaaactgcagcttatggttctcttaggctatc-3'. The PCR product was cloned into the Nhe I and Pst I sites of pRSET-A (Invitrogen) to generate pRSET-Odam. The E. coli strain, BL21 (DE3) pLysS, was transformed with pRSET-Odam and cultured at 37°C in Luria-Bertani (LB) broth. The protein was extracted and purified from the cell lysates (Elpis-Biotech). Fractions were analyzed using SDS-PAGE and Western blotting.

5. Fluorescence microscopy

Cells in Laboratory-Tek chambered cover glasses (Nunc, Rochester, NY) were washed with PBS, fixed with 4% paraformaldehyde in PBS for 10 min at room temperature, and then permeabilized for 4 min in PBS containing 0.5% Triton X-100. After washing, the cells were incubated with anti-Odam antibody (1:200 dilution) in blocking buffer (PBS

and 1% BSA) for 1 h and then with FITC-conjugated anti-rabbit IgG (1:200 dilution; Amersham Pharmacia Biotech). After washing, the cells were visualized using a fluorescence microscope (AX70; Olympus Optical Co, Tokyo, Japan). Chromosomal DNA in the nucleus was stained using propidium iodide.

6. Preparation of cytoplasmic and nuclear protein extracts

Cells were collected by centrifugation. Cells were lysed in ice cold hypotonic lysis buffer [10 mM HEPES (pH 7.9), 10 mM KCl, 0.1% NP-40] supplemented with protease inhibitors (Roche Molecular Biochemicals, Mannheim, Germany). Nuclear and cytoplasmic fractions were separated by centrifugation. The membrane pellet was resuspended in ice-cold hypertonic lysis buffer [10 mM HEPES (pH 7.9), 150 mM NaCl, 1% NP-40, 0.25% sodium deoxycholate, 10% glycerol]. The soluble fraction was isolated by centrifugation.

7. Western blot analysis

Proteins (30 μg) from the cells were separated by 10% SDS-PAGE and transferred to nitrocellulose membranes. Membranes were blocked for 1 h with 5% nonfat dry milk in PBS containing 0.1% Tween 20 (PBS-T), and incubated overnight at 4°C with the primary antibody diluted in PBS-T buffer (1:1000). After washing, membranes were incubated for 1 h with secondary antibodies. Labeled protein bands were detected using an enhanced chemiluminescence system (Dogen, Cambridge, MA).

8. Luciferase assay

Cells were seeded in 12-well culture plates at a density of 1.5×10^5 cells per well. Cells were transiently transfected with the reporter constructs and a SV40-driven β-galactosidase expression vector as an internal control. After 48h, following the addition of 50 μl Luciferin to 50 μl cell lysate, luciferase activity was determined using an Analytical Luminescence Luminometer according to the manufacturer's instructions (Promega, Madison, WI). β-galactosidase activity was determined in 96-well plates that were read at 405 nm using an ELISA reader. The luciferase activity was normalized to β-galactosidase activity.

9. Chromatin immunoprecipitation (ChIP) assay

Cells were treated with the cross linking reagent formaldehyde (1% final concentration) for 10 min at 37°C, rinsed twice with cold PBS, and swollen on ice in SDS lysis buffer (1% SDS, 10 mM EDTA, 50 mM Tris–HCl, pH 8.1) for 10 min. Nuclei were collected and sonicated on ice. Supernatants were obtained by centrifugation for 10 min and were diluted 10-fold in ChIP dilution buffer (0.01% SDS, 1.1% Triton X-100, 1.2 mM EDTA, 16.7 mM Tris–HCl, pH 8.1, 167 mM NaCl). The fragmented chromatin mixture was incubated with 2 ml antibodies on a rotator at 4°C for 4 h, then 20 μl protein A/G PLUS-agarose (Santa Cruz) was added and incubated for 1 h at 4°C with rotation to collect the antibody/chromatin complex. The final DNA pellets were recovered and analyzed by PCR using primers that encompass the promoter region (Table. 2).

Table 2. The list for ChIP assay primer

Promoter name		Primer
Odam	forward	5'-TCC ACC TCA TCT TAC CTC AA-3'
	reverse	5'-TGT AGT GGT CAT AGC ACT AC-3'
Mmp-20	forward	5'-ACC ATG TAG GTC CTG GGG AAT GAA-3' 5'-TAA AAG TCC TCT GGG TTG AC-3'
	reverse	5'-CTC CTC TCT TGC TTG ATG AT-3'

10. Analysis of Mmp-20 by zymography

The activity of Mmp-20 was assayed by casein zymography. Briefly, Conditioned medium was collected from cells following culture without serum for 24 h. Samples were mixed with loading buffer and electrophoresed on 12% SDS-polyacrylamide gels containing 2% casein (Invitrogen) at 140 and 110 V for 3 h. The gels were then washed twice in zymography washing buffer (2.5% Triton X-100 in double-distilled H_2O) at room temperature to remove SDS, followed by incubation at 37°C for 12–16 h in zymography reaction buffer (40 mM Tris-HCl [pH 8.0], 10 mM CaCl2 and 0.02% NaN3). Gels were stained with Coomassie blue R-250 (0.125% Coomassie blue R-250, 0.1% amino black, 50% methanol and 10% acetic acid) for 1 h, then de-stained with de-staining solution (20% methanol and 10% acetic acid in 70% double-distilled H_2O). Non-staining bands representing the level of the latent form of Mmp-20 were quantified by densitometry using a digital imaging analysis system.

11. Alizarin red S staining

Cells were fixed with 70% ethanol for 20 min and stained with 1% alizarin red S (Sigma-Aldrich) in 0.1% NH_4OH at pH 4.2-4.4. Mineralization assays were performed by treatment of ALC with or without recombinant Odam (rOdam) and staining with alizarin red S solution. The cells were evaluated at 0, 4, 7, 10, and 14 days.

12. Statistical Analyses

All quantitative data are presented as the mean ± standard deviation (SD). Statistical

differences were analyzed using Student's t-tests (*, $p<0.05$).

IV. RESULTS

1. Expression of Odam mRNA and protein during amelogenesis

In the first series of experiments, i determined the protein expression level of Odam during different stages of ameloblast differentiation and the subcellular localization of Odam protein during ameloblast differentiation by immunohistochemistry. Interestingly, the subcellular localization of Odam varied in a stage-specific fashion during ameloblast differentiation (Fig. 5A). Odam protein was not observed in presecretory phase that precedes the secretory and maturation stages. However, distinct expression was detected in secretory-stage ameloblasts (Fig. 5B). Strong staining was also observed in transition- and maturation stage ameloblasts (Fig. 5C). In secretory-stage ameloblasts, Odam staining was observed in the nucleus and cytoplasm, and the apex of ameloblasts stained strongly (Fig. 5D). However, in maturation-stage ameloblasts, Odam was strongly detected in the supranuclear region (Golgi complexes) as well as the interface between ameloblasts and the enamel layer, but not in the nucleus (Fig. 5E).

Selective and time-dependent induction of enamel matrix proteins and enzymes was observed during ALC differentiation. The level of protein and mRNA expression was assessed using Western blots and RT-PCR respectively. Similar to a previous report [11], expression of Odam and Klk-4 gradually increased with time during culture (Fig. 6A and B). In contrast, transcription of amelogenin and enamelin mRNA gradually decreased with cell differentiation (Fig. 6B). Runx2 was steadily expressed during ALC differentiation (Fig. 6A and B). Expression of Mmp-20 mRNA and protein increased slightly from the first day of culture until day 7 and decreased thereafter (Fig. 6A and B).

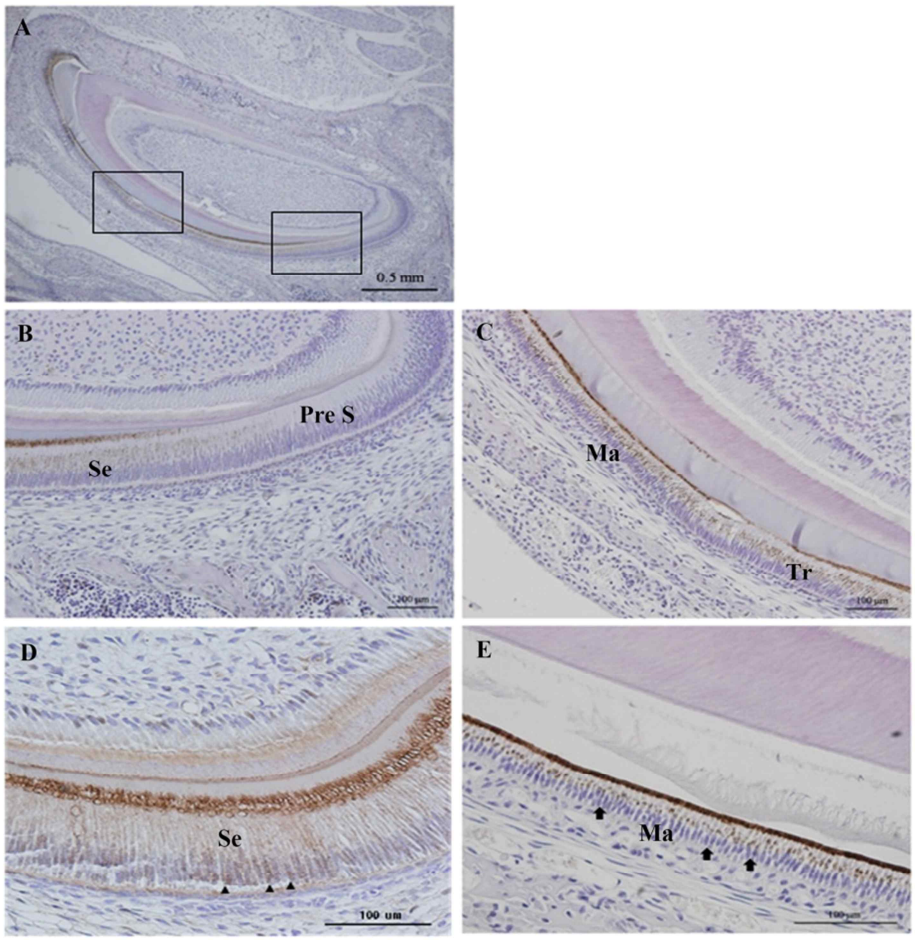

Figure 5. Immunohistochemical analysis of Odam expression during ameloblast differentiation in the mandibular incisor of a 16-day-old mouse.

(A, B) Presecretory ameloblasts lack Odam protein expression. (C) Transition-stage ameloblasts express Odam protein in the supranuclear region of the cytoplasm. (D) Secretory-stage ameloblasts express Odam in their nucleus (arrowheads) and cytoplasm. (E) Maturation-stage ameloblasts do not express Odam protein in their nucleus (arrows). PreS, pre-secretory; Se, secretory; Tr, transition; Ma, maturation.

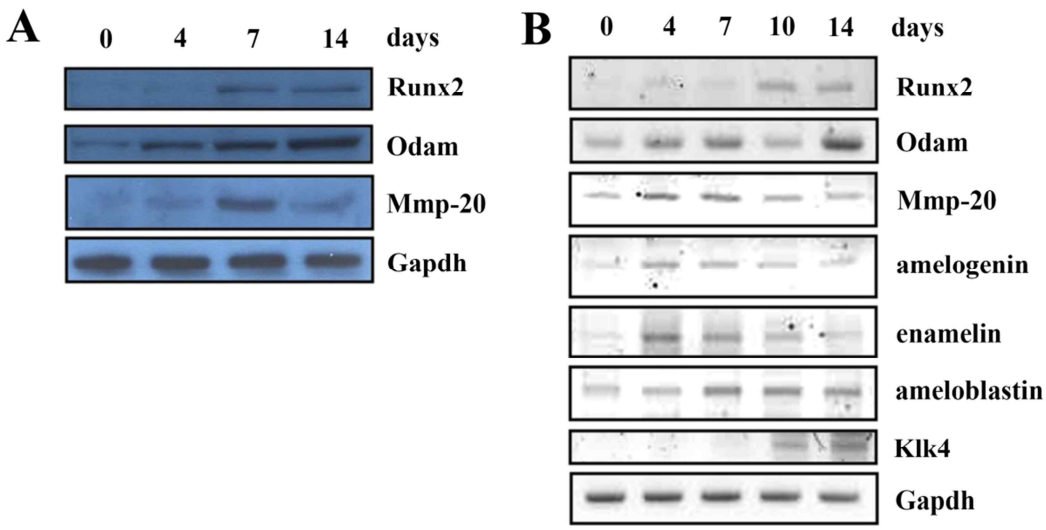

Figure 6. Odam and Mmp-20 protein and mRNA expression during ameloblast differentiation in vitro.

(A) Western blot analysis of the expression of Runx2, Odam, and Mmp-20 during differentiation of ALC in vitro. Odam expression was detected at the beginning of differentiation and increased at subsequent time-points. Expression of Mmp-20 increased slightly from days 0 to 7 and decreased thereafter. (B) RT-PCR analysis of mRNA expression of enamel matrix proteins and enzymes during differentiation of ALC in vitro. Expression of Mmp-20 was strongest at 4–7 days (equivalent to the secretory stage). Gapdh, glyceraldehyde-3-phosphate dehydrogenase; Klk-4, kallikrein-4; Mmp-20, matrix metalloproteinase-20.

2. Cellular and extracellular localization of Odam

The full-length rat *Odam* cDNA encodes a 279-amino acid protein with 15-amino acid signal peptide at the N-terminus that includes a cleavage point for signal peptidase [10].

Exogenous Odam protein was expressed in C_2C_{12} cells, which do not normally express Odam, and was readily detected in intracellular compartments and the CM collected from serum-free cultures (Fig. 7A). To evaluate whether the signal peptide affected the localization of ODAM, it was transfected ALC that expressed a reduced level of Odam with an *Odam* construct containing a mutant signal peptide. This mutant *Odam* was expressed in the cytoplasm and nucleus, but not in the CM (Fig. 7B), indicating that the Odam signal peptide plays an important role in Odam protein secretion.

To examine the time-line of Odam protein expression, I performed Western blot analysis of differentiating ALC. Odam protein was detected in the nucleus from days 0-10 of ALC differentiation *in vitro*, but was observed in the extracellular matrix after 10 days. The amount of Odam protein in the cytoplasm increased after the initiation of ALC differentiation, and the secreted Odam protein was smaller than intracellular protein (Fig. 7C). These data suggest that the subcellular localization of Odam varies in a stage-specific fashion during ameloblast differentiation.

To compare the subcellular localization of endogenous and exogenous Odam, rOdam was treated into ALC cells. In control ALC, faint Odam staining was seen in the nucleus and cytoplasm of ALC (Fig. 7D). After treatment with exogenous rOdam for 4 h, Odam protein was clearly visible in the nucleus and cytoplasm. Under the same conditions, some cells showed a punctuate pattern of fluorescence throughout the cytoplasm,

probably corresponding to rOdam internalized in endosomal compartments (Fig. 7D).

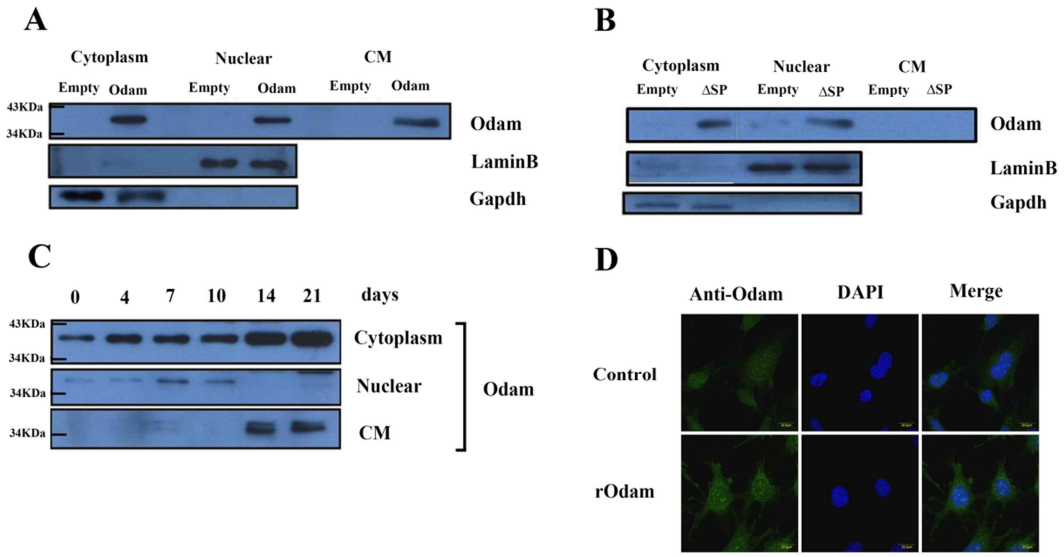

Figure 7. Subcellular and extracellular localization of Odam.

(A) C_2C_{12} cells were transfected with an *Odam*-expression plasmid and the cell lysates and conditioned medium (CM) were analyzed for the presence of Odam protein by Western blot. A strong Odam signal was observed in both the cell lysates and CM. (B) ALC stably expressing low levels of Odam protein were transfected with an expression construct encoding an *Odam* signal peptide mutant and analyzed by Western blot. The cell lysates exhibited a strong Odam signal, whereas the CM did not show a strong signal for the Odam protein. (C) Western blot analysis of the expression pattern of Odam in different cellular compartments during in vitro differentiation of ALC. Note the gradual increase in expression of Odam in the cytoplasm throughout differentiation. Odam was detected in the nucleus from days 0 to 10. The presence of Odam in the CM was strongly detected after 10 days. (D) Subconfluent ALC was cultured in the absence or presence of 10 μg rOdam. Odam localization was detected by immunostaining. Bars: 20 μm.

3. Effect of Runx2 and Odam on the transcriptional activity of Mmp-20

I next determined the effect of Runx2 and Odam on Mmp-20 expression. Overexpression of *Runx2* or *Odam* in ALC increased the expression of Mmp-20 protein (Fig. 8A). In contrast, siRNA-mediated silencing of *Runx2* or *Odam* decreased Mmp-20 expression (Fig. 8B). Odam expression was higher in cells overexpressing *Runx2* than in normal ALC (Fig. 8A). These studies suggest that Runx2 regulates Odam expression, which in turn regulates Mmp-20 expression.

4. ODAM cooperates with Runx2 to regulate Mmp-20

To correlate the role of Runx2 and Odam in Mmp-20 transcriptional activation with their function *in vivo*, ALC was transfected with a HA-tagged *Runx2* expression construct, a Flag-tagged *Odam* expression construct, and/or specific siRNA constructs. Runx2 specifically induced Odam and Mmp-20 protein expression, and overexpression of Odam augmented Mmp-20 expression (Fig. 8C). However, Odam expression did not affect the expression of Runx2 (Fig. 8C).

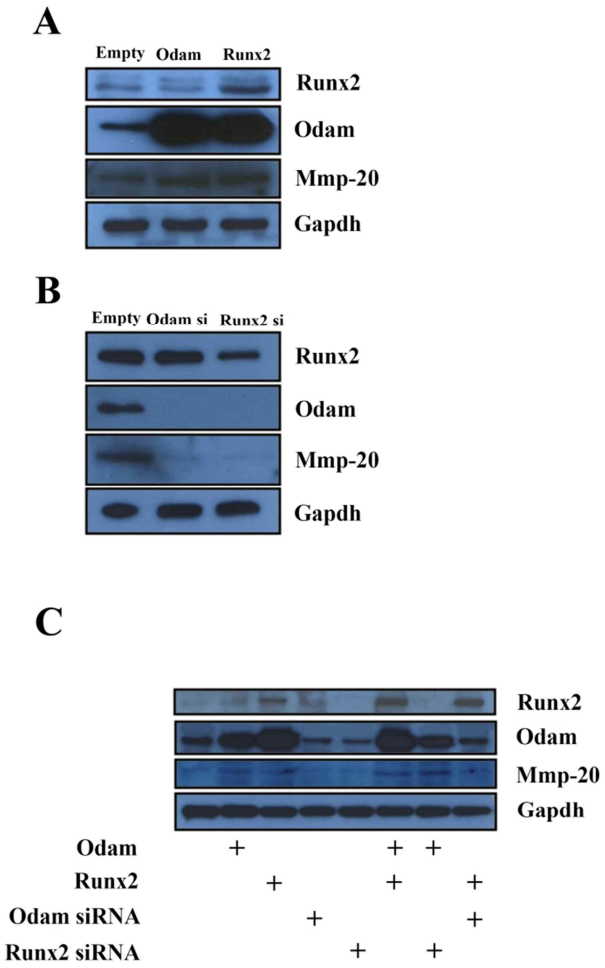

Figure 8. Regulation of Mmp-20 by Runx2 and Odam.

(A) ALC was transfected with *Runx2*- or *Odam*-expression plasmids and cell lysates were analyzed by Western blot with antibodies against Runx2, Odam, Mmp-20, or Gapdh (as a control). Overexpression of Runx2 or Odam induced an increase in the Mmp-20 expression level. (B) ALC was transfected with either a control siRNA (100 pM) or siRNA specific for *Odam* or *Runx2* (100 pM). After 2 days, the expression level of Runx2,

Odam, and Mmp-20 was determined by Western blot with the indicated antibodies. Mmp-20 expression was decreased following the expression of each siRNA. Gapdh was used as a loading control. (C) ALC was transfected with constructs expressing *Runx2*, *Odam*, *Runx2 specific siRNA*, *Odam specific siRNA*, or *control siRNA*, alone and in various combinations. Protein levels were analyzed by Western blotting with antibodies against Runx2, Odam, Mmp-20, and Gapdh. The data show that Runx2 regulated Odam expression and Odam induced Mmp-20 expression.

5. Runx2 attenuates Odam-mediated Mmp-20 transcriptional activation

To investigate the functional consequences of Runx2- or Odam-induced Mmp-20 expression, I determined the effect of Runx2 on Odam-mediated transcriptional activation. Increasing concentrations of Odam or Runx2 significantly increased the expression of a luciferase reporter gene under the control of the mouse Mmp-20 promoter (Fig. 9A). As expected, depletion of *Odam* or *Runx2* using specific siRNA suppressed the promoter activity of the Mmp-20 reporter construct (Fig. 9B). Next, I investigated whether Runx2, acting as an upstream regulator of Odam, is required for Odam-mediated Mmp-20 transcriptional regulation using the mouse Mmp-20-luciferase construct in ALC, which expressed a quantifiable level of Odam. As expected, overexpression of *Runx2* or *Odam* significantly induced Mmp-20 transcriptional activity in ALC cells. Overexpression of *Runx2* and *Odam* showed a synergistic effect on Mmp-20 transcriptional activity (Fig. 9C). On the other hand, when endogenous Runx2 or Odam was suppressed using siRNA, the positive effect of Runx2 or Odam on the activity of the Mmp-20 promoter was disrupted (Fig. 9C). Moreover, Odam increased the activity of the Mmp-20 promoter 2.5-fold in *Runx2*-deficient cells, whereas following the knockdown of Odam expression in ALC cells, Runx2 only weakly induced the activity of the Mmp-20 promoter (Fig. 9C). These results confirm the data presented in Figure 8 with respect to the role of the Runx2-Odam cascade in promoter activity.

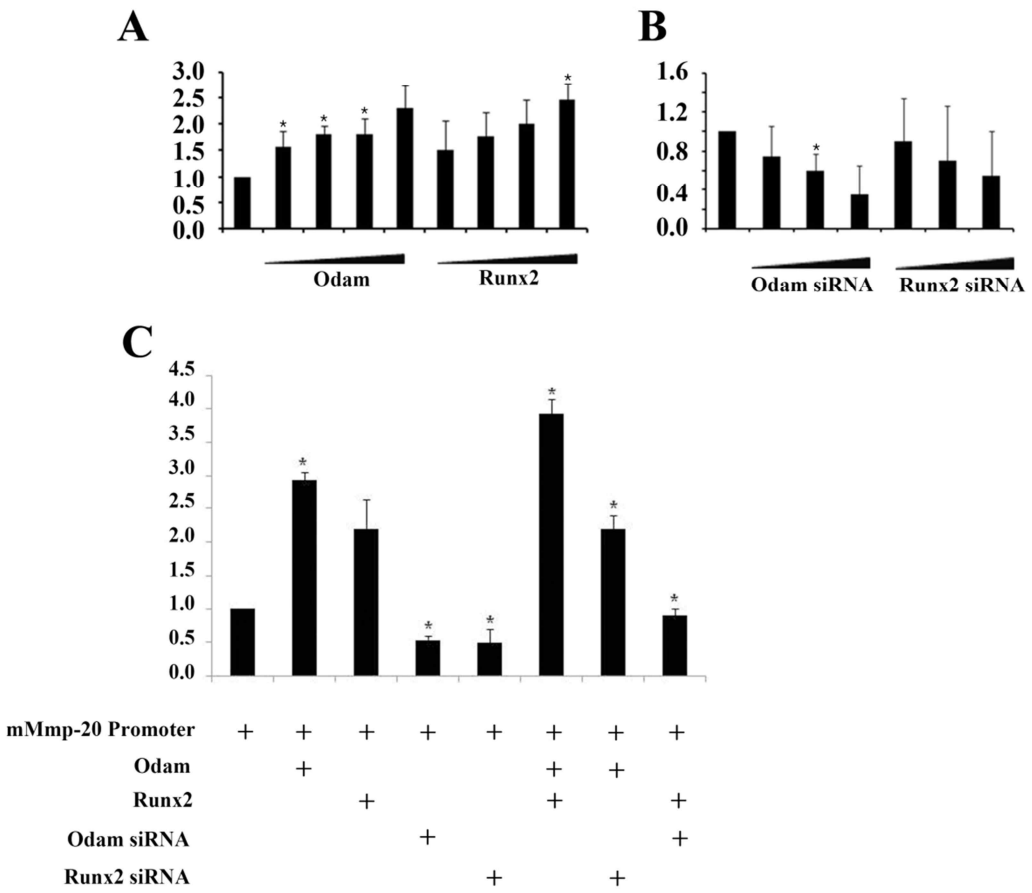

Figure 9. Mmp-20 promoter activity is induced by the cooperation of Runx2 and Odam.

(A) The transcriptional activity of the Mmp-20 promoter was altered by expression of Runx2 and Odam in ALC. ALC was transfected with increasing amounts of plasmid expressing *Runx2* or *Oda*m (0.1, 0.5, 1.0, or 2.0 μg). The *Mmp-20* promoter activity increased in a dose-dependent manner in response to increased concentration of Runx2 or Odam. (B) *Runx2* or *Odam* knockdown abolished Mmp-20 transcriptional activity. ALC was transfected with 40, 80, or 160 pmol of *Runx2* specific siRNA or 0.1, 0.5, or 1.0 μg

of *Odam* specific siRNA expression plasmid. The *Mmp-20* promoter activity decreased in a dose-dependent manner with reduced levels of Runx2 or ODAM. (C) ALC cells were transfected with luciferase reporter under control of the *Mmp-20* promoter (0.1 μg), and with various combinations of *Runx2* or *Odam* DNA (1 μg DNA) or *Runx2* or *Odam* specific siRNA (100 pmol). Cells extracts from the transfected cells were analyzed by luciferase assay. The data are presented as the meanstandard deviation for triplicate experiments. An asterisk denotes values significantly different from the control ($P < 0.05$).

6. Recruitment of Odam to the Mmp-20 promoter

To test whether Odam-mediated activation of the Mmp-20 promoter occurs through recruitment of Odam to the endogenous Mmp-20 promoter, I performed chromatin immunoprecipitation (ChIP) assay. ALC was transfected with the Flag-tagged *Odam* expression construct. Chromatin DNA fragments were precipitated with the indicated antibodies, and the DNA was amplified using primers selective for the Odam-response element in the Mmp-20 promoter. As shown in Fig. 10A, the Mmp-20 promoter could be precipitated using an Odam-specific antibody but not with the negative control antibody (pre-immune serum) or a Runx2-specific antibody. In addition, the result, that the Odam promoter could be precipitated using a Runx2-specific antibody, showed that Runx2 was recruited to the Odam promoter, but not the Mmp-20 promoter (Fig. 10A).

It was confirmed the interaction of Runx2 or Odam with DNA of Odam or Mmp-20 promoters by ChIP assay. ALC was transfected with the Flag-tagged *Odam* or HA-tagged *Runx2* expression construct. ChIP assays using a primer set for Odam or Mmp-20 indicated that Runx2 was not recruited to the Mmp-20 promoter, but Odam promoter. Furthermore, Flag-tagged *Odam* was also recruited to the Mmp-20 promoter following expression of Odam (Fig. 10B). The interaction of Runx2 or Odam protein and their specific antibody was not likely to interact non-specific binding.

It was then performed ChIP assays to examine whether overexpressed or silenced Runx2 or Odam influenced Odam or Mmp-20 promoters using ALC transfected with the HA-tagged *Runx2*, Flag-tagged *Odam*, *Odam siRNA* expression construct, or *Runx2 siRNA* oligo. Before the ChIP assay, it was performed immunoprecipitation of Runx2 and

Odam to determine whether Runx2 was recruited with Odam to the Mmp-20 promoter. Runx2 did not interact with Odam in ALC (data not shown). ChIP assays using a primer set for Mmp-20 indicated that inducing Odam was recruited to the Mmp-20 promoter following expression of either Odam or Runx2, which increases expression of Odam. In addition, increasing Runx2 bound the Odam promoter but not Mmp-20 promoter (Fig. 10C). Together, these results suggest that Runx2 interacted with the Odam promoter in vivo, and Odam was specifically recruited to the Mmp-20 promoter, where it induced Mmp-20 transcription.

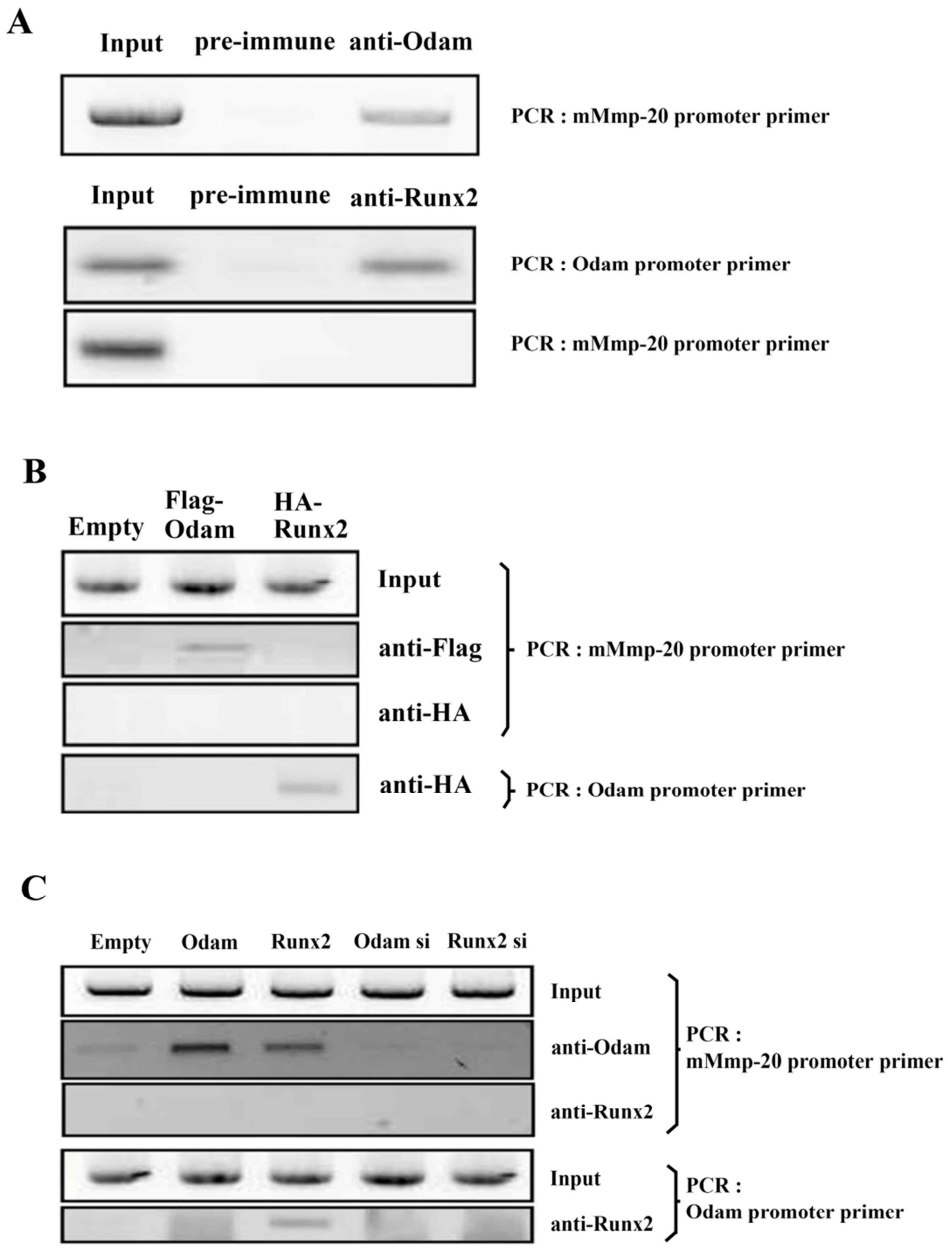

Figure 10. Recruitment of Odam to chromatin.

(A) Cross-linked chromatin was prepared and immunoprecipitated with pre-immune serum or Odam specific antibody. The precipitated DNA was analyzed by PCR with primer pairs spanning the mouse Mmp-20 promoter. The control represents PCR product obtained before precipitation. (B) ALC was transfected with expression vectors for Flag-*Odam* or HA-*Runx2*. ChIP was performed as in (A). Over-expressed *Odam* was recruited to the Mmp-20 promoter and overexpressed *Runx2* was recruited to the Odam promoter. (C) ALC was transfected with expression vectors for Flag-*Odam* or HA-*Runx2* or with *Odam*- or *Runx2-specific siRNAs*. PCR was performed with primer pairs spanning the mouse Odam or Mmp-20 promoter.

7. Role of Odam during amelogenesis in vitro

Amelogenin is digested by Mmp-20 during amelogenesis [33, 57]. To directly demonstrate that Mmp-20 cleaves amelogenin *in vivo*, amelogenins were extracted from ALC that had been differentiated for 4 days and the digestion was analyzed by Western blot with amelogenin specific antibodies. Mmp-20 cleaved intact amelogenin, generating a lower molecular weight fragment of approximately 17 kDa. Markedly different patterns of amelogenin degradation were observed in ALC in which *Runx2* or *Odam* were overexpressed or silenced. One amelogenin band less than 24 kDa in size was not present in the enamel from cells in which *Odam* was silenced, whereas the cleavage product in the controls and cells overexpressing *Odam* or *Runx2* had a lower molecular mass (Fig. 11A). Therefore, *in vivo* Mmp-20 activity resulted in different amelogenin isoforms that are present in naturally maturing dental enamel. The pattern of amelogenin cleavage products generated through *in vitro* digestion was similar to that observed in Western blot analyses of amelogenin cleavage products in porcine secretory stage enamel extracts [57].

To confirm the expression and function of Mmp-20, I performed Western blot analysis and casein zymography. Secretion of Mmp-20 into the extracellular matrix was induced by *Odam* (Fig. 11B). Since the crude protein extract containing the Mmp-20 enamel enzyme was used in the zymography assay, alterations in enzyme activity would probably go unnoticed. Therefore, to observe whether alterations in the activity of Mmp-20 were present, it was prepared zymograms containing casein as the substrate. The zymograms revealed no band in the negative control; however, as seen in Fig. 11B, in addition to the expected Mmp-20 fragment, a fragment at 78 kDa could be detected with expression of

Odam or Runx2. Mmp-20, induced by *Runx2* or *Odam*, was identified in the crude extract used in this study. The main lysis band was not observed with extracts from cells treated with *Runx2*- or *Odam*-specific siRNAs (Fig. 11B).

Finally, I determined the effect of altered Odam expression on enamel mineralization. In normal ALC mineralized nodules, visualized by staining with alizarin red S, appeared after 14 days of culture (Fig. 11C-a). In ALC that overexpressed *Odam* or were treated with rOdam mineralized nodule formation was initially observed on day 7 (Fig. 11C-b, C-c). Inactivation of Odam resulted in cells that failed to mineralize even after prolonged culture (Fig. 11C-d).

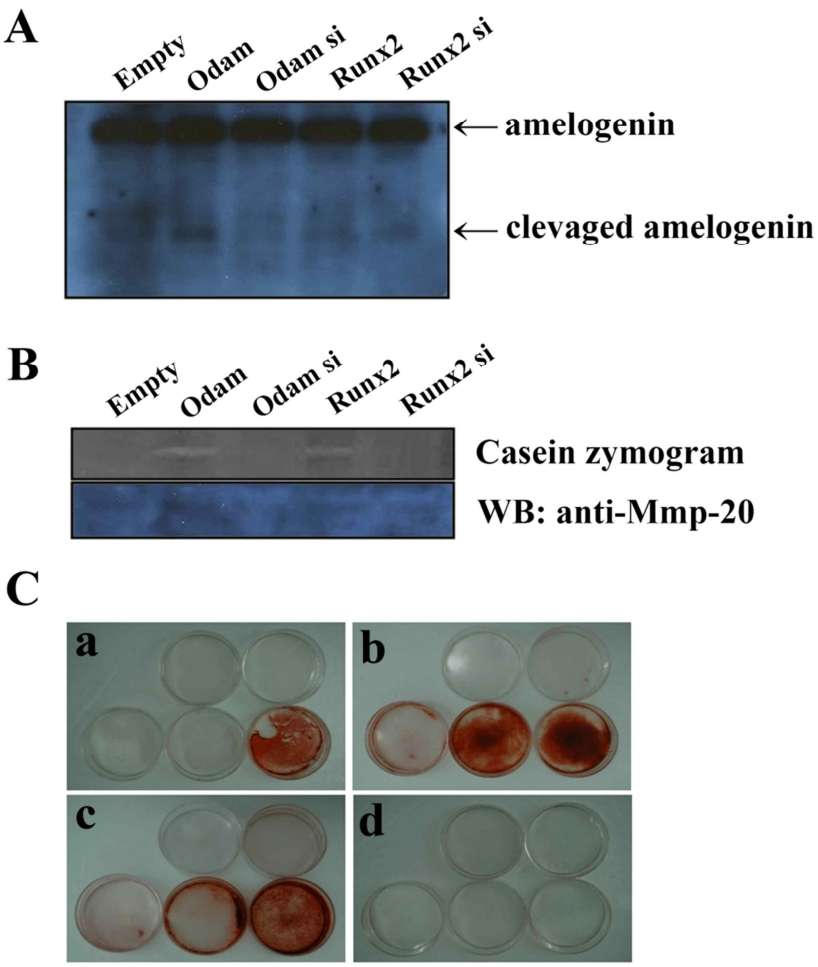

Figure 11. Increased expression of Odam enhances mineralization in ALC.

(A) ALC that were exposed to differentiation media for 4 days and then transfected with the appropriate constructs were used to examine amelogenin cleavage by endogenous Mmp-20 by Western blot analysis. Increasing Mmp-20 levels induced increased cleavage of amelogenin. (B) The kinetics of Mmp-20 expression of in ALC. Casein zymogram showing the relative proteolytic activity in equal volumes of transfected ALC samples; 10

ml of sample solution prepared from serum-free media was applied to each well (Top). Western blot analysis of 60 μg protein of extract using an anti-Mmp-20 antibody (Bottom). Induction of Mmp-20 resulted in increased protease activity. (C) Alizarin red S staining over a 14-day time course in differentiation and mineralization media for normal ALC (a), ALC treated with rOdam (3 μg/ml, b), *Odam* overexpressing cells (c), and *Odam* specific siRNA-expressing cells (d). The cells were evaluated at 0, 4, 7, 10, and 14 days.

V. DISCUSSION

The secretory stage precedes the maturation stage during amelogenesis [46]. If Odam is primarily expressed during the maturation stage of enamel development, it could not positively regulate Mmp-20 expression because Mmp-20 primarily detected during the secretory stage. The data supporting the expression of Odam in secretory ameloblasts are controversial. Although our laboratory has previously shown that Odam is expressed in secretory ameloblasts [11], other reports have indicated that Odam is not expressed during the secretory stage of amelogenesis [10, 12]. Therefore, one aim of the present study was to clarify the expression pattern of Odam during early amelogenesis. In the present study, Odam protein was localized to the nucleus and cytoplasm of the secretory ameloblasts in vivo. In addition, when ALC was cultured in differentiation media, expression of nuclear Odam was induced immediately and continued until day 10, which coincided with the secretory stage of amelogenesis. Interestingly, secreted Odam was detected in the CM of ALC from days 14 to 21, which coincided with the maturation stage of amelogenesis. I also showed that Mmp-20 was expressed during the same stage of amelogenesis as the expression of nuclear Odam. These results suggest that nuclear Odam may influence Mmp-20 expression during the secretory stage of amelogenesis.

To elucidate stage-specific role of Odam during amelogenesis, I used the ALC line as a study model. ALC is an ameloblastic cell line derived from neonate molar tooth organs [58]. ALC maintained the expression of several ameloblast specific genes (amelogenin, enamelin, Mmp-20, and Klk4) and also formed calcified nodules in long-term culture. It has been reported that ALC seems to maintain its original property as secretory

ameloblasts [59]. In the present study, the increase of Klk4 with time during the culture also implies the maturation of ALC. Collectively, these findings suggest that ALC expressing a typical ameloblast phenotype might be used for studying the stage-specific localization of Odam and further the mechanisms of Mmp-20 regulation mediated by Odam.

Mmp-20 cleaves amelogenin to produce fragments commonly observed *in vivo*, and is thought to regulate enamel mineralization [34]. Using the broad-spectrum Mmp inhibitor marimastat, inhibition of mineralization was found to be associated with the inhibition of Mmp-20 activation during amelogenesis [57]. Enamel formation in Mmp-20-deficient mice is severely defective, with enamel mineral content reduced by 50% and hardness decreased by 37% [33]. In the present study, stable cell lines in which Odam had been knocked down failed to initiate mineralized nodule formation. Notably, treatment of ALC that stably overexpress *Odam* or rOdam caused formation of an increased number of mineralized nodules and induced nodule formation earlier than in normal cells. These results suggest that increasing level of Odam, as the result of overexpression or treatment with rOdam, enhanced the onset of mineralization whereas Odam inactivation inhibited mineralization by inhibiting Mmp-20 activation.

Several secretory proteins that contain the signal sequence for targeting to the endoplasmic reticulum (ER), for example angiotensin converting enzyme, have been reported to localize to the nucleus [60, 61]. Interestingly, Odam contains the newly identified nuclear localization signal (NLS) motif that responds to extracellular stimuli and requires phosphorylation for transfer to the nucleus [62], in addition to several

potential consensus nuclear export sequence (NES) motifs [63]. This is similar to the secreted form of phospholipid transfer protein (PLTP), which contains an abnormal NLS and a consensus NES [64]. Therefore, nuclear import of the Odam fragment could be accomplished by a piggyback mechanism, involving binding to a NLS-containing partner. The predicted NES could play a role in the exit of intact Odam or Odam fragments from the nucleus. Odam showed strong positive nuclear and cytoplasmic expression in human breast tissue [24]. Because Odam is expressed in different cellular locations during the various stages of differentiation, it is likely to perform different functions intracellularly and extracelluarly. However, the functionality of these sequence motifs remains to be established.

CHAPTER IV.

Odam mediates junctional epithelium attachment to tooth via Integrin-Odam-Arhgef5-RhoA Signaling

* This Chapter has been largely reproduced from an article published by Lee HK. and Park JC. (2015). J Biol Chem., 290(23):14740-53.

I. ABSTRACT

Adhesion of the junctional epithelium (JE) to the tooth surface is crucial for maintaining periodontal health. Although odontogenic ameloblast-associated protein (Odam) is expressed in JE, its molecular functions remain unknown. I investigated Odam function during JE development and regeneration, as well as its functional significance in the initiation and progression of periodontitis and peri-implantitis. Odam was expressed in normal JE of healthy tooth but was absent in pathologic pocket epithelium of diseased periodontium. In periodontitis and peri-implantitis, ODAM was extruded from JE following onset with JE attachment loss and detected in gingival crevicular fluid. Odam induced RhoA activity and the expression of downstream factors, including Rock, by interacting with Rho guanine nucleotide exchange factor 5 (Arhgef5). Odam-mediated RhoA signaling resulted in actin filament rearrangement. Reduced Odam and RhoA expression in *integrin* β_3- and β_6-knockout mice revealed cytoskeleton reorganization in JE occurred via integrin-Odam-Arhgef5-RhoA signaling. Fibronectin and laminin activated RhoA signaling via the integrin-Odam pathway. Finally, Odam was re-expressed with RhoA in regenerating JE after gingivectomy *in vivo*. These results suggest that ODAM expression in JE reflects healthy periodontium, and that JE adhesion to the tooth surface is regulated via fibronectin/laminin-integrin-Odam-Arhgef5-RhoA signaling. I also propose that ODAM could be used as a biomarker of periodontitis and peri-implantitis.

II. INTRODUCTION

The junctional epithelium (JE) is a specialized epithelial structure that attaches the gingival soft tissue to the tooth surface [6]. In periodontal disease, oral microbes and the host response induce JE to migrate apically and invade the gingival connective tissue during its transformation to pocket epithelium. Inflammation around the pocket epithelium leads to the resorption of alveolar bone around the tooth, and thus to the loss of the periodontal ligament attachment, which is normally responsible for suspending the tooth within the bone [65]. Thus, JE represents the first line of defense against prevalent periodontal diseases [5, 66]. Breakdown of the JE attachment to the tooth surface in the development of periodontal disease has significant consequences for oral health.

The JE is derived from reduced enamel epithelium. After the tip of the tooth approaches the oral mucosa during tooth eruption, the reduced enamel epithelium and the oral epithelium meet, fuse, and form dentogingival junction [67]. However, reduced enamel epithelium is not essential for JE regeneration because it is completely restored from the adjacent sulcular or oral epithelium after pocket instrumentation or surgery. Newly regenerated JE exhibits the same structural and functional features as the original JE [18]. However, the molecular mechanisms responsible for inducing the formation of JE during regeneration remain unclear.

The odontogenic ameloblast-associated protein (Odam) has been implicated in diverse activities such as ameloblast differentiation, enamel maturation, and tumor growth [12, 14, 23, 68]. Odam is expressed during the developmental continuum from maturation stage ameloblasts to normal JE but is reduced after JE damage [7, 15, 18, 20, 69]. Odam is re-

expressed in regenerated JE after orthodontic tooth movement and surgical excision [19, 20]. However, the functional role of Odam in regenerating JE has not yet been established.

Epithelial integrins also participate in the regulation of periodontal inflammation [70]. Integrins are cell adhesion receptors that link the extracellular matrix (ECM) to the cellular cytoskeleton including fibronectin and collagens [71]. Integrin $\alpha_v\beta_3$ is crucial for bone resorbing function in periodontal disease [72]. Integrin $\alpha_v\beta_6$ is constitutively expressed in human and murine JE and *integrin* $\beta_6^{-/-}$ mice develop all of the classic hallmarks of chronic periodontal disease as the initial signs of periodontal disease [73].

During amelogenesis, ameloblasts undergo dramatic cytoskeletal changes, and RhoA protein levels are up-regulated [74]. Rho guanine nucleotide exchange factor 5 (Arhgef5/TIM) belongs to the Rho-GEF family and has GDP-GTP exchange activity for RhoA [75]. Arhgef5 can strongly activate RhoA and RhoB and stimulate Arhgef5-mediated activation of RhoA in dendritic cell chemotaxis [76]. However, although RhoA and Arhgef5 are expressed in ameloblasts and JE, the RhoA-Arhgef5 pathway in amelogenesis and JE formation remains unclear.

The objectives of the present study were to investigate the mechanism of JE attachment to the tooth surface for the formation of an epithelial barrier against periodontal pathogens in healthy and inflamed periodontal tissues. I also identified epithelial attachment loss using objective measures such as biomarkers in the gingival crevicular fluid (GCF) after destruction and apical migration of JE. I tested the hypothesis that certain ECM molecules induce Odam expression in JE via integrin receptors, and Odam subsequently triggers cytoskeletal changes of JE via Arhgef5-RhoA signaling during

dentogingival junction development and regeneration. In addition, I evaluated ODAM protein levels in GCF from periodontitis and peri-implantitis patients for early diagnosis and progress monitoring of periodontal disease.

III. MATERIALS AND METHODS

1. Reagents and Antibodies

The anti-Odam antibody was generated in rabbits by immunization with Odam peptides [16]. Anti-RhoA, F-actin, Gapdh, HA, Rock, His, lamin B, integrin β_1, integrin β_3, integrin β_6, horseradish peroxidase (HRP)-conjugated goat anti-mouse, HRP-conjugated goat anti-rabbit-IgG, and HRP-conjugated rabbit anti-goat-IgG antibodies as well as integrin β_1 and integrin β_6 siRNA were purchased from Santa Cruz Biotechnology (Santa Cruz, CA, USA). Anti-RhoA, E-cadherin, p-myosin, p-paxillin, paxillin, Rock, E-cadherin, and β-catenin antibodies were obtained from Cell Signaling (Beverly, MA, USA). The anti-GTP-RhoA antibody was purchased from Biosource. Anti-Arhgef5 was obtained from Proteintech Group (Chicago, IL, USA). Anti-Flag antibody, fibronectin, laminin, and collagen were from Sigma-Aldrich (St. Louis, MO). The Alexa Fluor® 488 Phalloidin (rhodamine-phalloidin) antibody was obtained from Invitrogen (Carlsbad, CA). Anti-fluorescein isothiocyanate (FITC) or Cy3-conjugated anti-mouse, rabbit, or goat IgG antibodies were purchased from Life Technologies (Grand Island, NY, USA). Y-27632 for Rock inhibition was obtained from Tocris Cookson (Avonmouth, UK).

2. Plasmids, Cloning, and Recombinant Odam (rOdam)

cDNAs of full-length *Odam* or its deletion mutants and siRNA targeting *Odam* were constructed and verified as described previously [16]. His-fused Odam proteins were extracted and purified as described previously [14]. The GFP-tagged *RhoAQ63L*

(constitutively-active RhoA) construct was provided by Dr. Hyun-Man Kim (Seoul National University, Seoul, Korea). Full-length Flag-tagged Arhgef5, ΔPH (amino acids 1341–1488), and Arhgef5 ΔDH (amino acids 1064–1340) were provided by Dr. Masato Okada (Osaka University, Osaka, Japan). The pOTB7-Arhgef5 construct was purchased from the Korea Human Gene Bank. Flag-tagged Arhgef5 ΔSH and SH (amino acids 1489-1581) were subcloned into Flag-tagged pcDNA3 (Invitrogen, Carlsbad, CA).

3. Experimental periodontitis

Experimental periodontitis in mice was induced by *Porphyromonas gingivalis* (PG) inoculation and dextran sulfate sodium (DSS) treatment. Mice were randomly divided into three groups: sham, DSS, and PG. The DSS group received daily application of 5% DSS (MP Biomedicals, Irvine, CA, USA). The PG group received oral inoculation of 10^9 cells of PG cells in 100 μl of 2% carboxymethylcellulose on days 4, 6, and 8. The sham group received vehicles instead of DSS and PG. All mice were euthanized on day 50.

4. Tissue preparation and Immunohistochemistry

All animal experiments were performed according to the Dental Research Institute guidelines of Seoul National University. Teeth blocks from WT and *integrin* $\beta_3^{-/-}$ mice were provided by Dr. Toshiyuki Yoshida and Teruo Okano (Tokyo Women's Medical University, Tokyo, Japan). Extracted human teeth and associated gingival tissue were obtained from Seoul National University Dental Hospital. These studies were approved

by the Institutional Review Board for Human Subjects of the Seoul National University (IRB No. S-D20140007). Rat and mice teeth were decalcified in 10% EDTA (pH 7.4), embedded in paraffin, and processed for immunohistochemistry. Sections were incubated overnight at 4°C with primary antibodies (dilutions of 1:100–1:200). Secondary anti-rabbit or -mouse IgG antibodies were added to the sections for 30 min at room temperature, followed by reaction with the avidin-biotin-peroxidase complex (Vector Laboratories, Burlingame, CA). Signals were converted using a diaminobenzidine kit (Vector Laboratories). Nuclei were stained with hematoxylin.

5. Gene expression profiling

Gene expression profile data (GSE2429) was obtained from the National Center for Biotechnology Information Gene Expression Omnibus (NCBI GEO) database (accession number GSE10526 to PG SerB mutant infection effect on immortalized gingival epithelial cells, GSE4250 to HGF, and GSE2255 to integrin β_6 deficiency model of emphysema).

6. Study subjects and Clinical examinations

After informed consent, 14 unrelated, systemically healthy adults were included in the study. This study protocol was approved by the Institutional Review Board for Human Subjects of the Korea University Anam Hospital (IRB No. ED13162). Periodontal examination included the assessment of plaque score, probing pocket depth, loss of attachment, and bleeding on probing. For peri-implantitis evaluation, two patients with

peri-implantitis were included in the study and two healthy implants served as control. This protocol was approved by the Institutional Review Board for Human Subjects of Seoul National University Bundang Hospital (IRB No. B-1410-271-003).*GCF Collection and ELISA*—Samples were obtained from teeth of one quadrant on the jaw that contained the teeth showing the deepest probing depth and the contralateral quadrant of the opposite jaw; therefore, a total of 222 samples were collected from 12 to 16 teeth of each subject. Each tooth site was gently dried for 10 s with compressed air and isolated from saliva with a cotton roll. GCF samples were obtained from 4 sites of one tooth using absorbing paper strips (Oraflow Inc., Plainview, NY, USA). Paper strips were placed in a single, labeled tube containing 100 μl PBS. The total levels of ODAM in GCF samples were assayed using an ODAM ELISA kit according to the manufacturer's instructions (Cusabio Biotech, Wuhan, China). Associations between probing depths and ODAM concentrations in GCF were analyzed using Kruskal-Wallis test and SPSS.

7. Cell Culture and Transient Transfection

Ameloblast lineage cells (ALCs) were cultured on collagen-coated dishes in MEM supplemented with 5% FBS, 10 ng/ml recombinant human epithelial growth factor (EGF; Sigma-Aldrich), and an antibiotic-antimycotic agent (Invitrogen) in a 5% CO_2 at 37°C. HAT7 cells, a dental epithelial *cell* line originating from a cervical loop epithelium of a rat incisor (a generous gift from Dr. Harada H, Department of Oral Anatomy II, Iwate Medical College School of Dentistry, Morioka, Japan), were grown and maintained in DMEM/ F12 (Gibco BRL, Carlsbad, NY). RAW264.7 cells, a macrophage-like cell line

derived from Balb/c mice, were grown and maintained in DMEM. To induce differentiation, 80%-90% confluent cells were cultured in MEM supplemented with 5% FBS, ascorbic acid (50 μg/ml), and β-glycerophosphate (10 mM) for up to 2 weeks. ALC or HAT7 cells were seeded in culture plates. Cells were transiently transfected with reporter constructs using Metafectene PRO reagent (Biontex, Planegg, Martinsried, Germany). In addition, cells were transiently transfected with siRNA (Santa Cruz) using Lipofectamine RNAi MAX reagent (Invitrogen).

8. Immunoprecipitation assay and His pull-down assay

Cell lysates were prepared by adding 1ml of RIPA buffer [50 mM Tris–Cl (pH 7.5), 150 mM NaCl, 1% Nonidet P-40, 1 mM EDTA, 1 mM PMSF, 1 mM Na_3VO_4, and 1 mM NaF] supplemented with protease inhibitors (Roche). Lysates were incubated at 4°C for 2 h with a 1:200 dilution of the indicated antibody. After incubation for 2 h at 4°C with A/G agarose beads (Santa Cruz), the beads were washed three times with RIPA buffer. Immune complexes were released from the beads by boiling. Following electrophoresis on 10% SDS-polyacrylamide gels, immunoprecipitates were analyzed by western blot using the indicated antibodies.

For His pull-down assays, twenty-four hours after transfection, cells were lysed in RIPA buffer. Lysates were incubated for 1 h at 30°C with His-ODAM C-terminal protein, followed by incubation for 2 h at 4°C with a 1:200 dilution of the anti-His antibody. After incubation for 2 h at 4°C with A/G agarose beads (Santa Cruz), beads were washed three times with RIPA buffer, and immune complexes were released from the beads by boiling.

Following electrophoresis on 10% SDS-polyacrylamide gels, immunoprecipitates were analyzed by western blot using the indicated antibodies.

9. Preparation of cytoplasmic and nuclear protein extracts

Cells were collected by centrifugation. Cells were lysed in ice cold hypotonic lysis buffer [10 mM HEPES (pH 7.9), 10 mM KCl, 0.1% NP-40] supplemented with protease inhibitors (Roche Molecular Biochemicals, Mannheim, Germany). Nuclear and cytoplasmic fractions were separated by centrifugation. The membrane pellet was resuspended in ice-cold hypertonic lysis buffer [10 mM HEPES (pH 7.9), 150 mM NaCl, 1% NP-40, 0.25% sodium deoxycholate, 10% glycerol]. The soluble fraction was isolated by centrifugation.

10. Western blot analysis

Proteins (30 μg) from the cells were separated by 10% SDS-PAGE and transferred to nitrocellulose membranes. Membranes were blocked for 1 h with 5% nonfat dry milk in PBS containing 0.1% Tween 20 (PBS-T), and incubated overnight at 4°C with the primary antibody diluted in PBS-T buffer (1:1000). After washing, membranes were incubated for 1 h with secondary antibodies. Labeled protein bands were detected using an enhanced chemiluminescence system (Dogen, Cambridge, MA).

11. Fluorescence microscopy

Cells in Laboratory-Tek chambered cover glasses (Nunc, Rochester, NY) were washed

with PBS, fixed with 4% paraformaldehyde in PBS for 10 min at room temperature, and then permeabilized for 4 min in PBS containing 0.5% Triton X-100. After washing, the cells were incubated with anti-ODAM antibody (1:200 dilution) in blocking buffer (PBS and 1% BSA) for 1 h and then with FITC-conjugated anti-rabbit IgG (1:200 dilution; Amersham Pharmacia Biotech). After washing, the cells were visualized using a fluorescence microscope (AX70; Olympus Optical Co, Tokyo, Japan). Chromosomal DNA in the nucleus was stained using propidium iodide.

12. RhoA activity assay

GTP-loaded RhoA levels were determined using the G-LISA RhoA activation assay kit (Cytoskeleton, Denver, CO) according to the manufacturer's instructions. Equal amounts of proteins from each experimental group were used in G-LISA RhoA activation assays to obtain values for RhoA activity per cell.

13. Cell adhesion assay

ALC cells were seeded on slides coated with recombinant Odam protein (rOdam) or collagen, and incubated for 4 h. Stable cells expressing *Odam* or *Odam shRNA* were seeded in 96-well plates and incubated for 4 hours. At the indicated times, plates were washed twice with PBS. Cells were fixed with 4% paraformaldehyde for 30 minutes, stained with crystal violet for 10 minutes, followed by the addition of Tween 20 for 30 minutes. Finally, we measured the OD at 595 nm.

14. Periodontal challenge procedures

Thirty healthy upper first molars from 24 eight-week-old Sprague-Dawley male rats were used for gingivectomy. Surgical areas were cleaned with 0.5% chlorhexidine. Removal of the gingiva and the JE along the maxillary molars (gingivectomy) was accomplished by scraping or ligature the tooth surface and extending 2 mm along the palate.

15. Statistical Analyses

All quantitative data are presented as the mean ± standard deviation (SD). Statistical differences were analyzed using Student's t-tests (*, $p<0.05$).

IV. RESULTS

1. ODAM expression was reduced after inflammation or chemical damage in JE

Odam was expressed in differentiating ameloblasts as well as in normal and regenerating JE [11, 18]. First, I investigated Odam protein expression during amelogenesis and JE formation by immunohistochemistry. Odam was clearly observed in reduced enamel epithelium, maturation-stage ameloblasts, and JE during rat tooth development (Fig. 12A). Odam expression was reduced in JE after damage by chemical drugs, DSS and PG compared to sham group (Fig. 12B). To investigate whether periodontitis affects ODAM expression in human JE, I immunohistochemically evaluated ODAM protein expression in a human tooth extracted because of severe periodontitis. In the extracted tooth, JE transforms to the invasive pocket epithelium. In the pocket epithelium, ODAM was no longer detected (Fig. 12C). ODAM expression significantly decreased in damaged gingival epithelial cells modulated with the oral pathogenic PG compared to normal epithelial cells (Fig. 12D). To confirm the alteration of ODAM expression after inflammation in JE, I analyzed microarray data from the NCBI Gene Expression Omnibus (GEO) data set. Hereditary gingival fibromatosis (HGF) associated with aggressive periodontitis typically results in severe, rapid destruction of the tooth supporting apparatus [77]. GEO data showed ODAM expression significantly decreased in gingival tissues with HGF compared to those of normal patients (Fig. 12E). These results suggest that ODAM was expressed in normal JE of healthy tooth but decreased after inflammation or chemical damage, and consequently disappeared in the pathologic

pocket epithelium of diseased periodontium.

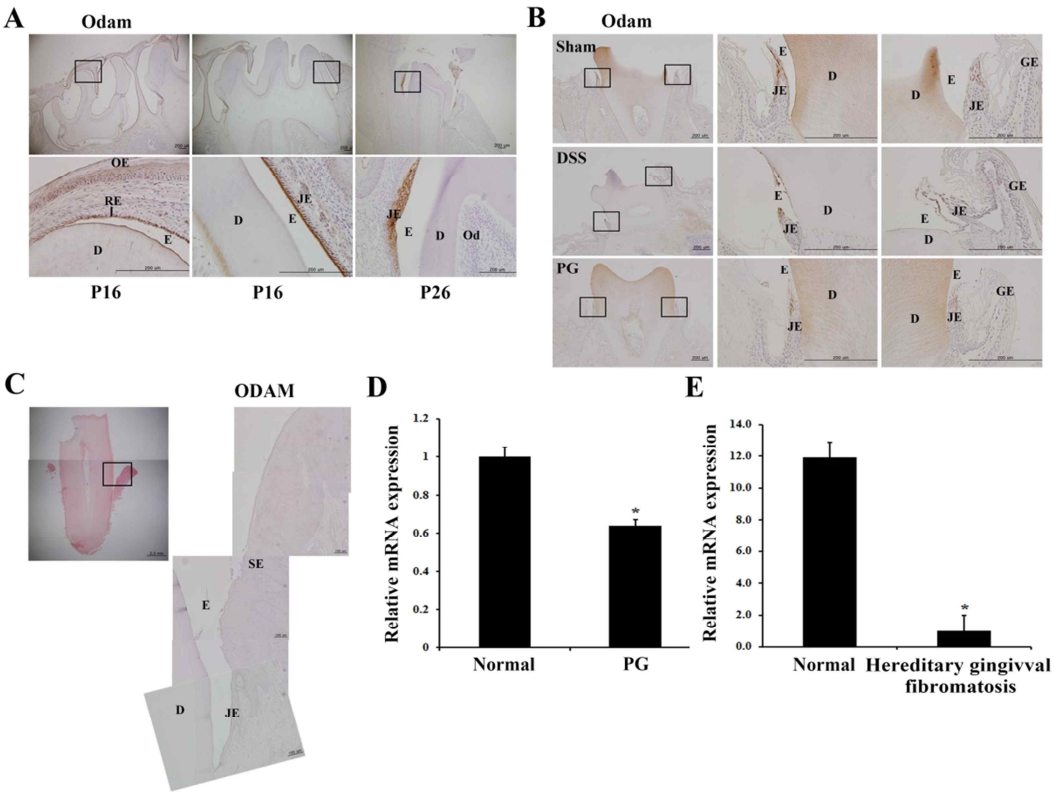

Figure 12. ODAM was expressed in normal JE but reduced after inflammation or damage.

(A) Immunohistochemistry indicates Odam was expressed in reduced enamel epithelium (left panels), maturation-stage ameloblasts (central panels), and JE (right panels) during rat tooth development on postnatal days 16 (P16) and P26. Scale bar: 200 μm. (B) Odam expression was reduced after inflammation by DSS treatment and PG inoculation in JE of 6-week-old mice (3 mice per treatment group). Scale bar: 200 μm. (C) Gingival sections from periodontitis patients did not express ODAM (n = 4). Scale bar: 100 μm. OE: oral

epithelium, RE: reduced epithelium, E: enamel, D: dentin, JE: junctional epithelium, Od: odontoblast, GE: gingival epithelium, SE: sulcular epithelium. (D) Expression of *ODAM* mRNA was analyzed from gene expression dataset GSE10526 deposited in GEO (n =4). (E) Expression of *ODAM* mRNA was analyzed from gene expression dataset GSE4250 deposited in GEO (n = 2).

2. ODAM was detected in the gingival crevicular fluid (GCF) from periodontitis and peri-implantitis patients

ODAM protein was detected in sera from late stage breast cancer patients [50]. I found that ODAM was expressed in normal JE. However, its expression was disappeared in pathologic pocket epithelium from periodontitis patients. Based on these findings, I investigated the expression of ODAM in GCF from periodontitis and peri-implantitis patients by ELISA analysis. As expected, the level of ODAM protein was significantly increased in GCF from periodontitis patients compared to healthy teeth without inflammation (Fig. 13A). Furthermore, the level of ODAM protein in GCF correlated with probing depth in periodontitis patients (Fig. 13B). Similar to periodontitis, ODAM protein level was also significantly increased in GCF from peri-implantitis patients compared to healthy teeth (Fig. 13C) and healthy implants (Fig. 13D). These results demonstrate that ODAM expression in JE reflects healthy periodontium. However, after JE attachment loss caused by periodontitis or peri-implantitis, ODAM is extruded from JE and detected in GCF.

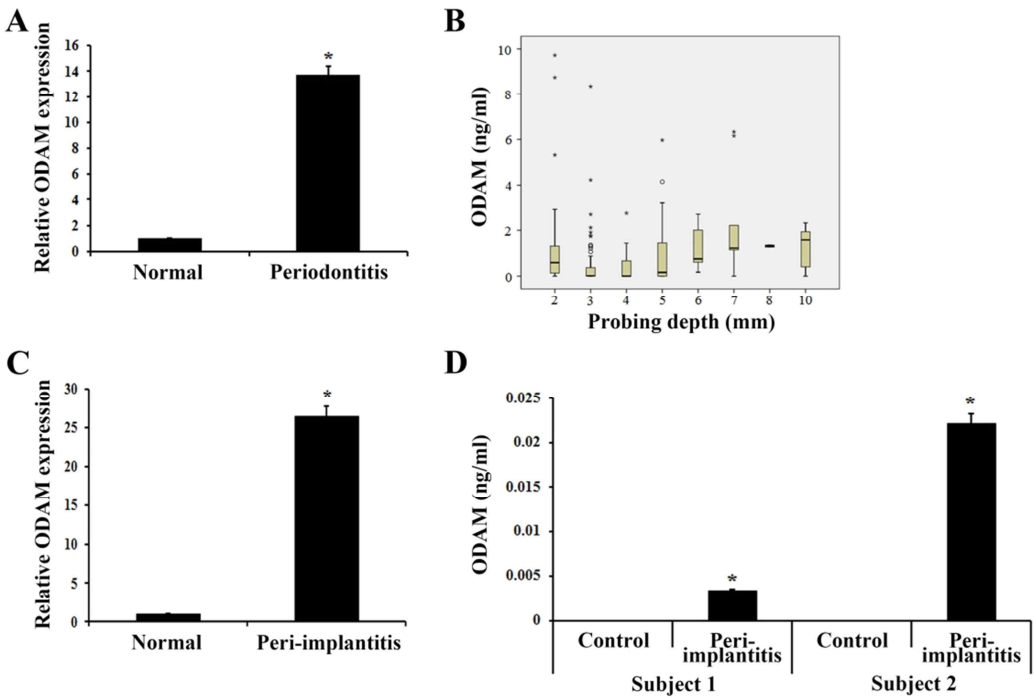

Figure 13. ODAM was detected in GCF from periodontitis and peri-implantitis patients.

(A) ODAM protein levels in GCF from healthy teeth (normal) and periodontitis patients were measured by ELISA. Summary results from 10 patients are shown. (B) The association between probing depths and ODAM concentration in the GCF by ELISA was analyzed using Kruskal-Wallis test (n = 4). (C) ODAM protein in GCF from healthy teeth (normal) and peri-implantitis patients was measured by ELISA (n = 2 per group). (D) ODAM protein in GCF from control and peri-implantitis patients was measured by ELISA. Healthy implants served as controls (n = 2). Data are the mean ± SD of triplicate experiments. *denotes values significantly different from control ($p<0.05$).

3. Odam interacted with Arhgef5 in ameloblasts

In our previous study, Arhgef5 was identified as an Odam-interacting protein by protoarray analysis [16]. In immunoprecipitation (IP) assay, Odam also showed endogenous interaction with Arhgef5 in ALCs (Fig. 14A). To confirm whether Odam could interact with Arhgef5, ALCs were cotransfected with *Arhgef5* and HA-tagged *Odam* constructs for IP assay. The results demonstrated the interaction of Odam with Arhgef5 (Fig. 14B). IP with the Flag antibody followed by blotting with the Arhgef5 antibody indicated that amino acids 127-279 of Odam affected the interaction between Odam and Arhgef5 (Fig. 14C). Pull-down assays also showed a direct interaction between these two proteins (Fig. 14D). Immunofluorescence microscopy revealed that the majority of GFP-tagged Odam and Flag-tagged Arhgef5 proteins co-localized to the periphery of ALCs (Fig. 14E). Overall, these data suggest the interaction between the C-terminus of Odam and the SH domain of Arhgef5 occurs in the cell periphery of ameloblasts.

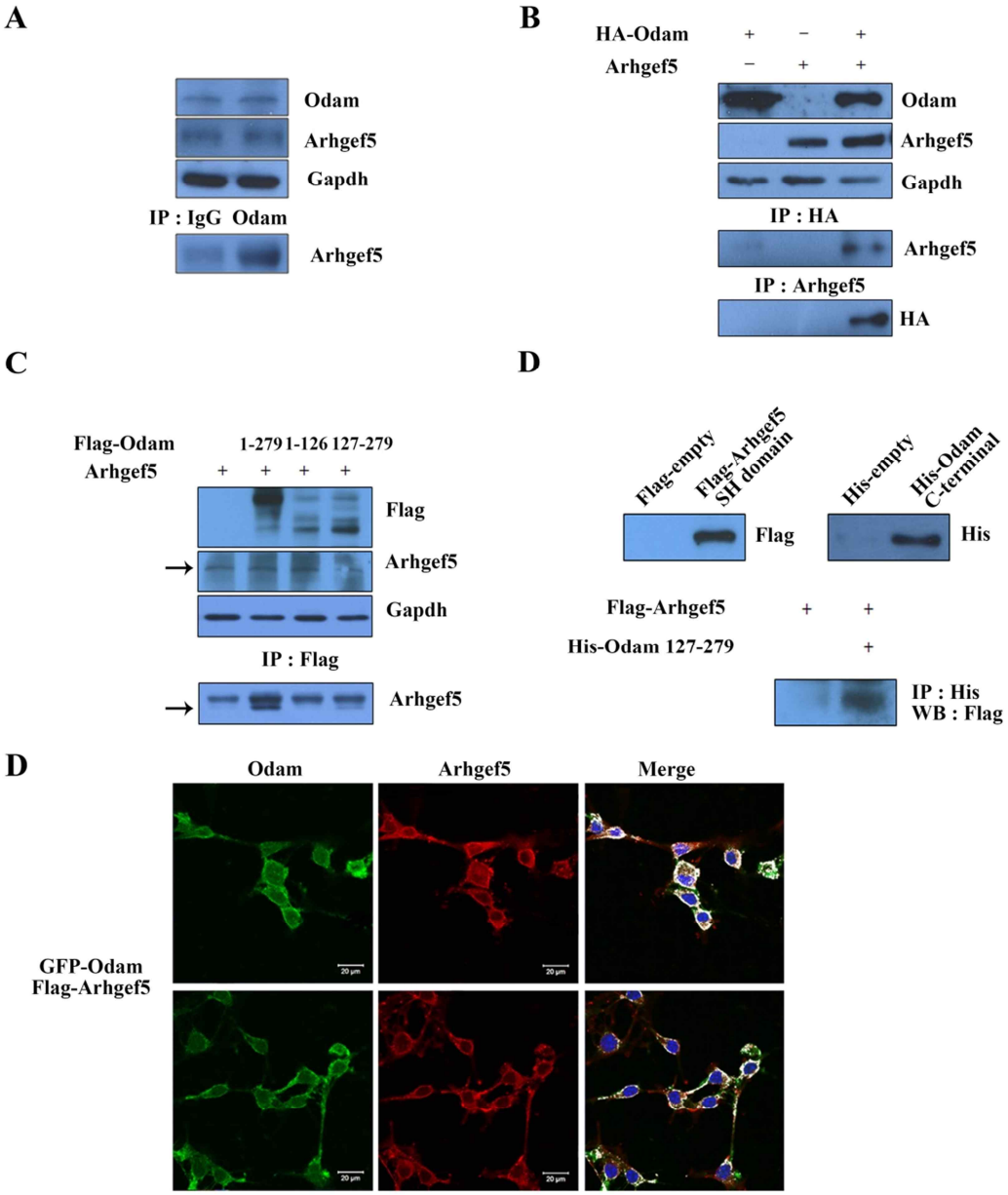

Figure 14. Odam interacted with Arhgef5 in ameloblasts.

(A) IP was performed using anti-Odam antibody in ALCs. Precipitated proteins were

visualized by western blot using anti-Arhgef5 antibody. (B) ALCs were co-transfected with HA-*Odam* and *Arhgef5* constructs. IP was performed using anti-HA or Arhgef5 antibodies. Precipitated proteins were visualized by western blotting using anti- Arhgef5 or HA antibodies. (C) Mapping of the Odam domain required for interaction with Arhgef5. Flag-*Odam* mutants were expressed in ALCs transfected with *Arhgef5*. The interaction was evaluated by IP using the anti-Flag antibody, followed by western blot using the anti-Arhgef5 antibody. (D) ALCs were transfected with the Flag-*Arhgef5* mutant containing only SH domain (amino acids 1489-1581). His pull-down assays were performed with cells expressing the *Arhgef5* SH domain. The Arhgef5 interaction was determined by pull-down using the His-Odam C-terminal mutant. Interactions were detected by western blotting using an antibody specific for the Flag tag expressed by the *Arhgef5* mutant. (E) GFP-tagged *Odam* and Flag-tagged *Arhgef5* constructs were transfected into ALCs. Exogenous Arhgef5 was immunostained using the anti-Flag antibody and GFP-Odam was detected by immunofluorescence. Scale bar: 20 μm.

4. Odam mediated RhoA signaling in ameloblasts and JE

GEFs-activated RhoA regulates downstream effectors, including Rho-associated kinase (Rock) and myosin [78]. To investigate the effects of Odam on RhoA signaling during amelogenesis, I examined the expression levels of RhoA downstream factors, including Rock, p-myosin, p-paxillin, and E-cadherin. *Odam* overexpression increased the phosphorylation activity of RhoA, myosin, and paxillin, as well as the expression of Rock and E-cadherin, whereas siRNA-mediated *Odam* inactivation decreased their activity and expression (Fig. 15A). However, the total expression of RhoA and paxillin were unaffected by *Odam* overexpression or inactivation. RhoA signaling was robust in *Odam*-, *Arhgef5*-, and active *RhoA*-expressing ALCs, but inhibited after siRNA-mediated *Odam* inactivation (Fig. 15B). To map the Odam functional domain that was required for RhoA activation with *Arhgef5*, I performed RhoA activity assay using *Odam* deletion constructs. RhoA activation demonstrated that deletion of the C-terminal region of *Odam* (amino acids 127–279) affected RhoA activation with *Arhgef5* (Fig. 15C). This result suggests that the C-terminal domain containing the amino acids 127–279 region of *Odam* is necessary for activation of RhoA signaling with *Arhgef5*. Confocal microscopy showed that Flag-tagged Odam and GFP-tagged RhoA proteins primarily co-localized to the cell periphery of ALCs (Fig. 15D). These data suggest that Arhgef5-Odam mediates activation of RhoA signaling in ameloblasts and JE.

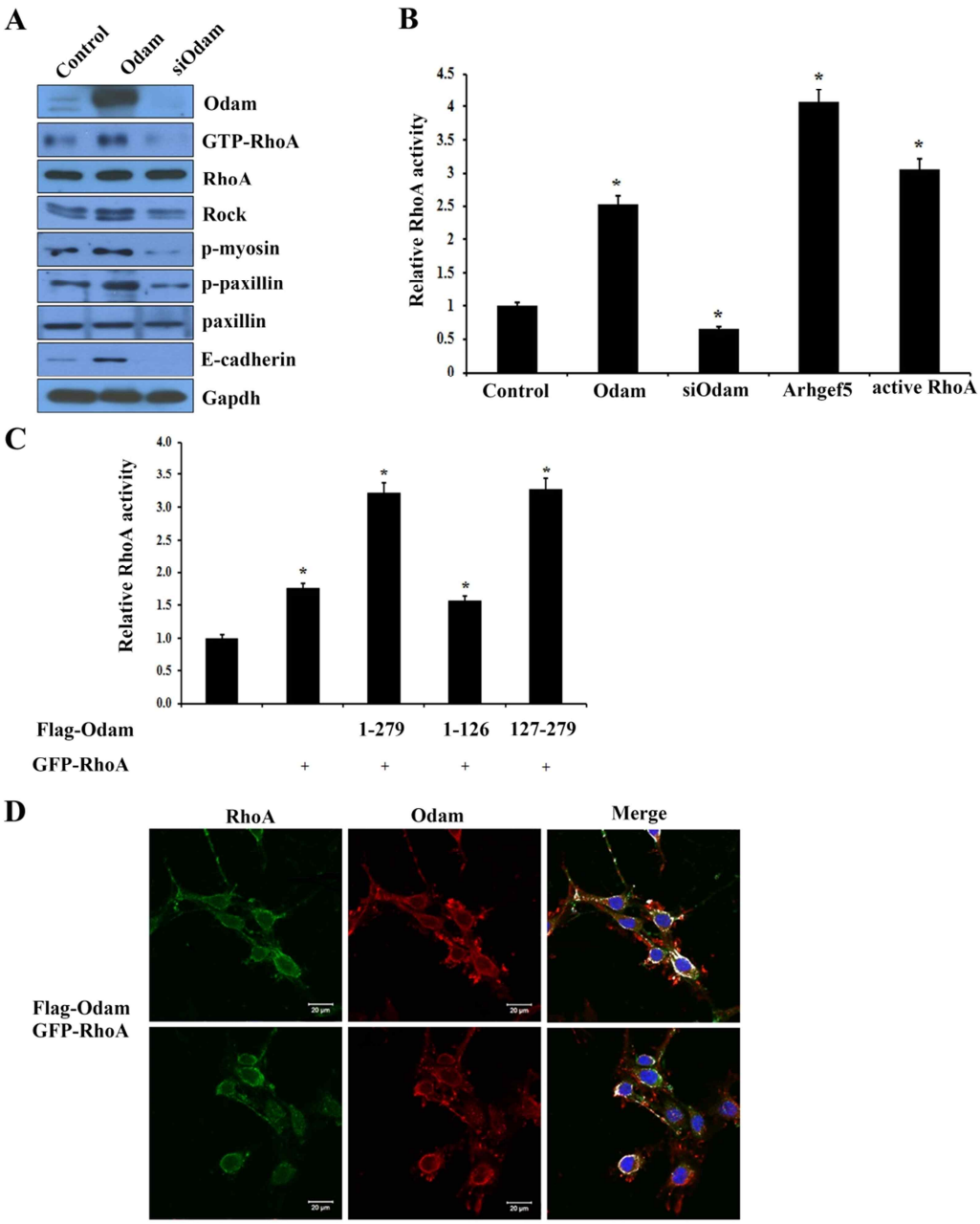

Figure 15. Odam induced RhoA signaling pathway in ameloblasts.

(A) ALCs were transfected with *Odam* or *Odam*-siRNA constructs. RhoA signaling components expression was analyzed by western blot. (B) ALCs were transfected with *Odam*, *Odam*-siRNA, *Arhgef5*, or active *RhoA* constructs. Equal amounts of cell lysates were used for G-LISA RhoA activation assays. (C) Mapping the Odam domain required for RhoA activation with Arhgef5. Flag-*Odam* mutants were expressed in ALCs transfected with the Arhgef5 construct. RhoA activity was determined by G-LISA RhoA activation assays. Data are the mean ± SD of triplicate experiments. *denotes values significantly different from the control ($p<0.05$). (D) Flag-tagged *Odam* and GFP-tagged *RhoA* constructs were transfected into ALCs. Exogenous Odam was immunostained using the anti-Flag antibody and GFP-RhoA was detected by immunofluorescence. Nuclei were stained with DAPI. Scale bar: 20 μm.

5. Odam-mediated RhoA signaling resulted in cytoskeleton reorganization in ameloblasts

As the cell reorganizes from a short epithelial cell to a secretory ameloblast, to a shorter cell able to alter its apical surface, and finally to a protective ameloblast, the actin cytoskeleton must continuously reorganize [79, 80]. To investigate whether Odam could affect F-actin distribution, I cultured ALCs for 24h on rOdam- or collagen-coated slides and examined ODAM and F-actin expression. Cells cultured on rOdam protein showed a greater density of F-actin filaments at the cell periphery compared to cells cultured on collagen (Fig. 16A). To confirm the effects of Odam on RhoA activation, I examined the activation levels of RhoA using G-LISA RhoA activation assay after rOdam treatment. RhoA signaling was powerful in rOdam-treated and active *RhoA*-expressing ALCs compared to control (Fig. 16B).

Next, I evaluated subcellular alterations in F-actin after exogenous *Odam* expression in ameloblasts. Confocal microscopy showed specific localization of GFP-tagged Odam in the nucleus and cytoplasm of ALCs and F-actin accumulated at the cell edge compared with control (Fig. 16C). To determine which functional domain of Odam is responsible for actin rearrangement and cell shape, several *Odam* deletion mutants were generated, and cells were examined using immunofluorescence analyses. *Odam* and *RhoA* overexpression resulted in a greater density of F-actin filaments at the cell periphery compared to cells transfected with *Odam* siRNA construct or treated with Rock inhibitor (Y-27632) (Fig. 16D). I also investigated whether Odam could affect the adhesion of ameloblasts to the substrate by adhesion assay. Odam- and Collagen-coated ALCs

exhibited significantly increased cell adhesion compared to control (Fig. 16E). These results suggest that Odam-mediated RhoA signaling resulted in actin filament rearrangement at the cell periphery of ameloblasts with promotion of cell adhesion.

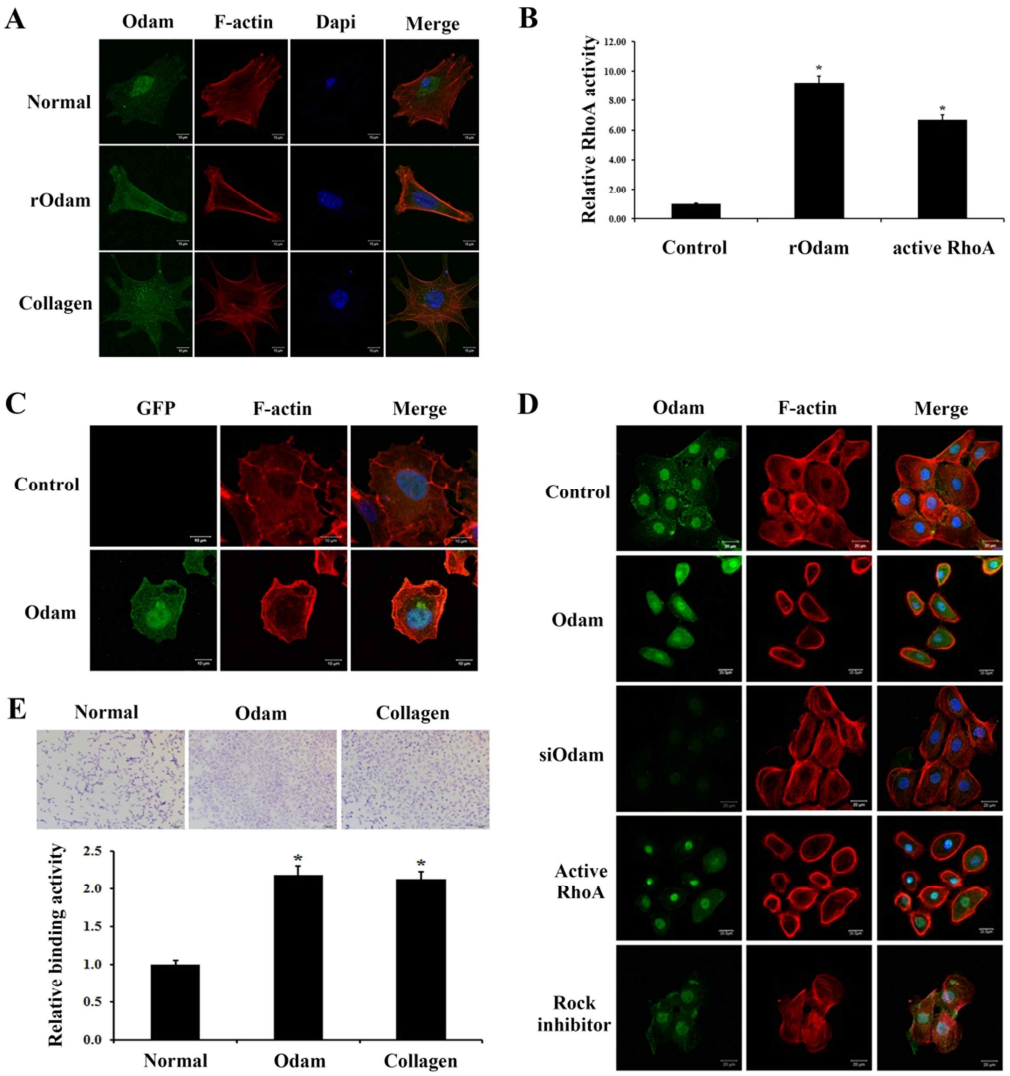

Figure 16. Odam induced actin rearrangement in ameloblasts via RhoA signaling.

(A) Cells were cultured on rOdam- or collagen-coated slides for 24 h. Fixed cells were treated with rhodamine-phalloidin to examine actin filaments rearrangement using confocal laser microscopy (red). Odam localization was investigated by

immunofluorescence. Scale bar: 10 μm. (B) ALCs were treated with rOdam or transfected with active *RhoA* constructs. Equal amounts of cell lysates were used for G-LISA RhoA activation assay. (C) ALCs were transfected with *Odam*, and rhodamine-phalloidin was used to examine the arrangement of actin filaments (red). Scale bar: 10 μm. (D) *Odam*, *Odam*-siRNA, or active *RhoA* constructs were transfected into ALCs. Rock inhibitor (Y-27632) was treated into ALCs. Rhodamine-phalloidin was used to examine the arrangement of actin filaments (red). Odam localization was investigated by immunofluorescence. Scale bar: 20 μm. (E) Adhesion of ALCs to rOdam- or Collagen-coated slides. Binding values are based on the absorbance of adherent cells. Data are presented as the mean ± SD of triplicate experiments. *denotes values significantly different from control ($p<0.05$).

6. Integrin-mediated Odam expression induced RhoA signaling

Integrin β_3 is requires for proper growth of the cervical loop, the promotion of the proliferation of preameloblastic cells, and iron transportation during enamel formation [81, 82]. *Integrin* $\beta_3^{-/-}$ mice exhibited shorter lower incisor, similar with *integrin* $\beta_6^{-/-}$ mice have severe attrition and an abnormal enamel surface [82, 83]. To examine whether integrin could affect Odam and RhoA expression in ameloblasts, I immunohistochemically analyzed *integrin* $\beta_3^{-/-}$mice. In the incisor, Odam was strongly expressed in maturation-stage ameloblasts of wild type (WT) mice but its expression was reduced in *integrin* $\beta_3^{-/-}$ mice (Fig. 17A). Interestingly, WT JE was strongly immunolabeled with the Odam antibody but was hardly expressed in JE of *integrin* $\beta_3^{-/-}$ mice (Fig. 17B). In order to investigate whether integrin β_3 disruption also affects the expression of GTP-RhoA in ameloblasts, I performed immunostaining in the molar tooth of WT or *integrin* $\beta_3^{-/-}$ mice. In *integrin* $\beta_3^{-/-}$ mice, ameloblasts showed little immunoreactivity with the GTP-RhoA antibody. In contrast, WT ameloblasts showed strong GTP-RhoA expression (Fig. 17C).

Integrin $\alpha_v\beta_6$ is expressed in ameloblasts and it plays a crucial role regulating amelogenin deposition and/or turnover and subsequent enamel biomineralization [83]. I analyzed GEO data using alveolar macrophages in *integrin* $\beta_6^{-/-}$ mice. Odam and RhoA expression were significantly decreased in alveolar macrophages of *integrin* $\beta_6^{-/-}$ mice compared with WT mice (Fig. 17D).

When RhoA is activated, Rock increases actin stress-fiber formation [84]. I examined

the effects of integrin β_3 disruption on actin arrangement in ameloblasts from 9-week-old WT and *integrin* $\beta_3^{-/-}$ mice incisors. In WT incisors, F-actin was distributed throughout the cytoplasm of ameloblasts and was concentrated at both the apical and basal ends. However, in *integrin* $\beta_3^{-/-}$ incisors, F-actin was weakly and diffusely detected in ameloblasts without polarity (Fig. 17E). Overall, these data indicated that integrin β_3 and β_6 expression is important for cytoskeleton reorganization via integrin-Odam-Arhgef5-RhoA signaling in ameloblasts and JE.

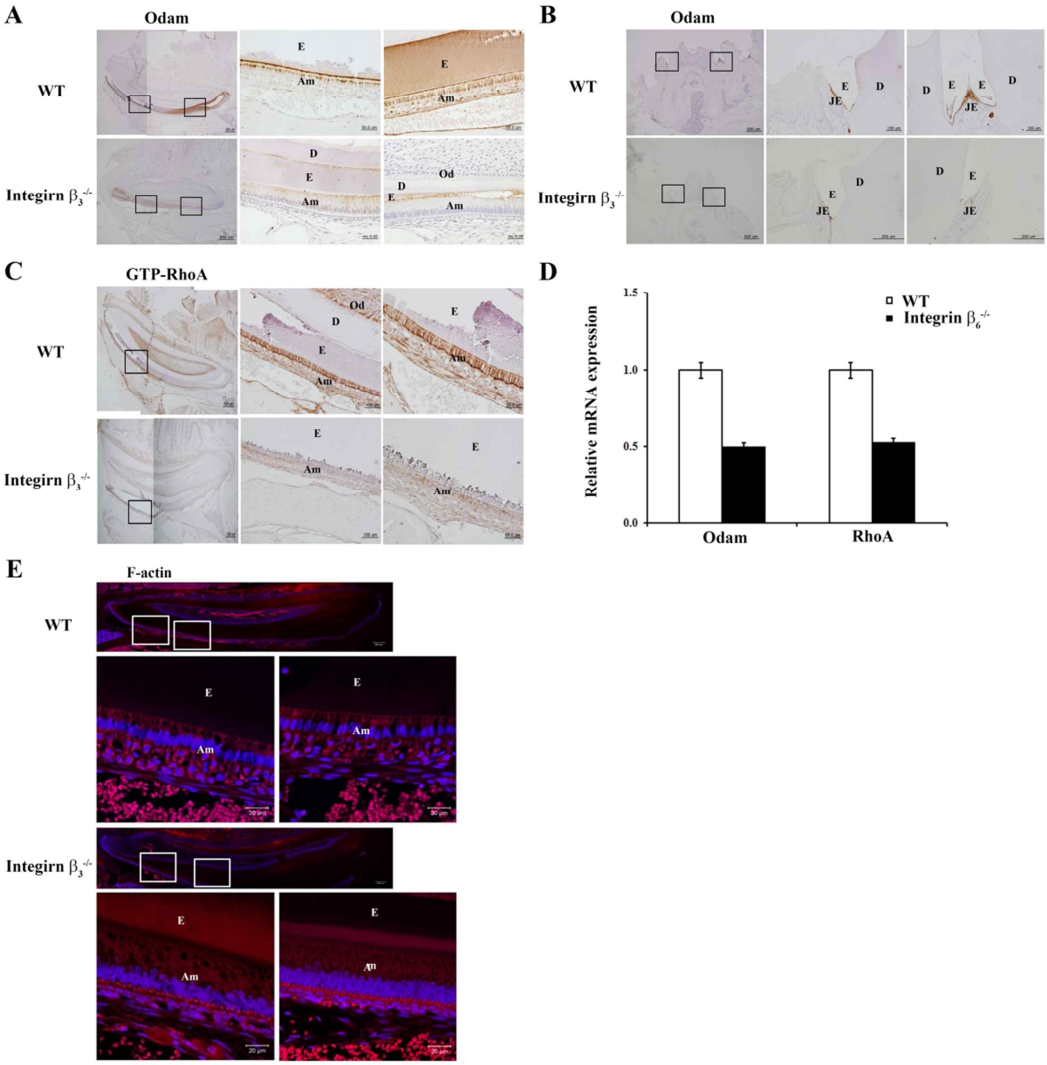

Figure 17. Integrin β3 depletion diminishes Odam, Arhgef5, and RhoA expression in ameloblasts and JE.

Tooth sections from *integrin* $\beta_3^{-/-}$ mice were evaluated. (A-C) Odam (panels A, B) and GTP-RhoA (panel C) protein expression was detected in ameloblasts and JE from WT and *integrin* $\beta_3^{-/-}$ mice aged 9 weeks by immunohistochemistry (n = 3 per group). Scale

bar: 500, 200, 100, or 50 μm. E: enamel, Am: ameloblast, D: dentin, Od: odontoblast, JE: junctional epithelium. (D) *Odam* and *RhoA* mRNA expression was analyzed from gene expression dataset GSE2255 deposited in GEO (n = 5). (E) F-actin expression was detected by immunofluorescence in teeth and JE of WT and *integrin* $\beta_3^{-/-}$ mice aged 9 weeks. Scale bar: 20 μm.

7. Fibronectin and laminin activated integrin-mediated Odam signaling

Fibronectin and laminin, which are components of the basement membrane, participate in the proliferation, differentiation, and attachment of preameloblasts and JE [85-88]. In addition, integrins associated with the cytoskeletal proteins, fibronectin and laminin, regulate cellular processes such as cell adhesion and differentiation [89]. To examine whether fibronectin and laminin could induce Odam-RhoA signaling via integrin, I investigated Odam and RhoA expression in ameloblastic HAT7 cells after fibronectin or laminin treatment by western blot. The expression levels of Odam, RhoA, and active RhoA were increased in HAT7 cells treated with fibronectin and laminin compared to control (Fig. 18A). To investigate whether fibronectin or laminin could induce the localization and expression of Odam and F-actin, I cultured HAT7 cells with fibronectin or laminin and then evaluated Odam and F-actin expression by western blot and immunofluorescence. Cytoplasmic Odam expression in HAT7 cells was significantly increased by fibronectin and laminin treatment, but nuclear Odam was slightly decreased (Fig. 18B). Cytoplasmic Odam expression was more intensive in fibronectin- or laminin-treated HAT7 cells than in control cells. Fibronectin- or laminin-treated cells showed a nearly complete disappearance of central actin stress fibers with a transition to circumferential actin cables (Fig. 18C).

The lack of integrin β_6 and β_1 could contribute to the periodontal phenotype [72]. I examined the effects of integrin β_6 and β_1 disruption in JE. In ameloblasts, increased ODAM expression by fibronectin or laminin was reversible by the addition of *integrin* β_6 or β_1 siRNA (Fig. 18D). To confirm RhoA activation in these conditions, I investigated

RhoA activity in ameloblasts. Surprisingly, RhoA signaling was robust in fibronectin- or laminin-treated ameloblasts similar with *Odam*-expressing cells, but inhibited by siRNA-mediated *integrin* inactivation (Fig. 18E). To confirm whether Odam could be regulated by fibronectin or laminin-integrin signaling, I investigated RhoA activity after fibronectin or laminin treatment and then *Odam* siRNA transfection. Odam, GTP-RhoA, and ROCK expression were increased by fibronectin and were reversible by the addition of *Odam* siRNA (Fig. 18F). In addition, RhoA activity was enhanced by fibronectin or laminin, but inhibited by siRNA-mediated *Odam* inactivation (Fig. 18G). These results indicate that fibronectin and laminin activated RhoA signaling, resulting in actin reorganization via integrin-mediated Odam signaling.

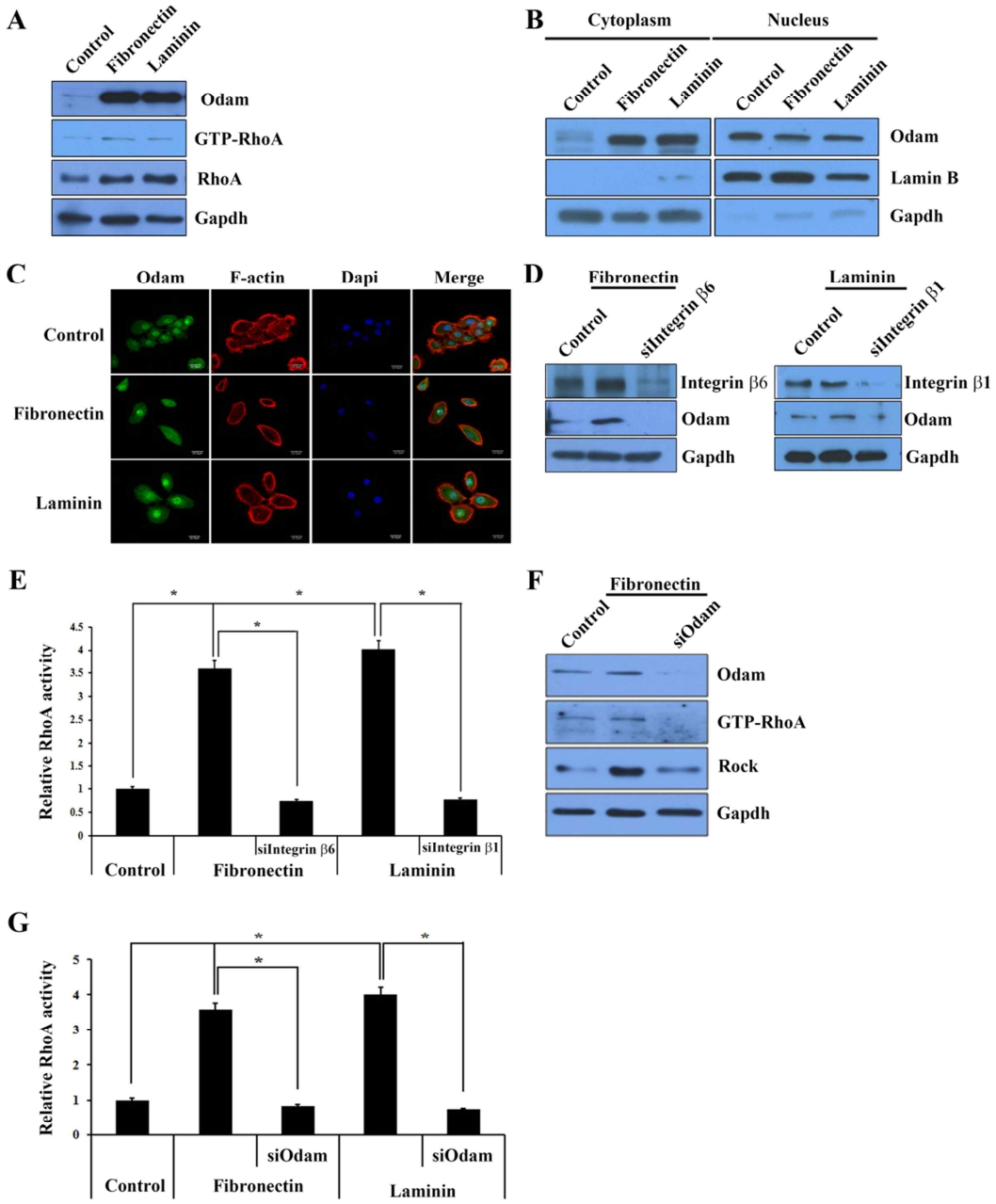

Figure 18. Fibronectin and laminin activated integrin-Odam signaling.

(A) Odam and GTP-RhoA protein expression were evaluated in ameloblastic HAT7 cells

after fibronectin or laminin treatment by western blot. (B) Effect of fibronectin and laminin on Odam expression and localization in HAT7 cells by western blot. (C) Immunofluorescence staining of Odam (green) and F-actin (red) in HAT7 cells after fibronectin or laminin treatment. Scale bar: 20 μm. (D) Odam expression levels were evaluated in ALCs by western blot transfected with *integrin* β_6- or β_1-siRNA for 48 hours after fibronectin or laminin treatment. (E) ALCs were treated with fibronectin or laminin and then transfected with *integrin* β_6- or β_1-siRNA. Equal amounts of cell lysates were used for the G-LISA RhoA activation assay. (F) Odam, GTP-RhoA, and Rock expression levels were evaluated in ALCs by western blot transfected with *Odam* siRNA for 48 hours after fibronectin treatment. (G) ALCs were treated with fibronectin or laminin and then transfected with *Odam* siRNA. Equal amounts of cell lysates were used for the G-LISA RhoA activation assay.

8. Odam was re-expressed in regenerating JE after gingivectomy in vivo or mechanical scratch in vitro

Odam expression decreased and subsequently disappeared at damaged JE and epithelial cell rests of Malassez (ERM) after gingival excision [18, 20, 69]. Consistent with these results, during JE regeneration at day 5 after gingivectomy, Odam was re-expressed in cells at the leading wound edge of the oral epithelium. Immunoreactive cell clusters were also found in the subjacent connective tissue. On day7, Odam was present in the regenerating JE at the tooth interface (Fig. 19A). GTP-RhoA showed a similar expression pattern in regenerating JE after gingivectomy (Fig. 19B). In addition, damaged cells by scratch secreted Odam immediately to the extracellular matrix. However, when the scratch wound healed, Odam was apparently localized to the cell as well as the extracellular matrix (Fig. 19C). These results suggest that intracellular Odam expression is important for the maintenance of JE attachment to tooth.

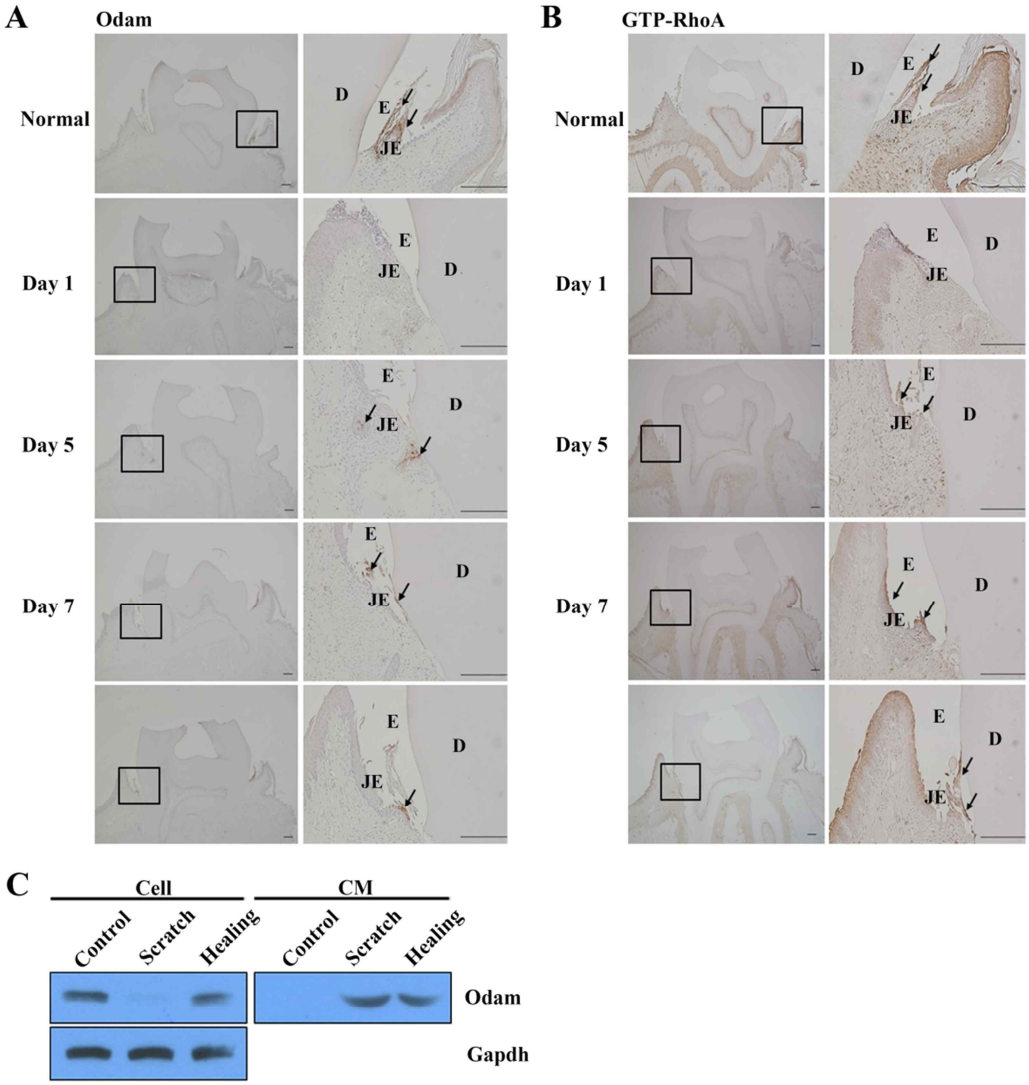

Figure 19. Odam was re-expressed in regenerating JE after gingivectomy.

(A, B) Odam (A, arrows) and GTP-RhoA (B, arrows) expression on days 1, 5, and 7 after gingivectomy in regenerating mouse JE by immunohistochemistry (n = 2 per group). Scale bar: 200 μm. E: enamel, JE: junctional epithelium, D: dentin. (C) Odam expression

was evaluated by western blot in cultured ALCs after scratch wounds.

V. DISCUSSION

Periodontal diseases are chronic inflammatory processes that affect more than one-third of the adult population and can lead to tooth loss and financial burden [90]. Of utmost importance for maintaining gingival and periodontal health are their defense mechanisms, particularly at the dentoepithelial level. JE, a critical tissue barrier, plays an important role in the formation of epithelial attachment, adhesion of gingiva to the tooth enamel surface, consisting of an internal basal lamina (BL) and hemidesmosomes [5, 6]. Peri-implantitis is a key factor responsible for implant failure [91]. The attachment of peri-implant epithelium to the titanium surface is similar to the mechanism by which JE cells connect to the natural tooth [92]. Peri-implant epithelium is attached to the implant via the internal BL and hemidesmosomes in the lower region of the peri-implant epithelium–implant interface. New findings presented in our paper demonstrate that ODAM function during JE development and regeneration, as well as its functional significance in the initiation and progression of periodontitis and peri-implantitis.

The BL of the JE and peri-implant epithelium is atypical because it constitutively expresses laminin, which contributes to epithelial cell adhesion [93, 94]. It is well known that the regenerative JE after gingivectomy is derived from the oral epithelium and JE maturation is induced by epithelial cell attachment to the tooth surface [95]. Immediately after gingivectomy, laminin expression transiently disappeared in the residual tissues [96, 97]. However, when the newly-formed JE had attached to the enamel surface, laminin 2 expression was apparent at the internal BL close to the cementoenamel junction, whereas its expression in connective tissue was reduced [98]. In the present study, laminin

activated RhoA signaling, resulting in actin reorganization via integrin-mediated Odam signaling. After gingivectomy, Odam expression transiently disappeared but re-expressed upon JE regeneration. Taken together, I suggest that laminin mediates the attachment of JE cells to the internal BL in normal dentogingival junctions and implant-tooth interface but not in those of inflammatory conditions such as periodontitis and peri-implantitis.

Fibronectin is important for cell adhesion, migration, and differentiation, and functions during wound healing by attracting macrophages and other immune cells to the injured area [99]. In tooth morphogenesis, fibronectin is synthesized in the dental papilla [100]. Fibronectin is associated with the basement membrane separating differentiating ameloblasts and odontoblasts and further data indicate that this protein is predominantly associated with the filaments of its lamina fibroreticularis [101]. In addition, fibronectin is found in the extracellular matrix of periodontium, cartilage, plasma, fibroblasts, as well as epithelial and endothelial cells, and plays a fundamental role in the early stages of healing, promoting cellular migration, and tissue regeneration after periodontal treatment [102, 103]. Compared to specific laminin expression in internal BL, fibronectin was constitutively expressed in the external BL adjacent to connective tissue [104, 105]. In the present study, fibronectin activated integrin-Odam-Arhgef5-mediated RhoA signaling, which resulted in cytoskeleton reorganization. These results suggest that fibronectin mediates the attachment of JE cells to the external BL in direct contact with the subepithelial connective tissue.

A significant increase in fibronectin and laminin, and vitronectin expression was found in human PDL from teeth treated with orthodontic force for 3 weeks. This result suggests

that over expression of fibronectin and laminin caused Odam re-expression in regenerating JE after orthodontic tooth movement [106]. Apical migration of JE often occurs in association with periodontal inflammation. Laminin was not detected at the migrating tip of JE [104]. However, fibronectin was demonstrated at the migrating tip of epithelial cells in inflammatory periodontium. Therefore, it was suggested that fibronectin in the subepithelial connective tissue at the apical tip of migrating epithelium could act as the trigger of cellular migration [105]. In the present study, in inflammatory periodontium, ODAM disappeared in pathologic pocket epithelium but was detected in GCF. These results suggest that fibronectin in the subepithelial connective tissue induced integrin-mediated Odam production from migrating epithelial cells. However, although migrating epithelial cells secrete ODAM, the protein was not detected in epithelial cells but in GCF because migrating epithelial cells cannot attach properly to the tooth surface. In addition, the ODAM protein was expressed in GCF from periodontitis and peri-implantitis patients and correlated with probing depth in periodontitis patients. Therefore, I propose ODAM in GCF could be used as a protein biomarker for periodontitis and peri-implantitis diagnosis.

Integrins play key roles in tooth development because several integrins, including α_6, α_v, β_1, β_3, β_4, β_5, and β_6 integrin subunits, are expressed in the dental epithelium [107, 108]. Integrin $\alpha_v\beta_6$ is part of the attachment apparatus in the JE that mediates adhesion of the gingival soft tissue to laminin-332 at the enamel interphase of the tooth [70]. In the present study, Odam was not expressed in JE of *integrin* $\beta_3^{-/-}$ mice. There was significantly reduced expression of Arhgef5, RhoA, and activated RhoA in *integrin* $\beta_3^{-/-}$

and $\beta_6^{-/-}$ mice. Our results suggest that integrin $\alpha_v\beta_3$ and $\alpha_v\beta_6$ are targets of the Odam-Arhgef5-RhoA signaling pathway and plays a significant role in tooth-cell adhesion and actin rearrangement during amelogenesis and JE formation.

In summary, I provided experimental evidence for the developmental mechanism of oral epithelial cells such as ameloblasts and JE that attach to the tooth, the mechanism of new attachment occurring after periodontal surgery, and the formation of peri-implant tissue healing in the clinic. Identifying the precise role of ODAM expression in regenerating JE should help clinicians provide better periodontal care for patients.

CHAPTER V.

ODAM inhibits breast cancer invasion and metastasis through activation of RhoA signaling

* This Chapter has been largely reproduced from an article published by Lee HK. and Park JC. (2015). Cell biochemistry & function, in press.

I. ABSTRACT

Odontogenic ameloblast-associated protein (ODAM) contributes to cell adhesion. In human cancer, ODAM is down-regulated and results in a favorable prognosis; however, the molecular mechanisms underlying ODAM-mediated inhibition of cancer invasion and metastasis remain unclear. Here, we identify a critical role for ODAM in inducing cancer cell adhesion. ODAM induced RhoA activity and the expression of downstream factors, including Rho-associated kinase (ROCK). ODAM-mediated RhoA signaling resulted in actin filament rearrangement by activating PTEN and inhibiting the phosphorylation of AKT. When ODAM is overexpressed in MCF7 breast cancer cells and AGS gastric cancer cells that activate RhoA at high levels, it decreases motility, increases adhesion, and inhibits the metastasis of MCF7 cells. Conversely, depletion of ODAM in cancer cells inhibits Rho GTPase activation, resulting in increased cancer migration and invasion. These results suggest that ODAM expression in cells maintains their adhesion, resulting in the prevention of their metastasis via the regulation of RhoA signaling in breast cancer cells.

II. INTRODUCTION

Breast cancer represents the first most frequent cancer, and the ratio of mortality to incidence is about 29% in women [109]. Metastasis at distant sites is the principal cause of death among breast cancer patients, being responsible for approximately 26% of deaths from this malignant disease [110, 111].

Odontogenic ameloblast-associated protein (ODAM), the protein product of a gene involved in tooth development is expressed in certain human epithelial neoplasms, including breast cancer [11, 12]. Notably, this molecule appeared to serve as a novel, favorable prognostic biomarker of malignancy, as demonstrated by the finding of a statistically significant correlation between the presence of ODAM and an improved 5-year survival of patients [24]. ODAM overexpression in MDA-MB-231breast cancer cells resulted in the inhibition of neoplastic and metastatic properties [23]. Additionally, a significant correlation was found between ODAM expression/nuclear localization and sentinel lymph node metastases indicative of poorer prognosis in melanoma [28]. These findings suggest that ODAM has a potentially significant role in regulating tumorigenesis and metastasis in breast cancer with possible clinical implications. However, the molecular mechanisms underlying ODAM-mediated inhibition of cancer metastasis and promotion of a favorable prognosis remain unclear.

Odam has been implicated in diverse activities such as enamel maturation, formation and regeneration of the junctional epithelium (JE), and tumorigenesis [12, 14, 23, 68]. Odam is expressed in maturation stage ameloblasts and normal

JE but is reduced after JE damage [7, 15, 18, 20, 69]. ODAM plays roles in enamel formation and mineralization during amelogenesis [11, 14, 16]. In our previous paper, we found that Odam induces RhoA activity and the expression of downstream factors by interacting with Arhgef5. Odam-mediated RhoA signaling results in actin filament rearrangement and enhancement of cell adhesion [112]. Although RhoA signaling pathway plays a role in the invasion of MDA-MB231 cells [113], which was not expressed ODAM in cell compartment [27], it has been also known that the inhibition of RhoA signaling pathway could induced the invasion of less-invasive breast cancer cells (MCF7), which was expressed ODAM [114]. However, the cancer inhibition by ODAM and RhoA in breast cancer cells has not yet been established. Therefore, it was evaluated the function of ODAM by interacting with RhoA in MCF7 cells because ODAM and RhoA were expressed in MCF7 and SK-BR-3 cells unlike MDA-MB231 cells and they induced cell adhesion in ameloblasts.

Cell motility, which is essential for metastasis, is a complex, multistep process that integrates multiple intracellular signaling and regulatory pathways [115]. Almost all aspects of tumor cell proliferation, motility, and invasion, including cellular polarity, cytoskeletal re-organization, and signal transduction pathways, are controlled through the interplay between the Rho-GTPases [116, 117]. The variations in the levels of Rho proteins directly correlate with the advancement of breast cancer [118, 119]. Our previous report demonstrated that Odam regulates RhoA signaling in oral epithelial cells [120].

However, the precise functions of ODAM-RhoA signaling, a key regulator of cell adhesion and motility in cancer cells, remain unclear. In this study, I further investigated the roles of ODAM in the migration and invasion of cancer cells *in vitro* and *in vivo*.

III. MATERIALS AND METHODS

1. Plasmids, reagents, and antibodies

Expression vectors encoding DDK (Flag)-tagged human ODAM and ODAM short hairpin RNA (shRNA) were purchased from Origene. Anti-ODAM antibody was generated in rabbits by immunization with ODAM peptides [16]. Anti-RhoA, F-actin, GAPDH, ROCK, horseradish peroxidase (HRP)-conjugated goat anti-mouse, HRP-conjugated goat anti-rabbit-IgG, and HRP-conjugated rabbit anti-goat-IgG antibodies were purchased from Santa Cruz Biotechnology. Anti-RhoA, ROCK, p-AKT, AKT, p-PTEN, PTEN, E-cadherin, and β-catenin antibodies were obtained from Cell Signaling. Anti-GTP-RhoA antibody was purchased from Biosource. Anti-Arhgef5 was obtained from Proteintech Group. Anti-Flag antibody was from Sigma-Aldrich. Alexa Fluor® 488 Phalloidin (Rhodaminephalloidin) antibody was obtained from Invitrogen. Anti-fluorescein isothiocyanate (FITC) or Cy3-conjugated anti-mouse, -rabbit, or -goat IgG antibody was purchased from Life Technologies.

2. Tissue preparation and immunohistochemistry

All experiments involving human cell lines were performed according to the Dental Research Institute guidelines and Institutional Animal Care and Use Committees of Seoul National University (SNU-111013-3). The experimental protocol was also approved by the Seoul National University's Institutional Review Board (S-D2011001). Malignant human tissue blocks were obtained retrospectively from the Seoul National University Hospital archive (Seoul, Korea) and Seoul National University Dental Hospital archive

(Seoul, Korea). Mouse bone blocks from metastatic breast cancer were provided by Dr. Zang Hee Lee (Seoul National University, Seoul, Korea). Sections were incubated overnight at 4°C with anti-ODAM or GTP-RhoA antibody as the primary antibody (dilutions of 1:100–1:200). Secondary anti-rabbit or mouse antibody was added to the sections for 30 minutes at room temperature, and then the sections were reacted with the avidin-biotin-peroxidase complex (Vector Laboratories). Signals were converted using a diaminobenzidine kit (Vector Laboratories). Nuclei were stained with hematoxylin.

3. Cell culture and transfection

MCF7, SK-BR-3, and MDA-MB231 cells (breast adenocarcinoma cells; ATCC) were grown and maintained in RPMI (Gibco BRL) supplemented with 10% FBS and antibiotics in a 5% CO_2 atmosphere at 37°C. The immortalized human mammary epithelial cell line MCF10A (ATCC) was cultured in complete MCF10A growth media, composed of DMEM/nutrient mixture F12 (DMEM/F12; Gibco BRL) supplemented with 5% fetal calf serum, 20 ng/ml EGF, 10 mg/ml insulin, 0.5 mg/ml hydrocortisone, and 100 ng/ml cholera toxin (Sigma-Aldrich). AGS cells (gastric adenocarcinoma, non-invasive cancer cells; ATCC) were grown and maintained in DMEM supplemented with 10% FBS and antibiotics.

MCF-10A, MCF7, SK-BR-3, MDA-MB231, or AGS cells were seeded in culture plates. Cells were transiently transfected with plasmid DNA using Metafectene PRO reagent (Biontex).

4. Western blotting

To prepare whole cell extracts, cells were washed three times with PBS, scraped into 1.5-ml tubes, and pelleted by centrifugation at 12,000 rpm for 2 minutes at 4°C. After the removal of the supernatant, pellets were suspended in lysis buffer [50 mM Tris-Cl (pH 7.4), 150 mM NaCl, 1% NP-40, 2 mM EDTA (pH 7.4)] and incubated for 15 minutes on ice. Cell debris was removed by centrifugation. Proteins (30 μg) were separated by 10% SDS-polyacrylamide gel electrophoresis and transferred to nitrocellulose membranes (Schleicher & Schuell BioScience, Dassel, Germany). Membranes were blocked for 1 hour with 5% nonfat dry milk in PBS containing 0.1% Tween 20 (PBS-T), and incubated overnight at 4°C with the primary antibody diluted in PBS-T buffer (1:1000). After washing, membranes were incubated for 1 hour with secondary antibodies. Labeled protein bands were detected using an enhanced chemiluminescence system (Dogen).

5. RhoA activity assay

The level of GTP-loaded RhoA was determined using the G-LISA RhoA activation assay kit (Cytoskeleton) according to the manufacturer's instructions. Because the expression level of RhoA varied depending on the type of substrate, equal amounts of proteins from each experimental group were used in the G-LISA RhoA activation assay to obtain values for the total amount of RhoA activity per cell.

6. Fluorescence microscopy

Cells on Laboratory-Tek chamber slides (Nunc) were washed with PBS, fixed for 10

minutes at room temperature with 4% paraformaldehyde in PBS, and permeabilized for 5 minutes in PBS containing 0.5% Triton X-100. After washing and blocking, cells were incubated for 1 hour with anti-ODAM (1:200) and Alexa Fluor® 488 Phalloidin antibodies in blocking buffer (PBS and 1% bovine serum albumin), followed by the addition of anti-FITC or Cy3-conjugated anti-rabbit IgG antibodies (1:200). After washing, cells were visualized using fluorescence microscopy (AX70; Olympus Optical Co). Chromosomal DNA in the nucleus was stained using DAPI.

7. Adhesion assay

Stable cells expressing *ODAM* or *ODAM shRNA* were seeded in 96-well plates and incubated for 4 hours. At the indicated times, plates were washed twice with PBS. Cells were fixed with 4% paraformaldehyde for 30 minutes, stained with crystal violet for 10 minutes, followed by the addition of Tween 20 for 30 minutes. Finally, we measured the OD at 595 nm.

8. Wound healing assay

After 24 hours of *ODAM* or *ODAM shRNA* transfection, cells were harvested, seeded in 6-well plates, and cultured until confluent. We used 200-μl pipette tips to make a straight scratch, simulating a wound. Cells were rinsed gently with PBS and cultured in fresh complete media. Cells were imaged using a 10× objective on a Leica DMLB microscope and acquired using QCapture Software (QImaging Software).

9. Invasion assay

Cell migration was analyzed using Transwell assays (Corning Inc., Corning, NY) with polycarbonate filters (pore size, 8 μm). Cells transfected with *ODAM* or *ODAM shRNA* were seeded in the upper chamber at a density of 1×10^5 cells/chamber in 100 μl of media. The lower chamber was filled with 600 μl of DMEM. Plates were incubated for 24 hours at 37°C, and cells in the upper chamber were carefully removed using a cotton swab. Migrated cells were fixed with 4% paraformaldehyde and stained with Hoechst trihydrochloride (1:5000; Invitrogen) for 10 minutes. The number of invading cells was counted using fluorescent microscopy. Four fields were randomly chosen, and the number of penetrated cells was counted.

10. Gene expression profiling

Gene expression profile data (GSE2429) were obtained from the National Center for Biotechnology Information Gene Expression Omnibus (NCBI GEO) database (http://www.ncbi.nlm.nih.gov/geo/). Publicly available gene expression datasets were downloaded from gene expression omnibus (GEO) (accession number GSE14938 to multiple normal tissues, GSE9574 and GSE20437 to breast cancer: histologically normal breast epithelium, GSE1299 to breast cancer cell expression profiles (HG-U133A), GSE35809 to an Australian patient cohort: gastric adenocarcinoma, GSE43346 to small cell lung cancers, and GSE3268 to squamous lung cancer), and ODAM and RhoA mRNA expression was analyzed using GEO data.

11. *In vivo* transfection of ODAM and histologic analysis

MCF7 cells and MDA-MB231 cells transfected with the *ODAM* construct and suspended in PBS containing 50% Matrigel were established and then were injected subcutaneously immunocompromised mice (BALB/c female mice). Four weeks later, the animals were euthanized, and the tumors were removed, fixed in formalin, embedded in paraffin blocks, and histologically examined.

12. Statistical analyses

All quantitative data are presented as the mean ± SD. Statistical differences were analyzed using Student's t-test (*, $p<0.05$).

IV. RESULTS

1. ODAM expression is decreased after tumorigenesis in normal tissues

ODAM was immunostained in dental epithelial cells of unerupted human tooth follicles and ameloblasts, tracheal gland, salivary gland, stomach, fetal lung, and bronchus [50]. To examine ODAM expression in human normal tissues, I analyzed microarray data from the NCBI GEO dataset. ODAM was expressed in the human adrenal gland, brain, cerebral cortex, colon, epididymis, kidney, lung, mammary gland, prostate, salivary gland, duodenum, ileum, stomach, thyroid, and trachea. Additionally, the expression levels of ODAM were stronger in the lung, mammary gland, prostate, salivary gland, stomach, thyroid, and trachea than in other tissues (Fig. 20A). Similarly, a search using the human protein atlas site (http://www.proteinatlas.org/ENSG00000109205-ODAM/tissue) showed a ubiquitous expression pattern of ODAM mRNAs in various human tissues (data not shown). To investigate the alteration of ODAM expression in breast, stomach, and lung cancer, I analyzed microarray data from the NCBI GEO dataset. ODAM mRNA expression was significantly decreased in breast cancer tissues and cell lines compared with normal breast epithelia (Fig. 20B). In addition, ODAM mRNA expression decreased in invasive gastric adenocarcinoma compared with that in metabolic gastric adenocarcinoma (Fig. 20C). Another GEO dataset showed that ODAM expression was significantly decreased in small cell lung cancer and squamous lung cancer tissues compared with that in normal tissues (Fig. 20D and E). However, ODAM expression remained in these cancer cells and was not completely eliminated. Immunohistochemistry data showed that ODAM

expression was detected overall in the normal mammary gland, stomach, and lung tissues of mice. However, compared with the overall expression in normal tissues, ODAM showed expression patterns at specific regions of benign but not malignant breast, stomach, and lung tumor tissues (Fig. 20F).

ODAM protein was detected in sera from late-stage breast cancer patients [50]. To assess whether the presence of ODAM in breast tumors has any physiologic relevance, I examined intracellular and extracellular ODAM protein expression in normal human breast epithelial cells (MCF10A), non-invasive breast cancer cells (MCF7 and SK-BR-3), and invasive breast cancer cells (MDA-MB231) by western blotting. Intracellular ODAM protein was expressed in normal and non-invasive cancer cells but was found to be expressed in the descending order of MCF10A, MCF7, and SK-BR-3 cells. However, ODAM expression was not detected in invasive MDA-MB231 cancer cells. On the other hand, extracellular ODAM protein was not observed in normal cells but was observed in MCF7, SK-BR-3, and MDA-MB231 cancer cells (Fig. 21A). These results suggest that intracellular ODAM reflects the invasiveness degree of breast cancer cells, while extracellular ODAM expression reflects their malignancy.

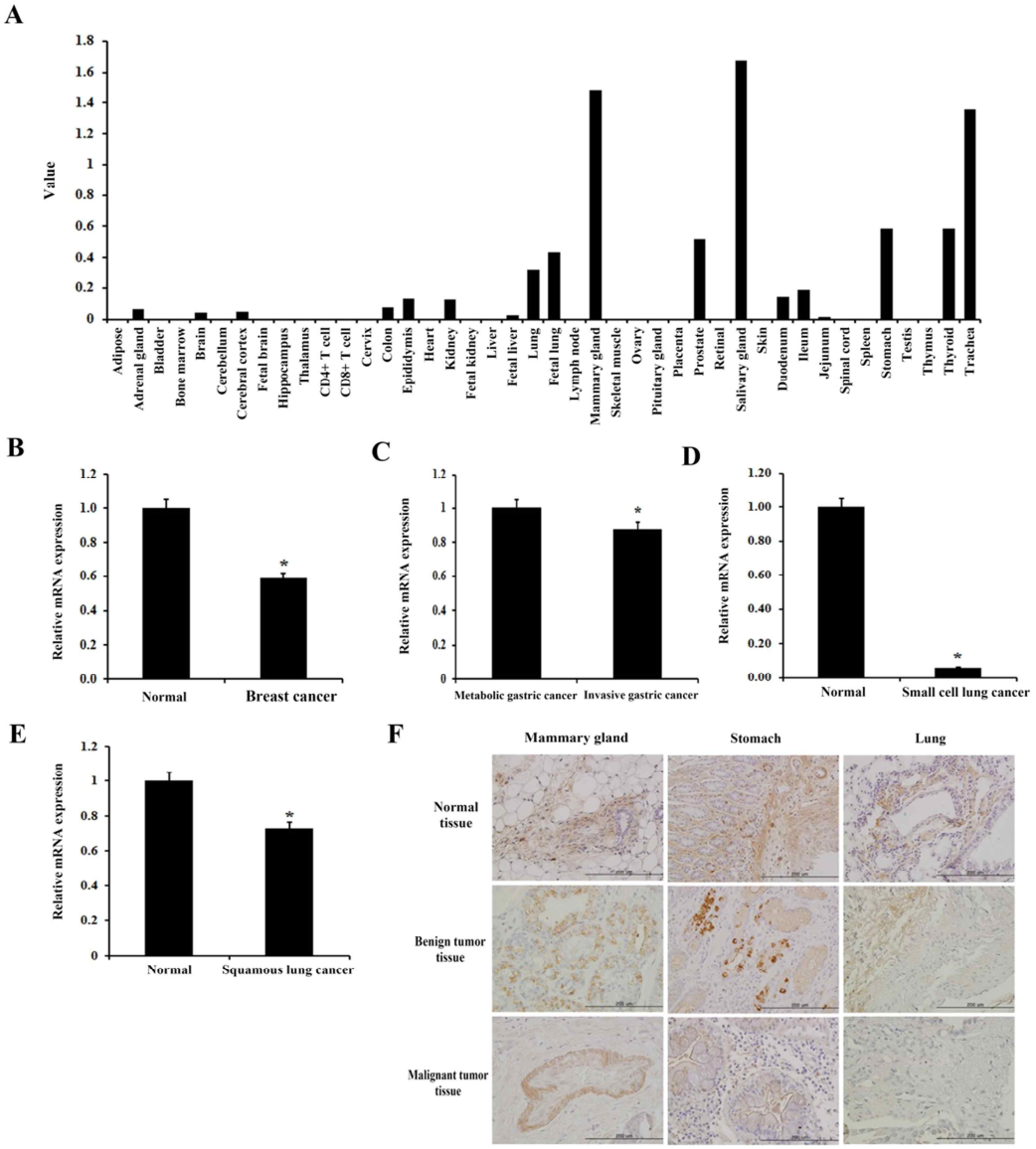

Figure 20. ODAM was expressed in normal and cancer tissues.

(A) Expression of *ODAM* mRNA is analyzed from the gene expression dataset GSE14938 (multiple normal tissues) deposited in GEO. (B-E) Expression of *ODAM*

mRNA is analyzed from gene expression datasets of breast cancer (GSE9574 and GSE20437), gastric cancer (GSE35809), and lung cancer (GSE43346 and GSE3268). (F) Immunohistochemistry indicates that ODAM is expressed in normal (upper panels) and cancer tissues (middle and bottom panels). Scale bar: 200 μm. * denotes values significantly different from the control (P<0.05).

2. ODAM interacts with ARHGEF5 and induces RhoA signaling in breast cancer cells

ODAM was expressed in normal or non-invasive cancer cells (Fig. 4), and related with cell adhesion (Fig. 16). Although RhoA signaling pathway plays a role in the invasion of MDA-MB231 cells [113], which do not express ODAM in cell compartment, the inhibition of RhoA signaling pathway could induced the invasion of non-invasive breast cancer cells (MCF7), which expressed ODAM [114]. The cellular ODAM, ARHGEF5, and RhoA were expressed in MCF7 and SK-BR-3 (Fig. 21A). Therefore, it was evaluated the function of ODAM by interacting with RhoA in MCF7 cells.

As expected, the expression of RhoA, and GTP-RhoA protein was similar to extracellular ODAM expression in MCF7, SK-BR-3, and MDA-MB231 cancer cells (Fig. 21A). In the previous paper, ODAM mediated RhoA signaling, resulting in cytoskeleton reorganization via the interaction with ARHGEF5 in ameloblasts [120].

To investigate the expression levels of RhoA and downstream factors by ODAM, it was examined the expression levels of RhoA and ROCK as a RhoA downstream factor. ODAM overexpression increased the expression of GTP-RhoA and ROCK, whereas ODAM inactivation by shRNA decreased their activity and expression (Fig. 21B). To examine the induction of RhoA activity by ODAM, it was performed RhoA activity assay experiments using *ODAM* and *ODAM shRNA* constructs. RhoA signaling was robust in ODAM-expressing MCF7 cells, but was inhibited after *shRNA*-mediated ODAM inactivation (Fig. 21C).

To confirm the alteration of RhoA expression in breast and lung cancer, it was analyzed

microarray data from the NCBI GEO dataset. RhoA expression was slightly decreased in breast cancer tissues compared with normal breast epithelium (Fig. 21D). Another GEO dataset showed that RhoA expression was significantly decreased in gastric cancer and lung cancer tissues compared with that in normal patients (Fig. 21E-F). I further investigated ODAM and GTP-RhoA expression in human breast cancer tissues by immunohistochemistry. ODAM and GTP-RhoA protein showed similar expression patterns in duct regions of benign breast cancer tissues (Fig. 21H). These data suggest that ODAM regulates RhoA signaling in breast cancer cells.

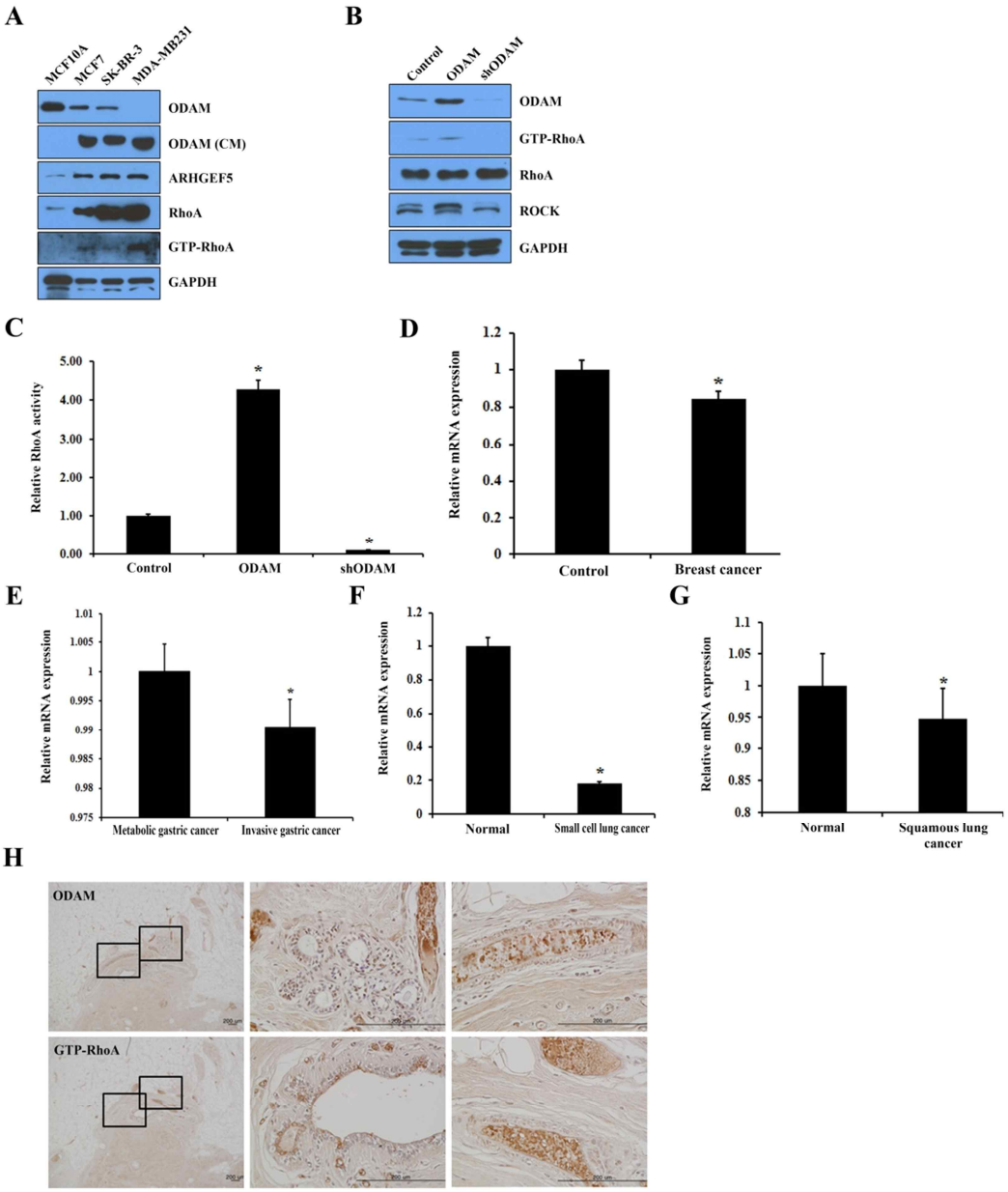

Figure 21. ODAM interacted with ARHGEF5 and induced RhoA signaling in breast cancer cells.

(A) The indicated cell lysates were analyzed by western blotting using antibodies against ODAM, ARHGEF5, RhoA, and GTP-RhoA in human MCF10A mammary epithelial cells, non-invasive MCF7 and SK-BR-3 breast cancer cells, and invasive MDA-MB231breast cancer cells. (B) MCF7 cells were transfected with *ODAM* or *ODAM shRNA* constructs. Expression of RhoA signaling components was analyzed by western blotting. (C) MCF7 cells were transfected with *ODAM* or *ODAM shRNA* constructs. Equal amounts of cell lysates were used for G-LISA RhoA activation assays. (D-G) RhoA expression was analyzed using gene expression data collected from breast cancer and normal breast epithelium in the GEO database GSE9574, breast cancer in the GEO databases GSE9574, GSE20437, and GSE1299, stomach cancer in the GEO database GSE35809, and lung cancer in the GEO databases GSE43346 and GSE3268. (H) ODAM (upper panels) and GTP-RhoA (lower panels) proteins in breast cancer tissues were analyzed by immunohistochemistry. Right panels are higher magnifications of boxed left panels, respectively. Scale bars: 200 μm. * denotes values significantly different from the control ($P<0.05$).

3. ODAM regulates PTEN and AKT signaling pathway via RhoA

ROCK is markedly activated to hinder cell proliferation and migration when adhesion signaling is weak. ROCK suppression promotes cell proliferation via PTEN and up-regulation of AKT phosphorylation or induces cell migration [121]. ODAM inhibited AKT phosphorylation but enhanced the expression of PTEN, a tumor suppressor gene, in melanoma cells [28]. Western blot analysis of breast cell lysates with phospho-specific antibodies revealed a marked decrease in AKT activation in *ODAM*-expressing cells evident as decreased phosphorylation at both the Ser 473 and Thr 308 residues associated with AKT activation; however, the overall levels of AKT protein were unaffected (Fig. 22A). Activation of AKT is antagonized by the PTEN tumor suppressor gene product through its PIP3-phosphatase activity [122]. To test whether the elevation of PTEN expression is specific to *ODAM*-expressing non-invasive breast cancer cells, it was examined PTEN expression in MCF7 cells. Significantly, the levels of PTEN protein and PTEN phosphorylation were elevated in *ODAM*-expressing MCF7 cells relative to controls (Fig. 22B).

Epithelial cells bind together through the binding of E-cadherins and the formation of an intracellular molecular complex with several molecules, including β-catenin and actin filaments [123, 124]. Thus, the gain of E-cadherin and β-catenin from the cell membrane was examined upon cell adhesion through ROCK activation using western blotting. *ODAM* overexpression clearly resulted in the gain of E-cadherin and β-catenin expression (Fig. 22C). However, MCF7 cells expressing *ODAM shRNA* induced the loss of ROCK, p-PTEN, PTEN, E-cadherin and β-catenin and the gain of AKT phosphorylation (Fig.

22A, B, and C). The gain of ROCK, p-PTEN, PTEM, E-cadherin and β-catenin was further confirmed through the constitutive overexpression of *active RhoA* (Fig. 22D). These results suggest that the construction of cell junctions upon RhoA signal activation by ODAM might be associated with the gain of adhesion signaling and intracellular molecular complexes such as E-cadherin and β-catenin

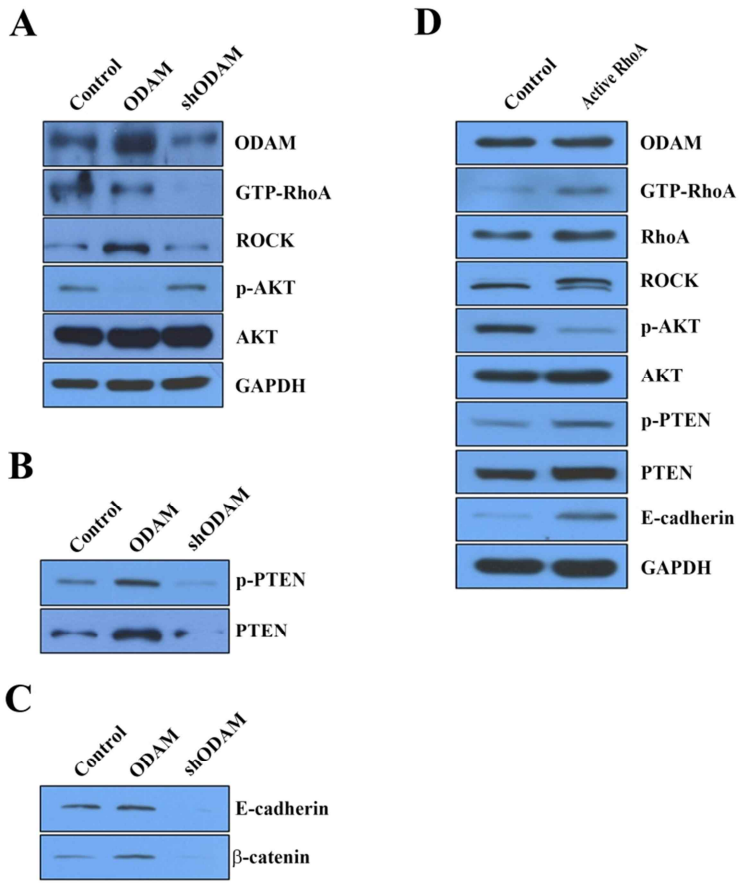

Figure 22. ODAM controlled PTEN and AKT signaling via the RhoA pathway.

(A) MCF7 cells were transfected with *ODAM* or *ODAM shRNA* constructs. AKT expression was analyzed by western blotting. (B) PTEN expression was analyzed by western blotting. (C) E-cadherin and β-catenin expression was analyzed by western blotting. (D) MCF7 cells were transfected with *active RhoA* constructs. Expression of RhoA and AKT/PTEN signaling components was analyzed by western blotting.

4. ODAM-induced RhoA signaling results in cytoskeletal rearrangement and cellular conformational changes

Actin rearrangement induces cell shape, adhesion, motility, and differentiation [125]. The actin cytoskeleton is continuously reorganized through the RhoA signaling pathway during tumorigenesis [84, 126]. To investigate whether ODAM-RhoA signaling changes actin filaments, it was evaluated subcellular alterations in F-actin after exogenous *ODAM* expression in MCF7 and AGS cells. Confocal microscopy showed specific localization of ODAM in the nucleus and cytoplasm of MCF7 and AGS cells, and F-actin accumulated at the cell periphery compared with control, but not in *shRNA*-mediated ODAM-inactivated cells (Fig. 23A, B). Next, to investigate whether ODAM could affect F-actin distribution and cell shape, MCF7 and AGS cells were cultured for 24 hours on rODAM- or collagen-coated slides and examined ODAM and F-actin expression. Cells cultured on rODAM protein showed a greater density of F-actin filaments at the cell periphery than cells cultured on collagen and retained their cell shape (Fig. 23C, D). I also investigated whether ODAM-induced RhoA activity and subsequent actin reorganization affect the adhesion of MCF7 and AGS cells to the substrates using adhesion assays. ODAM- and collagen-coated MCF7 and AGS cells exhibited significantly increased cell adhesion compared with control cells (Fig. 23E). These results suggest that ODAM-mediated RhoA signaling resulted in actin filament rearrangement at the cell periphery of MCF7 and AGS cells with the promotion of cell adhesion.

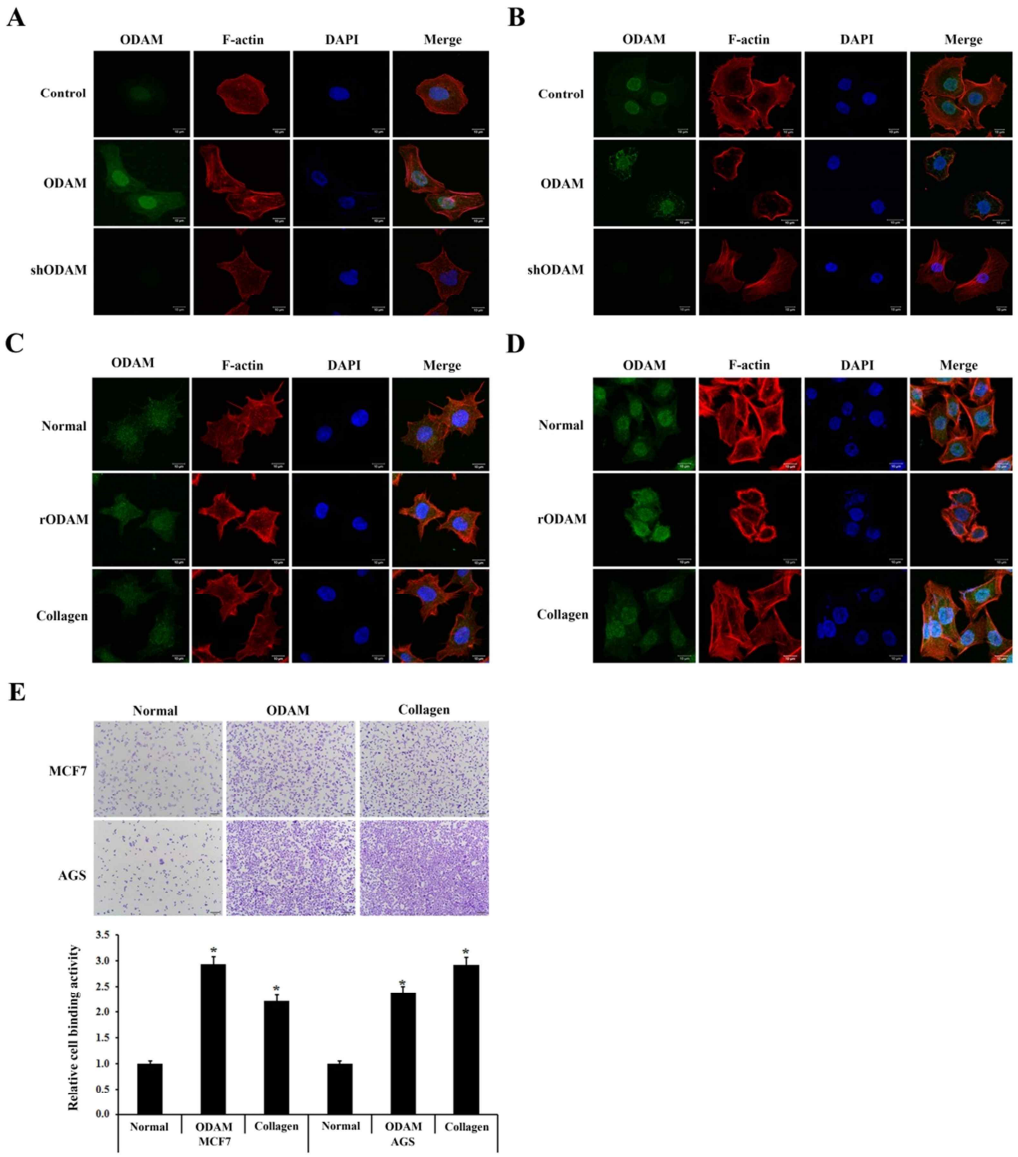

Figure 23. ODAM expression resulted in actin rearrangement in breast cancer and stomach cancer cells via RhoA signaling.

(A and B) MCF7 (A) and AGS (B) cells were transfected with *ODAM or ODAM shRNA*

constructs, and rhodamine-phalloidin was used to examine the arrangement of actin filaments (red). (C and D) MCF7 (C) and AGS (D) cells were cultured on ODAM- or collagen-coated slides for 24 h. Fixed cells were treated with rhodamine-phalloidin to examine ODAM and F-actin expression by confocal laser microscopy (red). (E) Adhesion of MCF7 and AGS cells to ODAM- or collagen-coated slides. Binding values are based on the absorbance of adherent cells. Data are presented as the mean ± SD of triplicate experiments. * denotes values significantly different from the control (P<0.05).

5. ODAM reduces tumor formation, growth, cellular migration, and invasion in breast and stomach cancer cells

Next, I asked whether ODAM controlled the migration and invasion of breast cancer cells. In wound healing assays, *ODAM* reduced the migration of MCF7 non-invasive breast cancer cells and AGS non-invasive stomach cancer cells. Conversely, ectopic *ODAM shRNA* enhanced MCF7 and AGS cell motility (Fig. 24A). Furthermore, transwell invasion assays demonstrated a significantly increased number of MCF7 and AGS cells when transfected with *ODAM shRNA*-expressing constructs compared with control cells (Fig. 24B). Conversely, the ectopic *ODAM* construct reduced MDA-MB231 cell motility (Fig. 24C). These results indicated that ODAM is crucial for the inhibition of breast and lung cancer cell migration and invasion *in vitro*. There is a strong correlation between the expression level of ODAM and invasiveness of cancer cells (Fig. 24A, B). To determine whether ODAM expression would affect the aggressive tumor-forming and metastatic properties of MCF7 and MDA-MB231 breast cancer cells *in vivo*, *ODAM*-expressing or control cancer cells were implanted subcutaneously into BALB/c mice. After 4 weeks of implantation, the tumors had grown in control and *ODAM*-expressing cells. Although tumor suppression by ODAM was relatively evident in MDA-MB231 cells, the tumors were smaller in the ODAM-expressing group than in the control group (Fig. 24D).

Breast cancer frequently metastasizes to the bone [127]. ODAM was also observed in osteoblast and osteoclast cell lines [27]. To investigate the role of ODAM in osteolytic bone metastasis, it was examined the expression of ODAM in normal tibia and tibia with breast cancer burden induced by the left cardiac ventricle injection of MDA-MB231

breast cancer cells [128]. Histomorphometric analysis revealed that bone tumor burden was clearly induced in mice-bearing MDA-MB231 cells compared with the bone of normal mice (Fig. 24E). ODAM was strongly expressed in normal tibia, but its expression was reduced in tibia with breast cancer burden (Fig. 24E). These results suggest that bone metastasis of breast cancer resulted the reduction of ODAM expression in the bone.

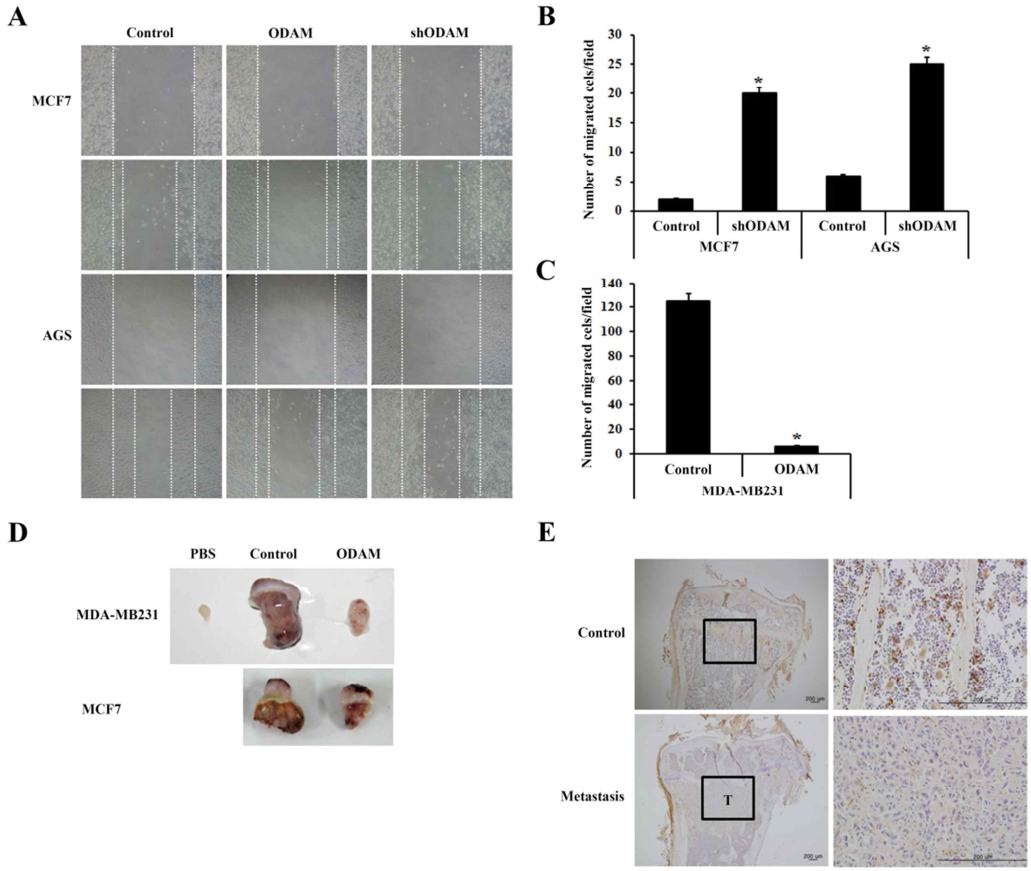

Figure 24. ODAM influenced the morphology, adhesion, migration, and invasion of breast and stomach cancer cells.

(A) Migration was analyzed by wound healing assays in MCF7 cells transfected with *ODAM* or *ODAM shRNA* constructs (Magnification: 200×). (B and C) The invasion capacity of MCF7, AGS, or MDA-MB231 cells, which were transfected with *ODAM* or *ODAM shRNA* constructs, was determined by matrigel-coated transwell assays. The average cell counts from representative fields for each condition are given as mean ± S.D.

* denotes values significantly different from the control ($P<0.05$). (D) Tumor formation was analyzed in BALB/c mice 4 weeks after subcutaneous implantation of MCF7 or MDA-MB231 cells (control) or *ODAM*-expressing MCF7 or MDA-MB231 cells (ODAM). (E) ODAM expression was observed in normal tibia and tibia with breast cancer burden by immunohistochemistry. Right panels are higher magnifications of boxed left panels, respectively. T: tumor. Scale bar: 200 μm.

V. DISCUSSION

ODAM was first identified as the protein constituent of calcifying epithelial odontogenic/Pindborg tumor (CEOT) and revealed high expression in ameloblasts and junctional epithelium [9, 11, 12, 22]. Further analysis showed that ODAM was expressed in epithelial malignancies including those of colon, breast, lung, stomach, and melanoma [27, 50, 51]. Intracellular ODAM showed a significant correlation with improved survival when analyzed between and across tumor stages [24]. Rho GTPases can influence the formation and progression of human tumors by the regulation of several neoplastic processes; an important future issue is the determination of the activity of these proteins in different tumors [129]. The importance of RhoA in this process has been demonstrated by *in vitro* studies in that low levels of activated RhoA were associated with cultured cells with a high migration phenotype [130, 131]; however, high RhoA activity has been linked to poor migration ability by high substrate adhesion [132-134]. This study demonstrated that ODAM induces RhoA activation and maintenance of MCF7 dormant breast cancer cells to assimilate through the integration of cell junctions concomitant with inhibited migration and invasion. The induced expression of E-cadherin, β-catenin, and actin filament bundles at the cell membrane, which maintains cell junctions, might explain the molecular basis underlying the assembly of MCF7 cell junctions through ODAM. Thus, these results indicate a good potential to inhibit MCF7 cells to metastasize to neighboring tissues or organs through ODAM. Thus, ODAM activation therapy should be cautiously administered, as there is a new potential for the inhibition of cancer cells.

ROCK, a downstream mediator of RhoA signaling, suppresses cell proliferation

through the up-regulation of PTEN and down-regulation of AKT phosphorylation, and accelerates cell migration [121, 135, 136]. The inhibition of ROCK activates the cell proliferation, migration and invasion of dormant MCF7 breast cancer cells, of which ROCK activity is dependent on the adhesion strength [114]. ODAM inhibits growth and migration through the elevation of the PTEN tumor suppressor and inactivation of PI3K/AKT signaling in melanoma and breast cancer cell lines [28]. MCF7 cell dissipation upon ROCK inhibition might be further peculiar because AKT activity might be involved in this process. The up-regulated AKT phosphorylation is associated with EMT. The active AKT induces EMT in squamous cell carcinoma cells [137]. The activation of AKT through leptin is associated with EMT in MCF7 cells [138]. In the present study, the integration of cell junctions through ROCK activation is directly associated with down-regulated AKT phosphorylation upon ROCK activation. In addition, cell migration and invasion were also up-regulated through RhoA, which was previously shown in MCF7 cells and strocytoma cells [126, 139]. The inhibition of cells in migration and invasion might substantially promote the association of dissociated MCF7 cells.

ODAM is localized in the nucleus, cytoplasm, and extracellular matrix of differentiating ameloblasts, JE, and diverse cancer cells [14, 27]. Although the presence of cytoplasmic ODAM and several interacting proteins in various cells and tissues imply multiple regulatory functions, the function of cytoplasmic ODAM in various cancer cell types has not yet been determined. In many cell types, cytoskeletal changes are regulated by low-molecular-weight GTP-binding proteins that belong to the Rho family [118, 140]. ROCK contributes to the polarity, proliferation, and differentiation of these cells by

regulating the organization of the actin cytoskeleton and cell-cell adhesion [141]. In the present study, I show for the first time that ODAM-mediated RhoA signaling resulted in cytoskeleton reorganization of non-invasive breast cancer cells. ODAM activates RhoA signaling, resulting in actin cytoskeleton reorganization and promotion of cell adhesion in MCF7 cells. Additionally, when the scratch wound in cultured breast cancer cells was healed, intracellular ODAM was apparently increased compared with extracellular ODAM, suggesting the adhesion function of cellular ODAM rather than migration function of extracellular ODAM. Taken together, the results suggest that intracellular/extracellular ODAM has a potentially significant role together with RhoA signaling in regulating the tumorigenesis and metastasis of various cancers with possible clinical implications.

In summary, the results of the present study suggest that the cell adhesion of MCF7 breast cancer cells might be up-regulated upon ODAM-RhoA signaling. Increased RhoA activity by ODAM might also inhibit cell migration/invasion. Thus, MCF7 cells upon ODAM-RhoA activation might hinder the metastasis into the surrounding tissues or organs. Moreover, these pathways are critical determinants of the motile and invasive phenotype of cancer cells in that ODAM regulates actin stress fibers, cell motility, and morphology in a RhoA-dependent manner.

CHAPTER VI. CONCLUDING REMARKS

In the study, intracellular and extracellular expression pattern of ODAM was investigated in odontogenic and cancer cells in vivo and in vitro. ODAM was present in developing ameloblasts, odontoblasts, osteoblasts, and various cancer cells including human lung, stomach, uterine cervix, and breast cancer cells. In these cells, ODAM protein was localized in the nucleus, cytoplasm, and extracellular matrix. Based on the observation presented here, it was proposed that ODAM has diverse functions that vary with protein location in various cell lines.

The nuclear ODAM was recruited to the MMP-20 promoter in secretory ameloblasts. Runx2 regulated expression of ODAM protein level, which in turn regulated MMP-20 promoter activity, thus suggesting that nucleus ODAM played a key role in efficient amelogenesis in higher eukaryotic cells.

Adhesion of the JE to the tooth surface is crucial for maintaining periodontal health. The cytoplasmic ODAM induced RhoA activity and the expression of downstream factors by interacting with ARHGEF5. ODAM-mediated RhoA signaling resulted in actin filament rearrangement and enhancement of cell adhesion. JE adhesion to the tooth surface was regulated via fibronectin/laminin-integrin-ODAM-ARHGEF5-RhoA signaling. ODAM was expressed in normal JE of healthy tooth but was absent in pathologic pocket epithelium of diseased periodontium. In periodontitis and peri-implantitis, ODAM was extruded from JE following onset with JE attachment loss and detected in gingival crevicular fluid. These results suggest that ODAM expression in JE

reflects healthy periodontium. Identifying the precise role of ODAM expression in regenerating JE should help clinicians provide better periodontal care for patients. It was also proposed that ODAM could be used as a biomarker of periodontitis and peri-implantitis.

Furthermore, I identified a critical role for ODAM in inducing cancer cell adhesion, in part through binding, a positive regulator of Rho GTPases. ODAM induced RhoA activity and the expression of downstream factors, including ROCK. ODAM-mediated RhoA signaling resulted in actin filament rearrangement by activating PTEN and inhibiting the phosphorylation of AKT. When ODAM was overexpressed in MCF7 breast cancer cells and AGS gastric cancer cells that activated RhoA at high levels, it decreased motility, increased adhesion, and inhibited the metastasis of MCF7 cells. Conversely, depletion of ODAM in cancer cells or ECM ODAM inhibited Rho GTPase activation, resulting in increased cancer migration and invasion. These results suggest that ODAM expression in cells maintains their adhesion, resulting in the prevention of their metastasis via the regulation of RhoA signaling in breast cancer cells.

These studies provided the first evidence for ODAM function in multiple cellular compartments of differentiating odontogenic and cancer cell lines with important functional implications.

REFERENCES

1. Moradian-Oldak J: **Protein-mediated enamel mineralization**. *Front Biosci (Landmark Ed)* 2012, **17**:1996-2023.
2. Smith CE: **Cellular and chemical events during enamel maturation**. *Crit Rev Oral Biol Med* 1998, **9**(2):128-161.
3. Simmer JP, Papagerakis P, Smith CE, Fisher DC, Rountrey AN, Zheng L, Hu JC: **Regulation of dental enamel shape and hardness**. *J Dent Res* 2010, **89**(10):1024-1038.
4. Lacruz RS, Smith CE, Moffatt P, Chang EH, Bromage TG, Bringas P, Jr., Nanci A, Baniwal SK, Zabner J, Welsh MJ *et al*: **Requirements for ion and solute transport, and pH regulation during enamel maturation**. *J Cell Physiol* 2012, **227**(4):1776-1785.
5. Schroeder HE, Listgarten MA: **The gingival tissues: the architecture of periodontal protection**. *Periodontol 2000* 1997, **13**:91-120.
6. Bosshardt DD, Lang NP: **The junctional epithelium: from health to disease**. *J Dent Res* 2005, **84**(1):9-20.
7. Ganss B, Abbarin N: **Maturation and beyond: proteins in the developmental continuum from enamel epithelium to junctional epithelium**. *Front Physiol* 2014, **5**:371.
8. Dey R, Son HH, Cho MI: **Isolation and partial sequencing of potentially odontoblast-specific/enriched rat cDNA clones obtained by suppression subtractive hybridization**. *Arch Oral Biol* 2001, **46**(3):249-260.
9. Solomon A, Murphy CL, Weaver K, Weiss DT, Hrncic R, Eulitz M, Donnell RL, Sletten K, Westermark G, Westermark P: **Calcifying epithelial odontogenic (Pindborg) tumor-**

associated amyloid consists of a novel human protein. *J Lab Clin Med* 2003, **142**(5):348-355.

10. Moffatt P, Smith CE, Sooknanan R, St-Arnaud R, Nanci A: **Identification of secreted and membrane proteins in the rat incisor enamel organ using a signal-trap screening approach**. *Eur J Oral Sci* 2006, **114 Suppl 1**:139-146; discussion 164-135, 380-131.
11. Park JC, Park JT, Son HH, Kim HJ, Jeong MJ, Lee CS, Dey R, Cho MI: **The amyloid protein APin is highly expressed during enamel mineralization and maturation in rat incisors**. *Eur J Oral Sci* 2007, **115**(2):153-160.
12. Moffatt P, Smith CE, St-Arnaud R, Nanci A: **Characterization of Apin, a secreted protein highly expressed in tooth-associated epithelia**. *J Cell Biochem* 2008, **103**(3):941-956.
13. Kawasaki K, Weiss KM: **Mineralized tissue and vertebrate evolution: the secretory calcium-binding phosphoprotein gene cluster**. *Proc Natl Acad Sci U S A* 2003, **100**(7):4060-4065.
14. Lee HK, Lee DS, Ryoo HM, Park JT, Park SJ, Bae HS, Cho MI, Park JC: **The odontogenic ameloblast-associated protein (ODAM) cooperates with RUNX2 and modulates enamel mineralization via regulation of MMP-20**. *J Cell Biochem* 2010, **111**(3):755-767.
15. Dos Santos Neves J, Wazen RM, Kuroda S, Francis Zalzal S, Moffatt P, Nanci A: **Odontogenic ameloblast-associated and amelotin are novel basal lamina components**. *Histochem Cell Biol* 2012, **137**(3):329-338.
16. Lee HK, Park JT, Cho YS, Bae HS, Cho MI, Park JC: **Odontogenic ameloblasts-associated protein (ODAM), via phosphorylation by bone morphogenetic protein receptor type IB (BMPR-IB), is implicated in ameloblast differentiation**. *J Cell Biochem* 2012,

113(5):1754-1765.

17. Yang IS, Lee DS, Park JT, Kim HJ, Son HH, Park JC: **Tertiary dentin formation after direct pulp capping with odontogenic ameloblast-associated protein in rat teeth**. *J Endod* 2010, **36**(12):1956-1962.

18. Nishio C, Wazen R, Kuroda S, Moffatt P, Nanci A: **Expression pattern of odontogenic ameloblast-associated and amelotin during formation and regeneration of the junctional epithelium**. *Eur Cell Mater* 2010, **20**:393-402.

19. Jue SS, Kim JY, Na SH, Jeon KD, Bang HJ, Park JH, Shin JW: **Localization of ODAM, PCNA, and CK14 in regenerating junctional epithelium during orthodontic tooth movement in rats**. *Angle Orthod* 2014, **84**(3):534-540.

20. Nishio C, Wazen R, Kuroda S, Moffatt P, Nanci A: **Disruption of periodontal integrity induces expression of apin by epithelial cell rests of Malassez**. *J Periodontal Res* 2010, **45**(6):709-713.

21. Dabija-Wolter G, Bakken V, Cimpan MR, Johannessen AC, Costea DE: **In vitro reconstruction of human junctional and sulcular epithelium**. *J Oral Pathol Med* 2013, **42**(5):396-404.

22. Murphy CL, Kestler DP, Foster JS, Wang S, Macy SD, Kennel SJ, Carlson ER, Hudson J, Weiss DT, Solomon A: **Odontogenic ameloblast-associated protein nature of the amyloid found in calcifying epithelial odontogenic tumors and unerupted tooth follicles**. *Amyloid* 2008, **15**(2):89-95.

23. Kestler DP, Foster JS, Bruker CT, Prenshaw JW, Kennel SJ, Wall JS, Weiss DT, Solomon A: **ODAM Expression Inhibits Human Breast Cancer Tumorigenesis**. *Breast Cancer (Auckl)*

2011, **5**:73-85.

24. Siddiqui S, Bruker CT, Kestler DP, Foster JS, Gray KD, Solomon A, Bell JL: **Odontogenic ameloblast associated protein as a novel biomarker for human breast cancer**. *Am Surg* 2009, **75**(9):769-775; discussion 775.

25. Ren C, Diniz MG, Piazza C, Amm HM, Rollins DL, Rivera H, Devilliers P, Kestler DP, Waite PD, Mamaeva OA *et al*: **Differential enamel and osteogenic gene expression profiles in odontogenic tumors**. *Cells Tissues Organs* 2011, **194**(2-4):296-301.

26. Crivelini MM, Felipini RC, Miyahara GI, de Sousa SC: **Expression of odontogenic ameloblast-associated protein, amelotin, ameloblastin, and amelogenin in odontogenic tumors: immunohistochemical analysis and pathogenetic considerations**. *J Oral Pathol Med* 2012, **41**(3):272-280.

27. Lee HK, Park SJ, Oh HJ, Kim JW, Bae HS, Park JC: **Expression pattern, subcellular localization, and functional implications of ODAM in ameloblasts, odontoblasts, osteoblasts, and various cancer cells**. *Gene Expr Patterns* 2012, **12**(3-4):102-108.

28. Foster JS, Fish LM, Phipps JE, Bruker CT, Lewis JM, Bell JL, Solomon A, Kestler DP: **Odontogenic ameloblast-associated protein (ODAM) inhibits growth and migration of human melanoma cells and elicits PTEN elevation and inactivation of PI3K/AKT signaling**. *BMC Cancer* 2013, **13**:227.

29. Sekiguchi M, Sakakibara K, Fujii G: **Establishment of cultured cell lines derived from a human gastric carcinoma**. *Jpn J Exp Med* 1978, **48**(1):61-68.

30. Takata T, Zhao M, Nikai H, Uchida T, Wang T: **Ghost cells in calcifying odontogenic cyst express enamel-related proteins**. *Histochem J* 2000, **32**(4):223-229.

31. Takata T, Zhao M, Uchida T, Wang T, Aoki T, Bartlett JD, Nikai H: **Immunohistochemical detection and distribution of enamelysin (MMP-20) in human odontogenic tumors**. *J Dent Res* 2000, **79**(8):1608-1613.

32. Hegedus L, Cho H, Xie X, Eliceiri GL: **Additional MDA-MB-231 breast cancer cell matrix metalloproteinases promote invasiveness**. *J Cell Physiol* 2008, **216**(2):480-485.

33. Caterina JJ, Skobe Z, Shi J, Ding Y, Simmer JP, Birkedal-Hansen H, Bartlett JD: **Enamelysin (matrix metalloproteinase 20)-deficient mice display an amelogenesis imperfecta phenotype**. *J Biol Chem* 2002, **277**(51):49598-49604.

34. Lu Y, Papagerakis P, Yamakoshi Y, Hu JC, Bartlett JD, Simmer JP: **Functions of KLK4 and MMP-20 in dental enamel formation**. *Biol Chem* 2008, **389**(6):695-700.

35. Vaananen A, Srinivas R, Parikka M, Palosaari H, Bartlett JD, Iwata K, Grenman R, Stenman UH, Sorsa T, Salo T: **Expression and regulation of MMP-20 in human tongue carcinoma cells**. *J Dent Res* 2001, **80**(10):1884-1889.

36. Dos Santos Neves J, Wazen RM, Kuroda S, Francis Zalzal S, Moffatt P, Nanci A: **Odontogenic ameloblast-associated and amelotin are novel basal lamina components**. *Histochem Cell Biol* 2012.

37. George A, Sabsay B, Simonian PA, Veis A: **Characterization of a novel dentin matrix acidic phosphoprotein. Implications for induction of biomineralization**. *J Biol Chem* 1993, **268**(17):12624-12630.

38. Terasawa M, Shimokawa R, Terashima T, Ohya K, Takagi Y, Shimokawa H: **Expression of dentin matrix protein 1 (DMP1) in nonmineralized tissues**. *J Bone Miner Metab* 2004, **22**(5):430-438.

39. MacDougall M, Gu TT, Luan X, Simmons D, Chen J: **Identification of a novel isoform of mouse dentin matrix protein 1: spatial expression in mineralized tissues**. *J Bone Miner Res* 1998, **13**(3):422-431.

40. Martinez EF, da Silva LA, Furuse C, de Araujo NS, de Araujo VC: **Dentin matrix protein 1 (DMP1) expression in developing human teeth**. *Braz Dent J* 2009, **20**(5):365-369.

41. Narayanan K, Ramachandran A, Hao J, He G, Park KW, Cho M, George A: **Dual functional roles of dentin matrix protein 1. Implications in biomineralization and gene transcription by activation of intracellular Ca2+ store**. *J Biol Chem* 2003, **278**(19):17500-17508.

42. Liu R, Yamamoto M, Moroi M, Kubota T, Ono T, Funatsu A, Komatsu H, Tsuji T, Hara H, Hara H *et al*: **Chlamydia pneumoniae immunoreactivity in coronary artery plaques of patients with acute coronary syndromes and its relation with serology**. *Am Heart J* 2005, **150**(4):681-688.

43. Kominsky SL, Argani P, Korz D, Evron E, Raman V, Garrett E, Rein A, Sauter G, Kallioniemi OP, Sukumar S: **Loss of the tight junction protein claudin-7 correlates with histological grade in both ductal carcinoma in situ and invasive ductal carcinoma of the breast**. *Oncogene* 2003, **22**(13):2021-2033.

44. Matter K, Balda MS: **Epithelial tight junctions, gene expression and nucleo-junctional interplay**. *J Cell Sci* 2007, **120**(Pt 9):1505-1511.

45. Nakamura T, Blechman J, Tada S, Rozovskaia T, Itoyama T, Bullrich F, Mazo A, Croce CM, Geiger B, Canaani E: **huASH1 protein, a putative transcription factor encoded by a human homologue of the Drosophila ash1 gene, localizes to both nuclei and cell-cell tight**

junctions. *Proc Natl Acad Sci U S A* 2000, **97**(13):7284-7289.

46. Reith EJ: **The stages of amelogenesis as observed in molar teeth of young rats**. *J Ultrastruct Res* 1970, **30**(1):111-151.

47. Hu JC, Sun X, Zhang C, Simmer JP: **A comparison of enamelin and amelogenin expression in developing mouse molars**. *Eur J Oral Sci* 2001, **109**(2):125-132.

48. Fukumoto S, Kiba T, Hall B, Iehara N, Nakamura T, Longenecker G, Krebsbach PH, Nanci A, Kulkarni AB, Yamada Y: **Ameloblastin is a cell adhesion molecule required for maintaining the differentiation state of ameloblasts**. *J Cell Biol* 2004, **167**(5):973-983.

49. Sire JY, Davit-Beal T, Delgado S, Gu X: **The origin and evolution of enamel mineralization genes**. *Cells Tissues Organs* 2007, **186**(1):25-48.

50. Kestler DP, Foster JS, Macy SD, Murphy CL, Weiss DT, Solomon A: **Expression of odontogenic ameloblast-associated protein (ODAM) in dental and other epithelial neoplasms**. *Mol Med* 2008, **14**(5-6):318-326.

51. Aung PP, Oue N, Mitani Y, Nakayama H, Yoshida K, Noguchi T, Bosserhoff AK, Yasui W: **Systematic search for gastric cancer-specific genes based on SAGE data: melanoma inhibitory activity and matrix metalloproteinase-10 are novel prognostic factors in patients with gastric cancer**. *Oncogene* 2006, **25**(17):2546-2557.

52. Hu JC, Sun X, Zhang C, Liu S, Bartlett JD, Simmer JP: **Enamelysin and kallikrein-4 mRNA expression in developing mouse molars**. *Eur J Oral Sci* 2002, **110**(4):307-315.

53. Golonzhka O, Metzger D, Bornert JM, Bay BK, Gross MK, Kioussi C, Leid M: **Ctip2/Bcl11b controls ameloblast formation during mammalian odontogenesis**. *Proc Natl Acad Sci U S A* 2009, **106**(11):4278-4283.

54. D'Souza RN, Aberg T, Gaikwad J, Cavender A, Owen M, Karsenty G, Thesleff I: **Cbfa1 is required for epithelial-mesenchymal interactions regulating tooth development in mice**. *Development* 1999, **126**(13):2911-2920.

55. Camilleri S, McDonald F: **Runx2 and dental development**. *Eur J Oral Sci* 2006, **114**(5):361-373.

56. Harbron L LL, Athanassion M, Simmer JP, Papagerakis P.: **Runx2 expression and function in ameloblasts.** *IADR Foster session* 2009, **#3093**.

57. Bourd-Boittin K, Fridman R, Fanchon S, Septier D, Goldberg M, Menashi S: **Matrix metalloproteinase inhibition impairs the processing, formation and mineralization of dental tissues during mouse molar development**. *Exp Cell Res* 2005, **304**(2):493-505.

58. Nakata A, Kameda T, Nagai H, Ikegami K, Duan Y, Terada K, Sugiyama T: **Establishment and characterization of a spontaneously immortalized mouse ameloblast-lineage cell line**. *Biochem Biophys Res Commun* 2003, **308**(4):834-839.

59. Takahashi S, Kawashima N, Sakamoto K, Nakata A, Kameda T, Sugiyama T, Katsube K, Suda H: **Differentiation of an ameloblast-lineage cell line (ALC) is induced by Sonic hedgehog signaling**. *Biochem Biophys Res Commun* 2007, **353**(2):405-411.

60. Arnoys EJ, Wang JL: **Dual localization: proteins in extracellular and intracellular compartments**. *Acta Histochem* 2007, **109**(2):89-110.

61. Lucero HA, Kintsurashvili E, Marketou ME, Gavras H: **Cell signaling, internalization, and nuclear localization of the angiotensin converting enzyme in smooth muscle and endothelial cells**. *J Biol Chem* 2010, **285**(8):5555-5568.

62. Chuderland D, Konson A, Seger R: **Identification and characterization of a general**

nuclear translocation signal in signaling proteins. *Mol Cell* 2008, **31**(6):850-861.

63. Hutten S, Kehlenbach RH: **CRM1-mediated nuclear export: to the pore and beyond**. *Trends Cell Biol* 2007, **17**(4):193-201.

64. Vuletic S, Dong W, Wolfbauer G, Day JR, Albers JJ: **PLTP is present in the nucleus, and its nuclear export is CRM1-dependent**. *Biochim Biophys Acta* 2009, **1793**(3):584-591.

65. Breuss JM, Gillett N, Lu L, Sheppard D, Pytela R: **Restricted distribution of integrin beta 6 mRNA in primate epithelial tissues**. *J Histochem Cytochem* 1993, **41**(10):1521-1527.

66. Schroeder HE, Listgarten MA: **The junctional epithelium: from strength to defense**. *J Dent Res* 2003, **82**(3):158-161.

67. Shimono M, Ishikawa T, Enokiya Y, Muramatsu T, Matsuzaka K, Inoue T, Abiko Y, Yamaza T, Kido MA, Tanaka T *et al*: **Biological characteristics of the junctional epithelium**. *J Electron Microsc (Tokyo)* 2003, **52**(6):627-639.

68. Lee HK, Park SJ, Oh HJ, Kim JW, Bae HS, Park JC: **Expression pattern, subcellular localization, and functional implications of ODAM in ameloblasts, odontoblasts, osteoblasts, and various cancer cells**. *Gene Expr Patterns* 2012, **12**(3-4):102-108.

69. Jue SS, Kim JY, Na SH, Jeon KD, Bang HJ, Park JH, Shin JW: **Localization of ODAM, PCNA, and CK14 in regenerating junctional epithelium during orthodontic tooth movement in rats**. *Angle Orthod* 2013.

70. Larjava H, Koivisto L, Hakkinen L, Heino J: **Epithelial integrins with special reference to oral epithelia**. *J Dent Res* 2011, **90**(12):1367-1376.

71. Hynes RO: **Integrins: bidirectional, allosteric signaling machines**. *Cell* 2002, **110**(6):673-687.

72. Larjava H, Koivisto L, Heino J, Hakkinen L: **Integrins in periodontal disease**. *Exp Cell Res* 2014, **325**(2):104-110.

73. Ghannad F, Nica D, Fulle MI, Grenier D, Putnins EE, Johnston S, Eslami A, Koivisto L, Jiang G, McKee MD *et al*: **Absence of alphavbeta6 integrin is linked to initiation and progression of periodontal disease**. *Am J Pathol* 2008, **172**(5):1271-1286.

74. Xue H, Li Y, Everett ET, Ryan K, Peng L, Porecha R, Yan Y, Lucchese AM, Kuehl MA, Pugach MK *et al*: **Ameloblasts require active RhoA to generate normal dental enamel**. *Eur J Oral Sci* 2013, **121**(4):293-302.

75. Snyder JT, Worthylake DK, Rossman KL, Betts L, Pruitt WM, Siderovski DP, Der CJ, Sondek J: **Structural basis for the selective activation of Rho GTPases by Dbl exchange factors**. *Nat Struct Biol* 2002, **9**(6):468-475.

76. Wang Z, Kumamoto Y, Wang P, Gan X, Lehmann D, Smrcka AV, Cohn L, Iwasaki A, Li L, Wu D: **Regulation of immature dendritic cell migration by RhoA guanine nucleotide exchange factor Arhgef5**. *J Biol Chem* 2009, **284**(42):28599-28606.

77. Casavecchia P, Uzel MI, Kantarci A, Hasturk H, Dibart S, Hart TC, Trackman PC, Van Dyke TE: **Hereditary gingival fibromatosis associated with generalized aggressive periodontitis: a case report**. *J Periodontol* 2004, **75**(5):770-778.

78. Bhadriraju K, Yang M, Alom Ruiz S, Pirone D, Tan J, Chen CS: **Activation of ROCK by RhoA is regulated by cell adhesion, shape, and cytoskeletal tension**. *Exp Cell Res* 2007, **313**(16):3616-3623.

79. Nishikawa S, Kitamura H: **Localization of actin during differentiation of the ameloblast, its related epithelial cells and odontoblasts in the rat incisor using NBD-phallacidin**.

Differentiation 1986, **30**(3):237-243.

80. Nishikawa S, Fujiwara K, Kitamura H: **Formation of the tooth enamel rod pattern and the cytoskeletal organization in secretory ameloblasts of the rat incisor**. *Eur J Cell Biol* 1988, **47**(2):222-232.

81. Yoshida T, Kumashiro Y, Iwata T, Ishihara J, Umemoto T, Shiratsuchi Y, Kawashima N, Sugiyama T, Yamato M, Okano T: **Requirement of integrin beta3 for iron transportation during enamel formation**. *J Dent Res* 2012, **91**(12):1154-1159.

82. Yoshida T, Iwata T, Umemoto T, Shiratsuchi Y, Kawashima N, Sugiyama T, Yamato M, Okano T: **Promotion of mouse ameloblast proliferation by Lgr5 mediated integrin signaling**. *J Cell Biochem* 2013, **114**(9):2138-2147.

83. Mohazab L, Koivisto L, Jiang G, Kytomaki L, Haapasalo M, Owen GR, Wiebe C, Xie Y, Heikinheimo K, Yoshida T *et al*: **Critical role for alphavbeta6 integrin in enamel biomineralization**. *J Cell Sci* 2013, **126**(Pt 3):732-744.

84. Maekawa M, Ishizaki T, Boku S, Watanabe N, Fujita A, Iwamatsu A, Obinata T, Ohashi K, Mizuno K, Narumiya S: **Signaling from Rho to the actin cytoskeleton through protein kinases ROCK and LIM-kinase**. *Science* 1999, **285**(5429):895-898.

85. Fukumoto S, Yamada Y: **Review: extracellular matrix regulates tooth morphogenesis**. *Connect Tissue Res* 2005, **46**(4-5):220-226.

86. Sorokin LM, Pausch F, Frieser M, Kroger S, Ohage E, Deutzmann R: **Developmental regulation of the laminin alpha5 chain suggests a role in epithelial and endothelial cell maturation**. *Dev Biol* 1997, **189**(2):285-300.

87. Tabata MJ, Matsumura T, Fujii T, Abe M, Kurisu K: **Fibronectin accelerates the growth**

and differentiation of ameloblast lineage cells in vitro. *J Histochem Cytochem* 2003, **51**(12):1673-1679.

88. Fukumoto S, Miner JH, Ida H, Fukumoto E, Yuasa K, Miyazaki H, Hoffman MP, Yamada Y: **Laminin alpha5 is required for dental epithelium growth and polarity and the development of tooth bud and shape**. *J Biol Chem* 2006, **281**(8):5008-5016.

89. Berrier AL, Yamada KM: **Cell-matrix adhesion**. *J Cell Physiol* 2007, **213**(3):565-573.

90. Eke PI, Dye BA, Wei L, Thornton-Evans GO, Genco RJ, Cdc Periodontal Disease Surveillance workgroup: James Beck GDRP: **Prevalence of periodontitis in adults in the United States: 2009 and 2010**. *J Dent Res* 2012, **91**(10):914-920.

91. Berglundh T, Persson L, Klinge B: **A systematic review of the incidence of biological and technical complications in implant dentistry reported in prospective longitudinal studies of at least 5 years**. *J Clin Periodontol* 2002, **29 Suppl 3**:197-212; discussion 232-193.

92. Atsuta I, Ayukawa Y, Furuhashi A, Yamaza T, Tsukiyama Y, Koyano K: **Promotive effect of insulin-like growth factor-1 for epithelial sealing to titanium implants**. *J Biomed Mater Res A* 2013, **101**(10):2896-2904.

93. Ikeda H, Yamaza T, Yoshinari M, Ohsaki Y, Ayukawa Y, Kido MA, Inoue T, Shimono M, Koyano K, Tanaka T: **Ultrastructural and immunoelectron microscopic studies of the peri-implant epithelium-implant (Ti-6Al-4V) interface of rat maxilla**. *J Periodontol* 2000, **71**(6):961-973.

94. Thesleff I, Barrach HJ, Foidart JM, Vaheri A, Pratt RM, Martin GR: **Changes in the distribution of type IV collagen, laminin, proteoglycan, and fibronectin during mouse tooth development**. *Dev Biol* 1981, **81**(1):182-192.

95. Caffesse RG, Nasjleti CE, Castelli WA: **The role of sulcular environment in controlling epithelial keratinization**. *J Periodontol* 1979, **50**(1):1-6.

96. Sabag N, Mery C, Garcia M, Vasquez V, Cueto V: **Epithelial reattachment after gingivectomy in the rat**. *J Periodontol* 1984, **55**(3):135-141.

97. Nakaya H, Kamoi K: **[Immunohistological study of wound healing in periodontal tissue of rats. Distribution of fibronectin and laminin after flap operation]**. *Nihon Shishubyo Gakkai Kaishi* 1989, **31**(2):462-490.

98. Masaoka T, Hashimoto S, Kinumatsu T, Muramatsu T, Jung HS, Yamada S, Shimono M: **Immunolocalization of laminin and integrin in regenerating junctional epithelium of mice after gingivectomy**. *J Periodontal Res* 2009, **44**(4):489-495.

99. Stenman S, Vaheri A: **Distribution of a major connective tissue protein, fibronectin, in normal human tissues**. *J Exp Med* 1978, **147**(4):1054-1064.

100. Thesleff I, Partanen AM, Kuusela P, Lehtonen E: **Dental papilla cells synthesize but do not deposit fibronectin in culture**. *J Dent Res* 1987, **66**(6):1107-1115.

101. Sawada T, Nanci A: **Spatial distribution of enamel proteins and fibronectin at early stages of rat incisor tooth formation**. *Arch Oral Biol* 1995, **40**(11):1029-1038.

102. Hynes RO, Yamada KM: **Fibronectins: multifunctional modular glycoproteins**. *J Cell Biol* 1982, **95**(2 Pt 1):369-377.

103. Dean JW, 3rd, Blankenship JA: **Migration of gingival fibroblasts on fibronectin and laminin**. *J Periodontol* 1997, **68**(8):750-757.

104. Hormia M, Owaribe K, Virtanen I: **The dento-epithelial junction: cell adhesion by type I hemidesmosomes in the absence of a true basal lamina**. *J Periodontol* 2001, **72**(6):788-797.

105. Sakai T, Ohsaki Y, Kido M, Goto M, Terada Y, Sakai H: **The distribution of fibronectin and laminin in the murine periodontal membrane, indicating possible functional roles in the apical migration of the junctional epithelium**. *Arch Oral Biol* 1996, **41**(8-9):885-891.

106. Redlich M, Shoshan S, Palmon A: **Gingival response to orthodontic force**. *Am J Orthod Dentofacial Orthop* 1999, **116**(2):152-158.

107. Salmivirta K, Gullberg D, Hirsch E, Altruda F, Ekblom P: **Integrin subunit expression associated with epithelial-mesenchymal interactions during murine tooth development**. *Dev Dyn* 1996, **205**(2):104-113.

108. Narani N, Owen GR, Hakkinen L, Putnins E, Larjava H: **Enamel matrix proteins bind to wound matrix proteins and regulate their cell-adhesive properties**. *Eur J Oral Sci* 2007, **115**(4):288-295.

109. Siegel R, Ma J, Zou Z, Jemal A: **Cancer statistics, 2014**. *CA Cancer J Clin* 2014, **64**(1):9-29.

110. Lin M, van Golen KL: **Rho-regulatory proteins in breast cancer cell motility and invasion**. *Breast Cancer Res Treat* 2004, **84**(1):49-60.

111. Wang Y, Zhou BP: **Epithelial-mesenchymal transition in breast cancer progression and metastasis**. *Chin J Cancer* 2011, **30**(9):603-611.

112. Lee HK, Ji S, Park SJ, Choung HW, Choi Y, Lee HJ, Park SY, Park JC: **Odontogenic Ameloblast-associated Protein (ODAM) Mediates Junctional Epithelium Attachment to Teeth via Integrin-ODAM-Rho Guanine Nucleotide Exchange Factor 5 (ARHGEF5)-RhoA Signaling**. *J Biol Chem* 2015, **290**(23):14740-14753.

113. Pille JY, Denoyelle C, Varet J, Bertrand JR, Soria J, Opolon P, Lu H, Pritchard LL, Vannier JP, Malvy C *et al*: **Anti-RhoA and anti-RhoC siRNAs inhibit the proliferation and**

invasiveness of MDA-MB-231 breast cancer cells in vitro and in vivo. *Mol Ther* 2005, **11**(2):267-274.

114. Yang S, Kim HM: **ROCK inhibition activates MCF-7 cells**. *PLoS One* 2014, **9**(2):e88489.

115. Jiang P, Enomoto A, Takahashi M: **Cell biology of the movement of breast cancer cells: intracellular signalling and the actin cytoskeleton**. *Cancer Lett* 2009, **284**(2):122-130.

116. Sahai E, Marshall CJ: **RHO-GTPases and cancer**. *Nat Rev Cancer* 2002, **2**(2):133-142.

117. Tang Y, Olufemi L, Wang MT, Nie D: **Role of Rho GTPases in breast cancer**. *Front Biosci* 2008, **13**:759-776.

118. Etienne-Manneville S, Hall A: **Rho GTPases in cell biology**. *Nature* 2002, **420**(6916):629-635.

119. Vega FM, Ridley AJ: **Rho GTPases in cancer cell biology**. *FEBS Lett* 2008, **582**(14):2093-2101.

120. Lee HK, Ji S, Park SJ, Choung HW, Choi Y, Lee HJ, Park SY, Park JC: **Odontogenic ameloblast-associated protein (ODAM) Mediates Junctional Epithelium Attachment to Tooth via Integrin-ODAM-Rho guanine nucleotide exchange factor 5 (ARHGEF5)-Ras homolog gene family member A (RhoA) Signaling**. *J Biol Chem* 2015.

121. Yang S, Kim HM: **The RhoA-ROCK-PTEN pathway as a molecular switch for anchorage dependent cell behavior**. *Biomaterials* 2012, **33**(10):2902-2915.

122. Sun H, Lesche R, Li DM, Liliental J, Zhang H, Gao J, Gavrilova N, Mueller B, Liu X, Wu H: **PTEN modulates cell cycle progression and cell survival by regulating phosphatidylinositol 3,4,5,-trisphosphate and Akt/protein kinase B signaling pathway**. *Proc Natl Acad Sci U S A* 1999, **96**(11):6199-6204.

123. Tomschy A, Fauser C, Landwehr R, Engel J: **Homophilic adhesion of E-cadherin occurs by a co-operative two-step interaction of N-terminal domains**. *EMBO J* 1996, **15**(14):3507-3514.

124. Gottardi CJ, Gumbiner BM: **Adhesion signaling: how beta-catenin interacts with its partners**. *Curr Biol* 2001, **11**(19):R792-794.

125. Lamouille S, Xu J, Derynck R: **Molecular mechanisms of epithelial-mesenchymal transition**. *Nat Rev Mol Cell Biol* 2014, **15**(3):178-196.

126. Wicki A, Lehembre F, Wick N, Hantusch B, Kerjaschki D, Christofori G: **Tumor invasion in the absence of epithelial-mesenchymal transition: podoplanin-mediated remodeling of the actin cytoskeleton**. *Cancer Cell* 2006, **9**(4):261-272.

127. Chen YC, Sosnoski DM, Mastro AM: **Breast cancer metastasis to the bone: mechanisms of bone loss**. *Breast Cancer Res* 2010, **12**(6):215.

128. Lee JH, Kim HN, Kim KO, Jin WJ, Lee S, Kim HH, Ha H, Lee ZH: **CXCL10 promotes osteolytic bone metastasis by enhancing cancer outgrowth and osteoclastogenesis**. *Cancer Res* 2012, **72**(13):3175-3186.

129. Karlsson R, Pedersen ED, Wang Z, Brakebusch C: **Rho GTPase function in tumorigenesis**. *Biochim Biophys Acta* 2009, **1796**(2):91-98.

130. Arthur WT, Burridge K: **RhoA inactivation by p190RhoGAP regulates cell spreading and migration by promoting membrane protrusion and polarity**. *Mol Biol Cell* 2001, **12**(9):2711-2720.

131. Jeon CY, Kim HJ, Lee JY, Kim JB, Kim SC, Park JB: **p190RhoGAP and Rap-dependent RhoGAP (ARAP3) inactivate RhoA in response to nerve growth factor leading to neurite**

outgrowth from PC12 cells. *Exp Mol Med* 2010, **42**(5):335-344.

132. Nobes CD, Hall A: **Rho GTPases control polarity, protrusion, and adhesion during cell movement**. *J Cell Biol* 1999, **144**(6):1235-1244.

133. Rousseau M, Gaugler MH, Rodallec A, Bonnaud S, Paris F, Corre I: **RhoA GTPase regulates radiation-induced alterations in endothelial cell adhesion and migration**. *Biochem Biophys Res Commun* 2011, **414**(4):750-755.

134. Ilic D, Furuta Y, Kanazawa S, Takeda N, Sobue K, Nakatsuji N, Nomura S, Fujimoto J, Okada M, Yamamoto T: **Reduced cell motility and enhanced focal adhesion contact formation in cells from FAK-deficient mice**. *Nature* 1995, **377**(6549):539-544.

135. Yang S, Tian YS, Lee YJ, Yu FH, Kim HM: **Mechanisms by which the inhibition of specific intracellular signaling pathways increase osteoblast proliferation on apatite surfaces**. *Biomaterials* 2011, **32**(11):2851-2861.

136. Zheng L, Kim HM: **Low-Rac1 activity downregulates MC3T3-E1 osteoblastic cell motility on a nanoscale topography prepared on polystyrene substrates in vitro**. *J Biomed Mater Res A* 2013, **101**(6):1629-1636.

137. Grille SJ, Bellacosa A, Upson J, Klein-Szanto AJ, van Roy F, Lee-Kwon W, Donowitz M, Tsichlis PN, Larue L: **The protein kinase Akt induces epithelial mesenchymal transition and promotes enhanced motility and invasiveness of squamous cell carcinoma lines**. *Cancer Res* 2003, **63**(9):2172-2178.

138. Yan D, Avtanski D, Saxena NK, Sharma D: **Leptin-induced epithelial-mesenchymal transition in breast cancer cells requires beta-catenin activation via Akt/GSK3- and MTA1/Wnt1 protein-dependent pathways**. *J Biol Chem* 2012, **287**(11):8598-8612.

139. Salhia B, Rutten F, Nakada M, Beaudry C, Berens M, Kwan A, Rutka JT: **Inhibition of Rho-kinase affects astrocytoma morphology, motility, and invasion through activation of Rac1**. *Cancer Res* 2005, **65**(19):8792-8800.

140. Heasman SJ, Ridley AJ: **Mammalian Rho GTPases: new insights into their functions from in vivo studies**. *Nat Rev Mol Cell Biol* 2008, **9**(9):690-701.

141. Otsu K, Kishigami R, Fujiwara N, Ishizeki K, Harada H: **Functional role of Rho-kinase in ameloblast differentiation**. *J Cell Physiol* 2011, **226**(10):2527-2534.

CHAPTER VII. ABSTRACT IN KOREAN

치아치은 접합과 암 발생 과정에서 ODAM의 기능적 특성

ODAM은 법랑모세포 분화, 법랑질 석회화, 치주 재생, 암 발생에 관여하는 인자이나 그 작용기전에 관해서는 잘 알려져 있지 않다. 치아치은 접합은 치주의 건강을 유지하는 데 있어서 중요한 요소이다. ODAM은 치아치은 접합상피에서 발현되지만, ODAM의 분자 기능에 대해서는 보고된 바가 없다. 또한, 암세포의 세포부착 특성은 암세포의 이동과 전이에 중요한 역할을 미친다. ODAM의 발현과 유방암 발생단계 사이의 상관관계는 확인되었으나, 그 메커니즘에 대해서는 연구된 바가 없다. 본 논문에서는 치아치은 접합상피 발생 및 재생과 암 발생 과정 동안의 ODAM의 기능을 조사하고, 치주염과 임플란트 주위염 초기에서 ODAM의 기능을 연구하였다.

ODAM은 세포의 종류와 분화 정도에 따라 발현 패턴과 발현 위치가 다양하였다. ODAM의 다양한 발현 양상은 치아세포와 암세포에서 ODAM의 기능과 상관관계가 있는 것으로 보인다. 법랑질 생성 과정동안 ODAM은 핵, 세포질, 세포외 기질에서 관찰되었다. 핵에서 ODAM은 Runx2의 조절을 받아 발현되었고, 증가된 ODAM은 MMP-20의 발현을 조절하여 법랑질 석회화 과정을 조절하였다.

ODAM은 건강한 치아의 정상 치아치은 접합상피에서 발현되나, 질병에 걸린 치주조

직의 주머니 상피에서는 발현되지 않았다. 치주염과 임플란트 주위염에서, ODAM은 치아치은 접합상피의 부착상실 부위를 따라 외부로 방출되어 치은열구액에 존재함을 확인하였다. ODAM은 Rho GTPases의 활성 유도인자인 ARHGEF5와 결합하여, RhoA 활성 및 ROCK 같은 하위인자의 발현을 유도하였다. ODAM을 매개로한 RhoA 신호는 actin filament의 재배열을 유도하였다. 치아치은 접합상피에서 ODAM의 발현은 치주조직의 건강 상태를 보여주고, 치아 표면에 부착된 접합 상피는 fibronectin/laminin-integrin-ODAM-ARHGEF5-RhoA signaling을 통해서 조절됨을 보여준다. 또한, ODAM이 치주염과 임플란트 주위염의 바이오 마커로서 사용될 수 있음을 나타낸다.

ODAM은 암세포에서도 RhoA의 신호를 활성화시켜 세포 부착을 증가시켰다. ODAM을 매개로한 RhoA 신호는 PTEN을 활성화하고 AKT의 인산화를 억제시킴으로서 actin filament의 재배열을 유도하였다. MCF7 유방암세포와 AGS 위암세포에 ODAM을 과발현 했을 때, RhoA의 활성도가 증가하였고, 세포의 부착이 증가하여 이동과 전이가 감소하였다.

이 결과들은 ODAM이 핵 내에서는 MMP-20를 조절하고, 세포질에서는 RhoA 신호전달 체계를 활성화 시킴으로서 세포 부착을 증가시키고, 염증성 치주에서는 세포외 기질로 방출됨을 보여준다.

주요어 : ODAM · ARHGEF5 · RhoA · 치아치은 접합상피 · 암세포 · 세포부착

학 번 : 2011-31199